

Remote river rating in resource constricted river basins

Exploring opportunities for ungauged basins through low-cost technological advancements

Samboko, H.T.

DOI

[10.4233/uuid:f74561e6-c8ba-4bbb-8ac2-19a6a18ed41d](https://doi.org/10.4233/uuid:f74561e6-c8ba-4bbb-8ac2-19a6a18ed41d)

Publication date

2023

Document Version

Final published version

Citation (APA)

Samboko, H. T. (2023). *Remote river rating in resource constricted river basins: Exploring opportunities for ungauged basins through low-cost technological advancements*. [Dissertation (TU Delft), Delft University of Technology]. <https://doi.org/10.4233/uuid:f74561e6-c8ba-4bbb-8ac2-19a6a18ed41d>

Important note

To cite this publication, please use the final published version (if applicable).
Please check the document version above.

Copyright

Other than for strictly personal use, it is not permitted to download, forward or distribute the text or part of it, without the consent of the author(s) and/or copyright holder(s), unless the work is under an open content license such as Creative Commons.

Takedown policy

Please contact us and provide details if you believe this document breaches copyrights.
We will remove access to the work immediately and investigate your claim.

Remote river rating in resource constricted river basins

Exploring opportunities for ungauged basins through low-cost technological advancements

A PhD study by Hubert Samboko



Remote river rating in resource constricted river basins

Exploring opportunities for ungauged basins through low-cost technological innovations

Remote river rating in resource constricted river basins

Exploring opportunities for ungauged basins through low-cost technological advancements

Dissertation

for the purpose of obtaining the degree of doctor
at Delft University of Technology,

by the authority of the Rector Magnificus, Prof.dr.ir. T.H.J.J. van der Hagen,
chair of the Board for Doctorates,

to be defended publicly on

Monday 11 September 2023 at 17:30 o'clock

by

Hubert Tafadzwa SAMBOKO

Master of Science in Water Resource Engineering and Management, University of Zimbabwe,
Zimbabwe,

born in Bulawayo, Zimbabwe.

This dissertation has been approved by the promotor.

Composition of the doctoral committee:

Rector Magnificus,
Dr.ir. H.C. Winsemius,
Prof.dr.ir. H.H.G. Savenije

Chairperson
Delft University of Technology, copromotor
Delft University of Technology, promotor

Independent members:

Prof.dr. H. Makurira
Dr. K.E. Banda
Dr.ir. A.M.J. Coenders
Prof.dr.ir. R. Uijlenhoet
Prof.dr.ir. N.C. van de Giesen

University of Zimbabwe
University of Zambia
Delft University of Technology
Delft University of Technology
Delft University of Technology



Nederlandse Organisatie voor Wetenschappelijk Onderzoek

This research has been funded by the Netherlands Organisation of Scientific Research, grant 07.303.102.

© 2023 Hubert T Samboko, Water Resources Section, Faculty of Civil Engineering and Geosciences, Delft University of Technology.

Title: Remote river rating in resource constricted river basins

Exploring opportunities for ungauged basins through low-cost technological advancements

Keywords: hydraulic modelling, poorly gauged, remote river rating, unmanned aerial vehicle, RTK GNSS

Printed by:

Front & Back Cover Design: Hubert T. Samboko

Copyright © 2023 by Hubert T Samboko

An electronic version of this dissertation is available at
<http://repository.tudelft.nl/>

Summary

The unavailability of consistent accurate river flow data is a significant impediment to understanding water resources availability, and hydrological extremes. This is particularly true for remote, difficult to access, morphologically active and therefore rapidly changing rivers. The state of global river discharge monitoring with respect to water infrastructure and frequency of data collection has been on the decline over the past few decades. This is despite the significant importance of these data for river flow predictions. Fortunately, rapid advancements in technologies open up possibilities for water resource authorities to increase their ability to accurately, safely and efficiently establish river flow observation through remote and non-intrusive observation methods. Low-cost Unmanned Aerial Vehicles (UAVs) in combination with Global Navigation Satellite Systems (GNSS) can be used to collect geometrical information of the riverbed and floodplain. Such information, in combination with hydraulic modelling tools, can be used to establish physically based relationships between river flows and permanent proxies. This study attempts to monitor flow in volatile, dangerous and difficult to access rivers using only affordable and easy to maintain new technologies. This thesis consists of three main components: i) generating a workable framework for monitoring rivers using low-cost technologies; ii) establishment of river geometry using a combination of airborne photogrammetry and low-cost GNSS equipment iii) and physically based rating curve development through hydraulic modelling of surveyed river sections.

The first three chapters of this thesis provide an introduction in the form of a literature review, justification for the study and a description of the study area. In chapter 4, a framework is developed through an intensive review of traditional river monitoring processes. Uniquely effective and low-cost individual components are selected and placed within a framework. The ideal outcome is an interconnected framework which clearly presents the steps which are necessary for river monitoring in remote locations. The manner in which each critical step is related to the other is explained. Furthermore, the method by which modern technologies are assimilated into the method is described. Within the framework, critical thresholds are set up in order to signal the to the water manager whether the proposed model in its current state continues to perform as required.

Chapter 5 investigates how low-cost technologies such as UAVs in combination with low-cost GNSS devices can be used to generate river geometry for the purposes of application in a hydraulic model. Furthermore, performance of the open-source photogrammetry software substantiated the claim that, free and open-source available packages are capable of producing results which are as good as proprietary alternatives as shown by the RMSE analyses. A novel approach to generate a seamless bathymetry through merging and volumization was successfully tested. Results presented in this chapter encourage future studies to investigate the impact of variations in the number of Ground Control Points (GCPs) on discharge estimations in a hydraulic model with different hydrodynamic boundary conditions. This follow up was instituted in Chapter 6.

In this sixth chapter we accept that uncertainties in the data acquisition may propagate into uncertainties in the relationships found between discharge and state variables. This uncertainty prompts the need to understand the impact of varying geometries on hydraulic models. Specific attention is placed on variations caused by differing GCP numbers since the task of GCP placement is time consuming, potential dangerous and resource intensive in certain location and instances. We are successfully able to determine the minimum number of control points required to reproduce geometry. Overall, we successfully develop and test a workable method for water resources authorities to estimate river flows accurately through the application of advanced, low-cost technologies with minimal contact with measured variables.

The development and application of low-cost technologies for river flow monitoring has led to the following important conclusions:

- For the purpose of flow estimation, there is no need to use more than seven GCPs to establish accurate UAV-based geometry. Rather, it is more crucial to distribute the available markers to be maximally representative of the terrain elevations. Furthermore, it may be necessary to place more markers in close proximity to locations where one may expect the largest challenge for photogrammetry software (e.g.: water, thick forest/vegetation)
- In order to limit the impact of the “doming” effect on terrain geometry measurements, one of the most effective, yet easily implementable mechanisms is to measure a river line using Real Time Kinematic (RTK) Global Navigation Satellite Systems (GNSS) equipment. This data can then be used to correct the terrain post photogrammetry processing.

List of Symbols

a	Rating curve parameter [m^{2-b}/s]
A	Cross-sectional area [m^2]
b	Rating curve parameter [-]
E_{ns}	Nash–Sutcliffe efficiency
h	Water stage [m]
h_0	Water level at zero flow [m]
i	Hydraulic slope [-]
n	Bed roughness [$s/m^{1/3}$]
n	Number of check points
O_i	Observed Record
O_{mean}	Average of all observed records
P_{bias}	Percentage bias [%]
P_i	Simulated record
Q	Discharge [m^3/s]
R	Hydraulic Radius [m]
$RMSE_{xy}$	Root Mean Square Error in the horizontal plane
$RMSE_z$	Root Mean Square Error in the vertical plane
ΔX_i	residual of the i th value in the x axis
ΔY_i	residual of the i th value in the y axis
ΔZ_i	residual of the i th value in the z axis

List of Abbreviations

ADCP	Acoustic Doppler Current Profiler
ASTER	Advanced Space-borne Thermal Emission and Reflection Radiometer
CM	Current Meter
CS	Cross Section
DAR	Light Detection and Ranging
DEM	Digital Elevation Model
D3DFM	D-Flow Flexible Mesh
DGPS	Differential Global Positioning System
DIY	Do It Yourself
DTM	Digital Terrain Model
FCP	Fixed Camera Parameter
GCP	Ground Control Point
GIS	Geographic Information System
GNSS	Global Navigation Satellite Systems
GPS	Global Positioning System
HEC-RAS	Hydrologic Engineering Center - River Analysis System
LSPIV	Large Scale Particle Image Velocimetry
MAD	Mean Average Deviation
MVS	Multi-view stereo
MW	Mega wats
NSE	Nash–Sutcliffe
ODM	Open Drone Map
OLS	Ordinary Least Squares
PBIAS	Percentage Bias
PIV	Particle image Velocimetry
QGIS	Quantum Geographic Information System
RAM	Random Access Memory
RGB	Red Green Blue
RMSE	Root Mean Square Error
RTCM	Radio Technical Commission for Maritime Services
RTK	Real Time Kinematic
SRTM	Shuttle Radar Topography Mission
SWOT	Surface Water Ocean Topography
UAV	Unmanned Aerial Vehicle

UNDRR	United Nations Office for Disaster Risk Reduction
USB	Universal Serial Bus
UTM	Universal Transverse Mercator
WARMA	Zambia Water Resources Management Authority
WGS	Whole-genome sequencing

Contents

Summary	vii
List of Symbols	x
List of Abbreviations	xi
1 Introduction	1
1.1 Remote river monitoring	1
1.2 Reconstruction of geometry/bathymetry for the purposes of river monitoring	3
1.3 River monitoring under ungauged conditions; justification of this study	4
1.4 Problem definition and research questions	4
1.5 Thesis outline	6
2. Study Area	7
2.1 Water Resource Management	8
3. An inventory of flow estimation and its data sources	9
3.1 Traditional river rating	9
3.1.1 What are the limitations of the traditional method?	10
3.2 Physically based river rating	10
3.3 Surveying instruments	11
3.3.1 ADCP	11
3.3.2 Unmanned Aerial Vehicle (Drone)	12
3.3.3 RTK GNSS	12
3.4 Large Scale Particle Image Velocimetry	13
3.4.1 LSPIV in its current state	13
3.5 Photogrammetry	14
4 Evaluation and improvement of remote sensing-based methods for river flow management	15
4.1 Inventory of flow observation techniques	15
4.1.1 In-situ flow observations for natural control sections	15
4.1.2 Satellite observation methods	18
4.1.3. The role of aerial photos and videos in river monitoring	19
4.2 Study area	20
4.3 Flow estimation framework	22
4.4 Discussion	28
4.5 Conclusions (and recommendations)	29
5 Evaluating low-cost topographic surveys for computations of conveyance	31
5.1 Introduction	31
5.2 Materials and methods	35
5.2.1 Study site	36
5.2.2 Data acquisition: Low-cost GNSS equipment	36

5.2.3 Flight plan.....	36
5.2.4 Dry river bathymetry	37
5.2.5 Wet river bathymetry.....	38
5.2.6 Processing the dry and wet bathymetry	39
5.3 Reconstruction experiments	41
5.3.1 Impact of the processing software used.....	41
5.3.2 Impact of GCP placement and density on accuracy	42
2.3.3 Impact of DEM variations on hydraulic conveyance	44
5.4 Results	45
5.4.1 Impact of the processing software used.....	45
5.4.2 Impact of GCP placement and density on accuracy of hydraulic features	46
5.4.3 Impact of DEM variations on hydraulic conveyance and slope	48
5.5 Conclusions and recommendations	52
6 Towards Affordable 3D Physics-Based River Flow Rating: Application Over Luangwa River Basin	54
6.1 Introduction	54
6.2 Material and Methods.....	55
6.2.1 Data collection methods	56
6.2.2 Study Site	56
6.2.3 Hydraulic Modelling	57
6.2.4 Description of Data Requirements for D3DFM	58
6.2.5 D3DFM setup, calibration and evaluation.....	59
6.2.6 Comparison of discharge estimations based on varying geometries	61
6.2.7 Evaluation of the propagation of continuous width and depth observations on uncertainty of discharge estimation	61
6.3 Results and discussion.....	62
6.3.1. Comparing the Rating Curve of the D3DFM Model with Traditional Methods.....	62
6.3.2. Comparison of discharge based on varying GCP numbers.	65
6.3.3 The impact of uncertainty in proxies of flow on discharge estimation.	66
6.4 Conclusion and Recommendations	69
7 Conclusions and Outlook	71
7.1 A proposed framework for remote river rating	72
7.2 Evaluation of the geometry for remote river rating in hydrodynamic environments.	72
7.3 The impact of geometry variations on discharge estimations	73
Outlook.....	73
7.4 Integration of satellite data to achieve truly remote river rating	73
7.5 Bathymetric Chart	74
7.6 Discharge Model	74

Appendix A	76
Appendix B	82
References	84
Acknowledgements	95
Funding and Support	95
Curriculum Vitæ.....	97
List of Publications.....	98

1 Introduction

1.1 Remote river monitoring

The unavailability of consistent accurate river flow data is a significant impediment to understand water resources availability, and hydrological extremes. This is particularly true for remote, difficult to access, morphologically active and therefore rapidly changing rivers. The state of global river discharge monitoring with respect to water infrastructure and frequency of data collection has been on the decline over the past few decades. This is despite the significant importance of these data for river flow predictions (Moramarco and Ranzi, 2018). To save time, labour and costs the river discharge is commonly estimated by a rating curve, relating water level to river discharge. This method by which flow is monitored has not changed for over 100 years (Costa et al., 2000). The method consists of the installation of gauging stations on sites which record water levels through continuous observations, and relating these water levels to discharge through a water level – discharge relationship, also known as a rating curve. A rating curve is constructed by fitting a curve through a number of measurements of water level and discharge. Each measurement must be collected using physical observations of in-stream velocities and integration to flow, which in practice may be a tedious task. Figure 1.1 shows an imaginary rating curve indicating the problem of extrapolation beyond the range of observations, particularly for extreme flow conditions. Normally there are limited or no measurements under extreme conditions, due to flooding. This can result in inaccessibility of the area of interest or damaged equipment making it impossible to carry out measurements. Extrapolation is applied for extreme flow conditions, which can induce errors and uncertainties in the stage-discharge relationship.

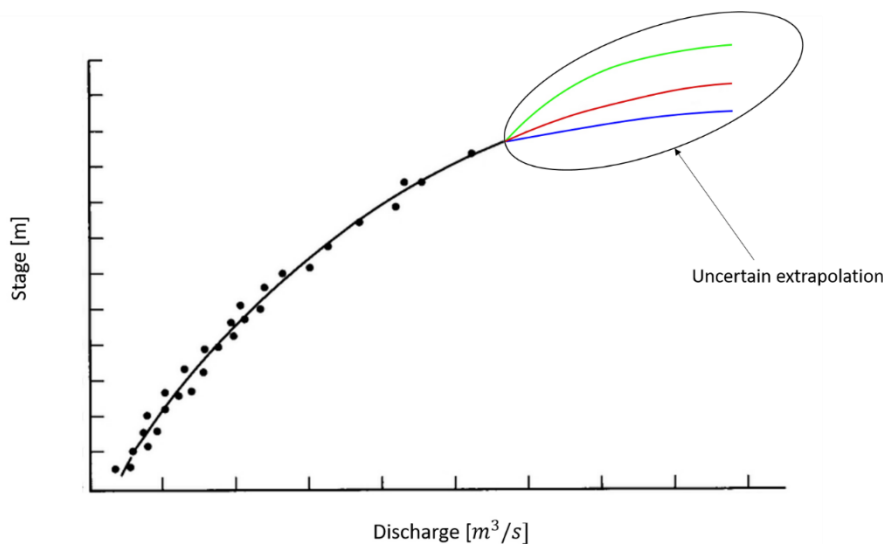


Figure 1.1 Imaginary Rating curve indicating the problem of extrapolation

Unfortunately numerous challenges have emanated from this labour-intensive and rigorous exercise. Some of the challenges include frequently changing flow channels due to soil erosion and deposition, vandalism of remotely located equipment, dangerous data collection conditions (e.g. wild animals, high

velocities, debris and flooding) and limited human and financial resources to manage large catchments. Consequently, the appreciation and willingness to adopt non-contact river monitoring techniques has increased tremendously. This is due to the benefits associated with minimisation of contact between survey personnel and measured variables.

Fortunately, advancements in technology have led to new opportunities in river monitoring for dam operators, water resources authorities, environmental agencies and scientists with limited financial capacities (Rafik and Ibrenk, 2001). These advancements have helped alleviate the dangers associated with data collection in potentially hazardous terrains. Key among these developments is the application of remote sensing instruments such as satellite derived data. To our knowledge, there are currently three remote sensing methods of estimating water level (Dobriyal et al., 2017). These are; (i) direct radar altimeter measurements of water surface level with respect to a common datum (Alsdorf et al., 2000), (ii) determination of water width and surface elevation through identification of the point of contact between land and water surface using high resolution satellite imaging, and (iii) satellite derived water surface area proxies (Revilla-Romero et al., 2014). Although all three remote sensing methods present significant improvements in earth observation for the purposes of river monitoring, by and large, they still fall short when dealing with more demanding spatial and temporal resolutions. For instance; freely available satellite data from Landsat 8 may not be able to detect river width changes in small rivers due to limitations in spatial resolution. Similarly, the impact of significant flood events which typically occur within minutes may be overlooked due to limitations in temporal resolution. Consequently, while satellite data is promising for larger rivers, their spatial and temporal resolution is not appropriate for small to medium rivers (Kim, 2006).

The demand for flow observation tools which can be applied at appropriate spatial and temporal scales has led to the application of low-cost Unmanned Aerial Vehicles (UAVs). The UAV collects overlapping images which are geotagged and subsequently merged together using photogrammetry (Skondras et al., 2022). The photogrammetric process in turn produces a number of outputs which include a digital elevation model (DEM). In addition to UAVs, there are other promising advances in technology in the form of smartphones and affordable yet very precise Global Navigation Satellite Systems (GNSS) positioning instruments. All these devices potentially play a critical role in the establishment of geometry for the purposes of flow observation using affordable and scalable methods. Estimation of discharge based on an observed geometrical property requires us to make use of empirical relationships between geometrical variables of the stream (width, water level, and wetted perimeter) and flow. An alternative approach is to introduce more physics in the equation. The physically based river rating makes use of the fact that river flow is a function of river slope, river-bed roughness and channel geometry, following hydraulic equations that prescribe mass and momentum of the water. One of the most commonly used equations is Manning's formula which is based on steady and uniform flow (Chow, 1959). From this, it follows that using a hydraulic model is an alternative strategy for flow

estimation from geometrical proxies (Mansanarez et al., 2019). In this instance discharge measurements of flow require information about the geometry of the channel in question and limited samples of flow (Costa et al., 2000).

1.2 Reconstruction of geometry/bathymetry for the purposes of river monitoring.

Hydraulic models may play an important role in river monitoring procedures. However, several different data inputs are required in order to calibrate, validate and implement hydraulic models. One of the most sensitive of these data inputs is the geometry and bathymetry of a river (Dey et al., 2019). The geometry is usually described in the form of Digital Elevation Models (DEMs). DEMs can be generated from a wide range of methods ranging from traditional ground surveying to remote sensing techniques applied to space- or air-borne imagery. Airborne-based Light Detection and Ranging (LiDAR) systems are capable of producing highly accurate DEMs (Liu et al., 2008). However, the data has limited spatial coverage and is expensive to acquire and process. In most cases, traditional ground surveying techniques are laborious, time inefficient, and potentially dangerous for personnel collecting the data (Samboko et al., 2019). Space-borne methods provide a non-contact, thus safer, alternative for surveying river terrains. The most common satellite-based topography data sources are the Shuttle Radar Topography Mission (SRTM) DEM and the Advanced Space-borne Thermal Emission and Reflection Radiometer (ASTER) DEM. For the purposes of hydraulic modelling, these data have also been treated in such a way as to represent bare earth terrain (Yamazaki et al., 2019). Unfortunately, there is a significant trade off which needs to be taken into account when applying satellite data for the purpose of river monitoring. Most freely available satellite-based terrain data sources such as ASTER (15m) and SRTM (30m) do not satisfy the required combination of spatial and temporal resolution necessary for accurate river monitoring. Consequently, while satellite data is promising for larger rivers, their spatial and temporal resolution is not appropriate for small to medium rivers (Kim, 2006).

It is within this technological gap that Unmanned Aerial Vehicles (UAVs) platforms equipped with cameras, continue to be developed and applied due to their relatively low-cost, high resolution and efficient application processes. Typically a consumer grade UAV is capable of mapping areas within 5 km range of the controller. However, most UAV regulations stipulate that the UAV must always be within line of sight. This regulation restricts the use to be range between 1 km and 3 km. The advantages of using UAVs are, (i) the portability of UAVs; ii) the option to self-design and modify integrated sensors; (iii) the availability of open source and user-friendly data processing software; (iv) and the collection of data in difficult to access terrains (Gindraux et al., 2017). UAVs, which operate at low altitudes, have a much higher spatial resolution than satellites. It is critical to note, however, that most UAVs come equipped with a consumer grade Global Positioning System which is not adequate to reproduce accurate and undistorted photogrammetric terrains. The implication is such that there is need to utilise Ground Control Points (GCPs) to correct the outputs of photogrammetry. However, the process

of GCP placement and measuring is notoriously laborious, time consuming and potentially dangerous in certain locations. Consequently it is useful to determine the optimal GCP number and GCP distribution necessary to reconstruct accurate elevation models.

1.3 River monitoring under ungauged conditions; justification of this study

Although these observations are useful, the continuous monitoring of rivers is jeopardised in many parts of the world by the absence or deterioration of gauging stations.

The scarcity of reliable river monitoring sites results in lack of operational records for e.g. flood forecasting, highly uncertain hydraulic models, used e.g. to assess and to manage water resources, design infrastructure or assess risks of flooding and lack of ability to monitor climate change (Sheffield et al., 2014). It is worth noting that flow is the sole integrating signal to measure the integrated effect of climate and land use change and therefore a crucial variable to monitor the effects of climate and land use change on the environment (Lamichhane and Shakya, 2019). Ironically, these data scarce river basins are exactly the areas where the need for hydrological predictions is high. To explain further; many ungauged regions are in developing countries. The limited resource availability associated with many developing countries means that there is a high level of vulnerability (UNDRR, 2015), i.e. the ability to recover from natural disasters/phenomena such as droughts or flooding is significantly compromised. This need for river monitoring culminates in a continuous search for innovative measurement techniques that are cheaper, require less human resources, and are easier to use with better accuracy than their predecessors.

Initiatives to advance flow predictions under ungauged or poorly gauged circumstances have been reported (Du et al., 2020; Hrachowitz et al., 2013; Kuzmin et al., 2019). A limited amount of research has been conducted in concrete applications to use UAVs in rating curve development. Firstly, an attempt made to develop an interconnected framework for establishing physically based remote river rating. This results in a stable and accurate flow estimation and it offers the potential to monitor river flow from space. The framework is investigated in a real-world relevant environment, so as to investigate the real-world challenges along with the scientific challenges. A suitable case study is the Luangwa River which is one of the major tributaries of the Zambezi basin in southern Africa. This river faces the typical challenges mentioned, i.e. remoteness, wide dimension, large seasonal variability, large morphological activity and dense wildlife activity. This study hypothesizes that advanced techniques can contribute and even improve efficient river flow monitoring.

1.4 Problem definition and research questions.

The water resources of poorly gauged river basins may be of strategic importance yet may be challenging in terms of data collection due to reasons such as poor accessibility, strong seasonal variability, and for

certain parts of the world, presence of large wild animals. Financial and physical resources are not the only challenge when it comes to data collection in areas of this nature; changes in river geometry also make it necessary to update stage discharge relationships through fieldwork more frequently than in other river systems. Remote sensing may reveal such rapid changes (Donchyts et al., 2016). These issues make it extremely important to investigate data collection methods which reduce the reliance on empirical relationships between flows and permanent flow proxy observations (typically water levels, but also wet area proxies or width with remote sensing, to eliminate or reduce the need for contact with water during surveys and permanent observations, and finally, to reduce the costs associated with such observations. In the case the Luangwa Basin, there are challenges with respect to a frequently changing water course due to volatile sandy soils, dilapidation of discharge monitoring infrastructure and limited resources to monitor the large basin.

This research mainly focused on the semi-arid Luangwa River in Zambia which is a large, poorly gauged tributary of the Zambezi in Sub-Saharan Africa. Here, accurate estimations of the water availability are important for water allocation planning especially during dry seasons (Hamududu and Ngoma, 2020), whereas reliable flow estimations are important for the management of the Cahora Bassa Dam downstream (Gumindoga et al., 2019; Winsemius, 2008). The Luangwa is also home to a wide range of resident and seasonal migrating animal species which require a safe and sustainable habitat. As a result, the Luangwa river basin is an interesting study region to analyse the added value of low-cost technological advancements to improve hydraulic model predictions despite the limited availability of ground observations similar to many other poorly gauged river basins in the world.

Hence, the main research question of this thesis is:

How can low-cost technologies be applied for accurate river monitoring through hydraulic modelling?

The research question is answered through several developments that are outlined below.

1. Development of an interconnected framework which clearly presents the steps which are necessary for river monitoring in remote locations.
2. Investigation if low-cost methods for data collection and processing, i.e. a combination of precise bathymetry points with low-cost RTK, and UAV photogrammetry, can be used to provide satisfactory quality elevation models for hydraulic models, quantified in hydraulic geometry characteristics.
3. To develop a method to derive a rating curve using affordable data collection methods and basic principles of physics. This involves the generation of a 3D hydraulic model using a combination of inputs that have been collected through low-cost methods and tools.

If we are able to tackle the 3 mentioned research areas, this opens doors to a new hydrological understanding of previously ungauged catchments through low-cost, high accuracy monitoring. It allows for optimal utilisation of the upcoming SWOT satellite mission as well as other satellite missions, but also low-cost readily available sensors such as cameras on smartphones, so as to ultimately monitor flows from space or locally without requiring contact with the water.

1.5 Thesis outline

The study area, motivation for its choice and description of hydrology and water resources is presented in Chapter 2. A description of the data sources used in this study and the way these are processed is given in Chapter 3. In the three following chapters, real cases are presented that show the integration of surveyed ground data with UAV and hydraulic model. Chapter 4 proposes a framework for monitoring volatile, dangerous and difficult to access rivers using only affordable and easy to maintain new technologies. The four main components of the framework are: establishment of geometry using airborne photogrammetry and bathymetry; physically based rating curve development through hydraulic modelling of surveyed river sections; determination of non-intrusive observations with for instance simple cameras or satellite observations; and evaluating the institutional and societal impacts of using new technology. Chapter 5 sought to compare open source and commercial photogrammetry packages to verify if water authorities with low resource availability have the option to utilise these without significant compromise on accuracy; assess the impact of variations in the number of Ground Control Points (GCPs) and the distribution of the GCP markers on the quality of Digital Elevation Models (DEMs), with a particular emphasis on characteristics that impact on hydraulics; and investigate the impact of variations in DEMs on flow estimations based on the number of GCPs used. In chapter 6, the rating curve based on a 3D hydraulic model is compared with conventional methods and an investigation is conducted on the impact of geometry uncertainty on estimated discharge when applied in a hydraulic model. Finally, an Investigation on how uncertainties in continuous observations of depth and width from satellite platforms may propagate into uncertainties in river flow estimates using the rating curves obtained is conducted. The thesis ends in an elaborate discussion and conclusions, summarised in Chapter 7.

2. Study Area

The study was conducted in Southern Zambia along the Luangwa River, downstream of the Luangwa Bridge. The Basin has a catchment area of approximately 160,000 km² which is about 10% of the Zambezi River Basin. The river originates in the Mafinga Hills in the North-Eastern part of Zambia and is approximately 850 km in length, flowing in South-Western direction (The World Bank, 2010). The river drains into the Zambezi River, shaping a broad valley along its course, which is well-known for its abundant wildlife and relatively pristine surroundings (WARMA, 2016). The basin is poorly gauged, mostly unregulated and sparsely populated with about 1.8 million inhabitants in 2005 (The World Bank, 2010). The mean annual precipitation is around 970 mm/year and potential evaporation around 1555 mm/year (The World Bank, 2010). The main land cover consists of broad-leaf deciduous forest (55%), shrub land (25%) and savannah grassland (16%) (GlobCover, 2009). During the dry season, the river meanders between sandy banks while during the wet season from November to May it can cover flood plains several kilometres wide.

For purposes of comparison, the specific location of the study site is only a few kilometres from the Zambia Water Resources Management Authority (WARMA) permanent gauging station. These sites may be considered similar in their hydraulic conveyance properties, given that they are geographically close to each other and their geomorphological characteristics are similar. *Figure 2.1a* shows the location of the basin within the administrative boundaries of Zambia. *Figure 2.1b* shows the location of the study site within the basin and *Figure 2.1c* shows the specific study site.

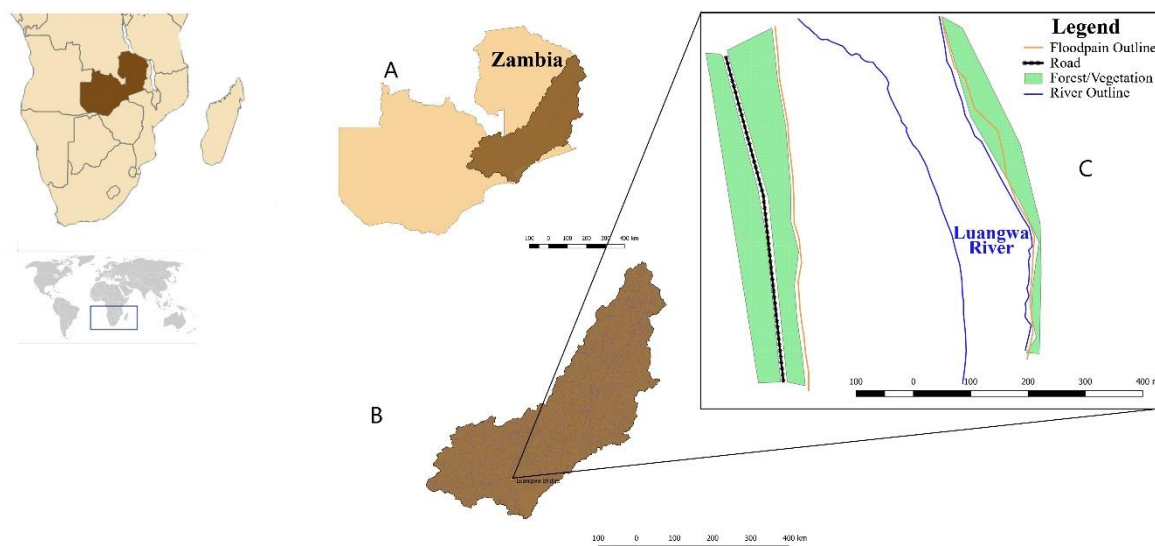


Figure 2.1 Study area a) Zambia b) Luangwa river c) river profile

2.1 Water Resource Management

A large majority of the Luangwa Basin falls within the jurisdiction of the Republic of Zambia and as such is governed under the Water Resource Management Act (Zambia, 2011). The Water Resources Authority of Zambia is the government institution which is tasked with management, development, conservation, protection and preservation of the water resources in the country. The sheer enormous size of the Luangwa makes it extremely difficult to maintain a reliable network of hydrological data collection stations. Vandalism and theft of valuable infrastructure makes the process of management expensive. Dilapidation of water infrastructure (weirs, canal, dams etc.) in the absence of repair and replacement funding further hampers efforts to sustain water works. Despite these considerable challenges, WARMA has a responsibility to manage and distribute water in a fair and equitable manner. There are many stakeholders involved in the allocation of water resources, ranging from small-scale local users (e.g. agriculture and fisheries) to large agricultural companies, copper mining and household use. The Luangwa River is one of the largest tributaries of the Zambezi River, which makes it extremely important for the management of downstream projects such as the Cahora Bassa hydropower station. The Cahora Bassa is the largest hydroelectric plant in Southern Africa (Sainz Sanchez, 2018). It currently produces 1,450 MW from the water passing through the five turbines. Consequently, credible information on upstream flows from the Luangwa is critical for dam management. The many stakeholders, combined with the extremes related to the semi-arid nature of the river basin, makes it a challenge to manage the resource appropriately (Winsemius, 2008).

Given that the Luangwa is one of the largest tributaries of the Zambezi, management, it play an important role in the management of downstream water infrastructure. For instance, Mozambique which is downstream of the Luangwa frequently experiences life threatening flooding (CDS, 2007). With better knowledge of upstream releases and response to rainfall in ungauged basins, the severity of these floods can be significantly reduced. Additionally early warnings can be issued to evacuate vulnerable persons and manage disasters more efficiently. The complex nature of challenges facing the Luangwa make it suitable for investigation into how flows can be estimated accurately so as to safeguard the interest of all stakeholders appropriately.

3. An inventory of flow estimation and its data sources

As the availability of data increases rapidly and data become more easily accessible, the capacity for responsible authorities to monitor flow has improved significantly. Even during the realisation of this thesis, many new data collecting technologies were introduced to users worldwide. Others are more experimental or classified and are only available through research centres. This chapter gives an overview of the most important data sources used throughout this thesis, and the way in which these may be applied in monitoring flow in poorly gauged basins. Firstly, a description of the traditional method of river monitoring is provided and some of the shortcomings of this method are stated. Thereafter, the more physical based river monitoring method is described. An outline of the application and continued improvement of survey instruments is then provided. The instruments that are described are the Acoustic Doppler Current Profiler (ADCP), Unmanned Aerial Vehicle (UAV) and the Real Time Kinematic Global Navigation satellite System (RTK GNSS). Finally, an explanation of the method of Large Scale Particle Image Velocimetry (LSPIV) and the technique of photogrammetry is provided.

3.1 Traditional river rating

Traditional river rating is based on the relationship between stage and discharge. In order to obtain a continuous record of discharge data, the river stage is recorded and the discharge is computed from the stage-discharge relationship. The discharge is then extracted from the stage-discharge relationship (Herschy, 2009; Luxemburg and Coenders, 2015). The power law function is the most commonly applied relationship for the approximation of the rating curve (Petersen-Øverleir et al., 2009). Equation 3.1 shows the power law function:

$$Q = a(h - h_0)^b \quad \text{Eq 3.1}$$

Where Q is the discharge [m^3/s], h is the water stage [m], h_0 represents the water level at zero flow [m] and a [m^{2-b}/s] and b [-] are coefficients, which are determined through curve fitting. In order to establish a reliable rating curve discharge measurements are carried out over a range of water stages. The lower and medium stages are usually relatively easily measured, because the area is still accessible and the river is not as wide as it can be. However, during higher stages there are challenges associated with flooding, turbulent water and poor access.

3.1.1 What are the limitations of the traditional method?

The main shortcoming of the traditional method is based on curve fitting (Strijker, 2017). In general, sufficient measurements during low or moderate flows are available, but little during peak flow conditions. In order to obtain discharge estimation for high flows the common practice is to extrapolate the curve. However, the process of extrapolation can induce errors and uncertainties within the rating curve (Petersen-Øverleir et al., 2009). This drawback was exemplified by Strijker (2017) who showed that the exponent b in Equation 1 has a minor influence on the rating curve for regular flow conditions, while under high flow conditions it can have a significant influence on the flow estimation. Limited observations in the extrapolation zone can result in an unreliable flow estimations, this is an important limitation of traditional river rating. Furthermore, the traditional method has a limited validity in time. Therefore the rating curve needs calibration as frequently as required by the rate of change in the stage-discharge relation (Luxemburg and Coenders, 2015). A list of factors that can cause changes in the relationship between water stage and discharge are presented below (Hersch, 2009; Rantz and Others, 1982):

- Degradation or aggradation of the river bed.
- Cross-sectional changes caused by growth and decay of aquatic weeds.
- Cross-sectional and river course changes after floods.
- Over-bank flow or spilling and ponding in areas adjoining the stream channel.
- Backwater effects due to obstructions or a confluence

3.2 Physically based river rating

Physically based river rating is based on integrating the river geometry into the power-law expression. River flow is a function of the river geometry, the river slope and the bed (Chow, 1959). The equations are derived from the shallow water equations. There are two commonly applied equations when it comes to physically based river rating. These are the Chézy and the Manning (-Strickler) formulas. These two equations are based on steady and uniform flow which assumes that the force of resistance cancels out the component of the gravitational force (Battjes and Labeur, 2014). The Manning's equation can be rewritten in the same form as the power-law function as shown in Equation 3.2:

$$Q = \underbrace{n^{-1}\sqrt{i}}_{X1} \underbrace{AR^{2/3}}_{a'(h-h_0)^b} \underbrace{a'(h-h_0)^b}_{X2} \quad \text{Eq 3.2}$$

Where the first part (X1) includes the bed roughness and the hydraulic slope, and the second part (X2) represents the geometry of a river also referred to as the conveyance (Note: $a=a'X1$). Using the physically based method means that the conveyance of the river can completely be described by the

geometry of a river section. It is important to note that the critical exponent b is thus completely determined by the geometry of the river bed, which is independent of the flow and can in principle be derived from an accurate DEM. The DEM reflecting river geometry can be measured in the field through aerial photography of the floodplains and by means of an ADCP for the part of the river under water. In this thesis both techniques are applied, more detailed descriptions of the methodologies will follow. The physically based method has the benefit of requiring less physical contact between the surveyor and the measured variable. This is significant for personal safety and time management which is otherwise required by the traditional method.

3.3 Surveying instruments

3.3.1 ADCP

An Acoustic Doppler Current Profiler (ADCP) is a hydro-acoustic current meter often mounted on a small boat or canoe that uses acoustic pulses to measure flow velocity over the depth of a water column (Figure 3.1a & 3.1b). The ADCP can determine the discharge using the velocity-area method and is a fairly accurate discharge measurement instrument (Mueller et al., 2013). However, challenges may be faced when required to operate during high flows, high sediment transport or when the water is turbid (Fiedler et al., 2009). During high flows turbulence may cause instability of the boat/canoe which in turn creates an unsafe environment for the surveyor. When the water is turbid, the ADCP may have difficulties penetrating towards the bottom i.e. the ADCP cannot measure the velocity close to the river bed. During low flow, the water is generally clear and these problems do not arise.

In this research the Teledyne RiverRay ADCP is used with a velocity profiling range up to 60 metres in combination with the accompanying software WinRiver II (WinRiver, 2001). An ADCP generally comes equipped with a consumer grade GNSS device to show its location. However in this study we forgo this GNSS device in favour of a more accurate RTK GNSS device in order to obtain precise locations.



Figure 3.1 a) ADCP attached to Canoe b) ADCP attached to motorised boat (Section 5.2.6 presents the method by which the ADCP was used)

3.3.2 Unmanned Aerial Vehicle (Drone)

An Unmanned Aerial Vehicle (UAV) is the collective term for all autonomously flying air-crafts. In this research the term refers to a drone. The UAV is equipped with a camera and deployed above the floodplain in order to collect images and videos for photogrammetry and surface velocity measurements. The particular UAV that is used in this thesis called a DJI Phantom 4 Pro (*Figure 3.2*) with a standard camera able to record in 4K resolution. The DJI Phantom 4 UAV has a battery life of approximately 27 minutes and can be operated within a range of 5 km. Furthermore, the UAV is equipped with a 64GB U3 SD card in order to have enough storage space and writing speed to record high quality videos at high frequency. The flight planning software which we use are Pix4DCapture and Drone Deploy.



Figure 3.2 DJI Phantom 4 UAV

3.3.3 RTK GNSS

In order to measure specific locations during fieldwork an accurate Global Navigation Satellite System (GNSS) is required. Most consumer grade GNSS devices are single-frequency (e.g. smartphones, ADCP, UAV) and have an average accuracy varying between five and ten meters (Schaefer and Woodyer, 2015). This level of accuracy is not sufficient for our research objectives. More accurate is a Differential Global Positioning System (DGPS). This special type of GNSS makes use of a fixed ground station (base) that sends corrections to a GNSS receiver used for the actual measuring (rover), this allows a DGPS to have an accuracy within the range of decimetres (Jiang et al., 2012). An even more accurate measurement, in the order of centimetres (or even millimetres for long-term measurements), can be achieved with Real Time Kinematic (RTK) GNSS. Like the DGPS, RTK makes use of a base station, a rover and the GNSS (Kim and Kim, 2022). However the difference is that the RTK uses phase differences of the satellite signals to correct the position instantly (both base and rover). The time between starting the base station and measuring with the rover determines in part the absolute accuracy of the measurements since the base will be able to determine its location more accurate over a longer time span (Peyret et al., 2000). Other factors are the distance between the rover and base, meteorological conditions, the line of sight between the receivers and the use of single or multi-band frequency. In this particular research both the Trimble DGPS and the low-cost RTK GNSS were used to record

measurements. The RTK GNSS has two SimpleRTK2B boards with u-blox-ZED9P modules (u-blox, 2021). These boards are able to convert multi-band signals with a centimetre level precision. The first board is configured as base station using U-center (related software, version 19.10) with the standard configuration file provided by u-blox. The second board is configured with the standard rover configuration file. The GNSS receivers are able to support GNSS, GLONASS, Galileo, and BeiDou. The connection between the base and the rover can either be made with a 4G network connection or with long range radio modules. The study area under investigation did not have 4G connectivity, therefore long range radio modules were applied.

3.4 Large Scale Particle Image Velocimetry

Large-Scale Particle Image Velocimetry (LSPIV) is an image based measurement technique used to visualize and quantify flow velocities at the free surface of a water body (Muste et al., 2008). LSPIV originates from Image Velocimetry (PIV), a technique that observes small scale displacement in a fluid based on recognizable features, so called 'tracers'. As opposed to PIV, LSPIV focuses on a larger observational area (e.g. a river surface). In order to determine velocity LSPIV determines the displacement between two or more consecutive images using a cross correlation function that can identify patterns of tracers within the images. First, each image is divided in several smaller areas called windows. Then a cross correlation function is used to search for tracer patterns in each window. It is possible to control the extent to which the function searches for tracers. When similar tracer patterns are identified, a displacement value for each window can be calculated. The resultant displacement is divided by the time difference of the two images so as to derive surface velocity. Thereafter the velocity-area method can be used to estimate the river discharge through the vector field of surface flow velocities (Le Coz et al., 2010).

3.4.1 LSPIV in its current state

A number of studies have explored the possibilities of LSPIV as a method of discharge measurement. For instance, a study by Le Boursicaud (2016) estimated discharges post-flood occurrence based on YouTube videos. Similarly a study by Fujita (2003) used images which were collected by use of a helicopter to estimate discharges. The use of a helicopter may come across as excessive, however it satisfies the basic requirement of LSPIV which are; the necessity of recording images from a high standpoint in order to cover the entire width of the river. There are several options which have been investigated for placing a camera at a high highpoint, e.g., a telescopic mast (Kim et al., 2008), a bridge (Armstrong et al., 2022) or UAV (Lewis et al., 2018b). At present the application of UAVs seems to be the most common practice (Lewis et al., 2018a; Lewis and Rhoads, 2018; Pearce et al., 2020). The causal factor seems to be the ease at which videos can be recorded at a nadir angle (vertically downwards). However, it is possible to record off-nadir though an extra processing step called orthorectification.

Orthorectification corrects the image from an off-nadir angle to a nadir point of view. This is implemented based on known positions which are called GCPs (Zhu and Lipeme Kouyi, 2019).

PIV techniques have been integrated into different software packages to aid in user friendly application. For instance, Fudaa-LSPIV is a freely distributed software package which can be used for surface flow estimation (Le Coz et al., 2014). Overall, LSPIV is now regarded as a reliable and broadly used technology to measure river surface flow velocity (Dal Sasso et al., 2021; Fakhri et al., 2020). However, there are still several limitations to its application which must be taken into consideration (Schweitzer and Cowen, 2021). The following are a selection of limitations applicable to this thesis;

- Measuring surface flow velocities of large rivers (i.e. large width) is challenging due to the trade-off between distance and camera resolution.
- Natural tracers are often neither available nor sufficiently distributed.
- Reflection on the water surface makes tracking difficult.
- Generally the surface velocity is directly linked to discharge with a velocity index or a log-function, this link often entails high uncertainty.

The first limitation is rather practical, natural tracers are generally too small to detect and seeding significant amounts of large tracers on a wide river is at least inconvenient. Attempts can be made to combine two videos recorded simultaneously so as to hover the UAVs much closer to the water surface. The second and third limitations are dependent on the river characteristics and weather conditions. These challenges can be overcome by proper location choice, seeding artificial tracers and recording at suitable moments. The final limitation is perhaps the most interesting or challenging. This challenge can be overcome by substituting the velocity-area method with a method that does not link the velocity directly to the discharge like a three dimensional discharge model.

3.5 Photogrammetry

(Stereo-) photogrammetry is the science of making measurements from photographs (Walford, 2017). This research makes use of aerial photography, where air photos are taken from an Unmanned Aerial Vehicle (UAV) using a highly-accurate camera. Overlapping photographs are used to identify common points on each image (Government of Canada, 2016; Pix4D, 2018c). A line of sight can be constructed, from the camera location to the point of interest. It is the intersection of those lines that determine the three dimensional location (x, y, z) of a particular point (Balogh and Kiss, 2014). This technique is called "structure from motion" and is used to create a 3D surface model and a highly-accurate digital elevation model (DEM). The DEM will be used to map the height differences of the floodplains of a river section.

4 Evaluation and improvement of remote sensing-based methods for river flow management

The application of remote sensing products for the purposes of river flow management has been on the rise (Chawla et al., 2020). Frequent changes in river geometry also make it necessary to update stage discharge relationships through fieldwork more regularly than in other river systems. Remote sensing may reveal such rapid changes (Donchyts et al., 2016). These issues make it extremely important to investigate data collection methods which reduce the reliance on empirical relationships between flows and permanent flow proxy observations (typically water levels), to eliminate or reduce the need for contact with water during surveys and permanent and finally, to reduce the costs associated with such observations. This paper sets forth research requirements that will lead to a framework for remote river flow observations, suitable for rivers that are difficult to access frequently, and difficult to equip with permanent water-borne instruments and applicable with little financial resources. We make a strong case for utilisation of Unmanned Aerial Vehicles (UAVs), which may eliminate the risk in dangerous and difficult to access places (Gustafsson and Zuna, 2017) and allow for rapid collection of geometrical data as well as calibration snapshots of flows and flow proxies in areas with limited direct accessibility to the stream. A limited amount of research has been done in concrete applications to use UAVs in rating curve development. We exemplify that the framework will work by relating these to a typical application environment, the Luangwa River, one of the major tributaries of the Zambezi basin. This river faces the typical challenges mentioned, i.e. remoteness, large seasonal variability, large morphological activity and dense wildlife activity. This study hypothesizes that advanced techniques can contribute and even improve efficient river flow monitoring. The ideal outcome is an interconnected framework which clearly presents the steps which are necessary for river monitoring in remote locations. We explain how each critical step is related to the other and how modern technologies are assimilated into the method. Section 4.1 describes an overview of currently practiced methods to observe flow or flow proxies using ground, contact or non-contact remote observations including satellite remote sensing. Section 4.2 introduces the selected illustration case, the Luangwa River. Section 4.3 describes our proposed flow observation framework. In Section 4.4, a summary of a number of research questions that need to be addressed to establish this framework is presented.

4.1 Inventory of flow observation techniques

4.1.1 In-situ flow observations for natural control sections

Despite the importance of discharge data for hydrological modelling, the number of monitoring stations has declined over the years (Shiklomanov et al., 2002). The traditional method by which flow is

monitored has not changed for over 100 years (Costa et al., 2000). River observations consist of three general steps: surveying in the classical sense whereby corresponding sets of discharge, and water levels, or other flow dimensions such as surface area or width in the vicinity of the site are recorded. These sets comprise an empirical relationship between flows and dimensions (also known as the “rating curve”). Through installation of gauging stations on site which record the proxy dimension and continuous observations are realised). In classical gauge sites, the dimension that is observed is typically the water level. Proxies of flow such as surface area and river width can also be recorded.

In order to determine discharge during the surveys it is important to record the water velocity across a cross-sectional surface. There are a number of methods that can be used to do this. These include floats, dilution gauging, trajectory, current meter and Acoustic Doppler Current Profiler (ADCP) methods. The float method only provides velocity at the surface and involves placing objects on the surface of a flowing water body at several locations within the cross section for a predetermined distance and consequently calculating the surface velocity (Gordon et al., 2013). This method is only suitable for small and straight streams (Hudson, 1993). The dilution method utilises the rate of diffusion of a particular tracer to determine streamflow (Comina et al., 2014). Inaccuracies can occur as a result of insufficient mixing. The method is therefore limited to relatively small and turbulent water bodies. It is difficult and impractical to use this method in large streams with discharge which is above 2 m³/s because a large amount of tracer is required to distinguish concentration differences properly, and full mixing may become problematic to achieve.

A study which was undertaken by Sentlinger (2019) applied the automated salt dilution method to estimate flows for larger discharges. In some situations it is difficult to obtain permission to insert tracers into water bodies due to risk of contamination (Moore, 2004). In the current meter method, the velocity is determined by assuming it as proportional to the rate of rotation of a rotor in a specified amount of time (Chauhan et al., 2014). This method has relatively high accuracy and time efficiency but requires that a sensitive instrument is brought into contact with water, compromising its use during high velocities.

The trajectory method involves diversion of streamflow into a pipe so as to estimate flow (Salguero et al., 2008). This can only be used in small streams where the flow is small enough so that it can be directed through a pipe (Liu et al., 2014). Finally, an ADCP, which transmits sound into the water, determines water particle velocity by calculating the differences in the frequency of the transmitted sound and echoes (Costa et al., 2006). Similar to the current meter, the ADCP is expensive, requires trained personnel to use it and must be used in contact with water. The ADCP is best utilised in large rivers with flat terrains (Flener et al., 2015). Similar to other contact-based methodologies, the ADCP may be difficult and dangerous to use especially when velocities are very high and debris is flowing through the stream’s section. In fact, all above mentioned methods have limitations in applicability,

especially during high flows since the surveyor and instruments need to be in contact with water during potentially dangerous conditions. Furthermore, the empirical rating curve method, typically requires quite a large number of points to collect and prepare the relationship, and are applied under the assumption that the relationship remains stable. Table 4.1 shows a summary of the different methods and gives a brief outline of some of the advantages and disadvantages of each method.

Table 4.1 Summary of advantages and disadvantages of flow estimation methods

Method	Advantages	Disadvantages
Float	Typically easy and quick to conduct.	Only suitable for small straight streams. Can be affected by weather conditions such as wind Requires contact with water. Large degree of uncertainty.
Salt dilution	Capable of determining not only velocity but total discharge.	Can be affected by lack of sufficient mixing. Only applicable in small rivers.
Trajectory	Very accurate as it collects total volume	Usually more difficult to conduct due to high resource requirements required to conduct the experiment. Permission to divert water required. Requires contact with water
Current meter	Easy to use. Relatively accurate.	Affected by location of measurement across the river cross section. Requires contact with water with a person in the water, or a construction.
Acoustic Doppler Current Profiler (ADCP)	Relatively accurate. Relatively fast to apply over large streams	Relatively expensive equipment. Cannot be used for shallow river channels (less than 1m)

When it comes to continuous observations, flow dimension observations (classically water levels) can be obtained with a pressure transducer in a stilling well or manual reading of a staff gauge. Lin et al (2018) was able to successfully test an automated water reading mechanism using single camera images pointed on a staff gauge providing efficient non-contact water level monitoring. Heusinkveld (2014) developed an application which uses a smartphone to automatically record water levels even when it is raining or when there is dirt on the scale. Besides water levels, it may be beneficial to record proxies of water level such as surface area and river width to identify changes in discharge.

4.1.2 Satellite observation methods

Besides ground or close to ground observations to observe continuous proxies for river flow, satellites may also be used to obtain proxies in large but difficult to access sites. There are currently three remote sensing methods of estimating proxies of river discharge (Dobriyal et al., 2017). These are; (i) direct radar altimeter measurements of water surface level with respect to a common datum (Alsdorf et al., 2000; Plant and Keller, 1990), (ii) determination of water width and surface elevation through identification of the point of contact between land and water surface using high resolution satellite imaging, and (iii) satellite derived water surface area proxies (Revilla-Romero et al., 2014). The first method utilised radar altimetry to derive water surface levels within acceptable accuracy standards (Bogning et al., 2018). This method is best utilised if we expect change in flow is particularly sensitive for changes in depth. The altimetry method is limited in spatial resolution by the specific overpass locations which may not coincide effectively with a user's point of interest. Altimetry is well placed to make use of the upcoming Surface Water Ocean Topography Mission (SWOT) (Biancam et al., 2016) which will present an even higher resolution and a much more robust temporal scale. The SWOT mission is designed to observe all rivers wider than 100m. The mission will observe all rivers regardless of nadir (camera/sensor looking vertically downwards) overpass. It will provide the very first discharge variations and river storage data in a globally consistent manner. The second approach can be applied using high-resolution imagery such as Sentinel-2 with spatial resolution in the order of 10m and temporal revisit time of at least 5 days. This method is however compromised by cloud cover, but can still offer many width estimates over non-clouded areas in high resolution imagery (Huang et al., 2018). A number of researchers have shown that satellite derived surface area in conjunction with appropriate ground data can be used to estimate river discharge changes (Bjerklie et al., 2005; De Groeve, 2010; Temimi et al., 2005).

The third approach makes use of the relationship between the surface area of a water body as viewed from satellites and flow. Bjerklie (2005) showed that empirical relationships between discharge and water surface area can be established. This can be done by establishing water surface and maximum channel width from orthophotos coupled with slope estimates derived from topographic maps so as to determine discharge. If discharge is particularly sensitive for changes in the floodplain inundation

extent, this implies that these two can be used interchangeably when it comes to monitoring flows (Zimba et al., 2018). This is the case to a greater extent in wide relatively flat terrain places like wetlands and floodplains. All methods require some form of a relationship between the observed satellite signal, and the in-situ flow. The relationship which is calibrated using ground data works best when the surface area co-varies most strongly with discharge. Satellite passive microwave sensors can be very useful due to their reduced impact from cloud cover in estimating river discharge and temporal revisit times (Brakenridge et al., 2007). Van Dijk et al.(2016) showed a strong correlation using a combination of optical, and microwave sensor inundation extent proxies (i.e. not actual surface areas) to determine river discharge of many rivers worldwide.

All these non-contact satellite-based monitoring methods have some disadvantages. Remote sensing is susceptible to the high reflective nature of trees in the visible and infrared section of the spectrum which can affect accurate estimation of water body surface area and width (Ward et al., 2013). Satellite based remote sensing however only show river variability (and either vertically or horizontally, not both simultaneously) and not river flow itself, always requiring in-situ information to achieve a flow estimate. A further limitation is the temporal resolution of most satellite data which typically has an inverse relationship with the spatial resolution. This means in the instances where relatively high resolution is required, there will be the limitation of having less observations per unit time. Remote sensing methods ultimately, cannot estimate discharge directly yet (Costa et al., 2000). Ground observations are required to make the translation into flow estimates.

4.1.3. The role of aerial photos and videos in river monitoring

UAVs and smartphones are much closer to the ground than satellites and therefore present an opportunity for non-contact monitoring at a much higher spatial resolution and at any time convenient to the user. This can help in taking efficient snapshots of flow and flow dimensions in areas that are typically difficult to access, and help translating remote sensing proxy observations into actual flow estimates (Bandini et al., 2017). Compared to other velocity estimation methods, a normal RGB camera UAV is priced at approximately 10% of a typical ADCP. Ordinary cameras on smartphones can also be used to record movies. In combination with Large Scale Particle Image Velocimetry (LSPIV) software and simple surveys, these can be turned into surface flow estimates (Tauro et al., 2016a, 2016b). LSPIV is made up of five main components: flow visualization, illumination, image recording, orthorectification and image processing (Muste et al., 2010). Despite needing validation due to the indirect nature of the method, LSPIV gives accurate readings in comparison with other methods (Hauet et al., 2008a). LSPIV methods have been developed to estimate water flow by focusing only on natural tracers, such as foam, ripples generated by turbulence and differences in water colour created by sediments or suspended solids (Beat et al., 2014; Kim, 2006). These new methods overcome the requirement for manual addition of tracers onto the water surface (Gustafsson and Zuna, 2017). The open source LSPIV software Fudaa-LSPIV provides a user-friendly method of surface velocity

estimation. The method is based on the LSPIV technique and the output includes surface velocity and combined with cross-section surveys, also river discharge using assumptions on the vertical velocity distribution (Jodeau et al., 2017). Topography and bathymetry of a river bed and floodplain can be constructed using photos acquired with an UAV using the process of photogrammetry.

4.2 Study area

In this section, the Luangwa Basin is exemplified as a typical location on which UAVs and other new technologies can be used to establish a flow observation site and data collection process. In addition to this, the site was also chosen due to the positive working relationship with the Water Management Authority of Zambia (WARMA).

The Luangwa river basin is pristine and the valley is well-known for its abundant wildlife (WARMA, 2016). Strategic locations for research are Luangwa Bridge, Mfuwe and Mulopwe village, as these are in close proximity to WARMA stations where results of our framework can be benchmarked. The site is relatively uniform in sediment type and channel form with easy access to the floodplain to observe Ground Control Points (GCP).

To exemplify the potential use of new observation sites, we refer to two use cases. The Luangwa's confluence into the Zambezi, is closely upstream of Lake Cahora Bassa, one of the largest hydropower schemes in Southern Africa. Rapid variations in inflows make it difficult to manage Cahora Bassa. Furthermore, near the outlet of this river (south of Luangwa bridge in Fig. 4.1), a large flood-prone area is located, making the river relevant to monitor upstream. For these reasons it may prove useful to predict

flows several days ahead in time near the outlet for humanitarian aid (Zambia Red Cross, personal communication) or for prediction of inflow variability (Cahora Bassa, personal communication).

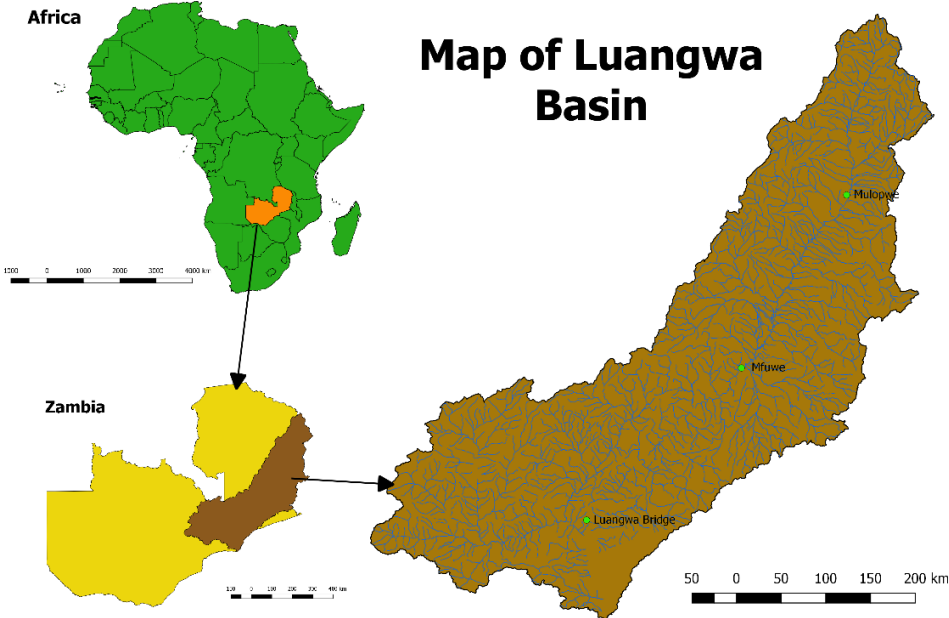


Figure 4.1 Study area map of Luangwa Basin

To this end, monitoring upstream flows is highly important, because a river gauge location in the upstream area (for instance Mfuwe, see Fig. 4.2) may provide significant skill for such forecasts. Fig. 4.2, shows the Luangwa River at Mfuwe in the dry season. The complex nature of the river is depicted by the branching of the river into different channels. The river channel shown in the figure primarily flows on the left-hand side of the river, however, it could easily be on the right or in the middle in the next season. This makes it difficult to setup permanent gauging infrastructure. Furthermore, extreme floods have repeatedly caused observation sites to get seriously damaged. The floods of 2019 washed away the stilling well and pressure transducers (Hulsman, personal communication). This makes it an ideal and relevant location to test the usability of UAV based flow estimation in difficult to access places.



Figure 4.2 Site Mfuwe - Luangwa River. Photo taken on November 6, 2018.

4.3 Flow estimation framework

In this section, we propose a framework, which combines all the elements necessary for river flow monitoring from surveying to the ultimate goal of non-intrusive monitoring with limited field assessment using novel and low-cost methods. Fig. 4.3 presents the framework. We propose that remote river flow observations entail the following 5 major steps: Step 1 which is node 1 defines requirements and possible benefits of site characteristics for our workflow. The site has to be a suitable compromise among some of the following aspects:

- The site should be relatively uniform in sediment type and channel form with accessibility to the floodplain to observe Ground Control Points (GCP).
- The site must be reasonably far from flow impediments like bridges to avoid backwater effects (similar to classical site selection requirements)
- A reasonable amount of accessibility to the permanent stream is necessary in order to conduct bathymetry cross-section observations or snapshot flow proxy observations.
- The stretch must be reasonably long enough to make slope estimates

Beneficiary characteristics include:

- A site may be selected where an altimetry satellite overpass is available so that altimetry heights can be used as flow proxy
- A site may be selected where the flow is particularly sensitive to increases in inundation surface areas, such as wetlands or floodplains. In this case satellite surface area, width or surface area proxies (see Section 4.2) can be used as permanent observation instead of water level instruments.

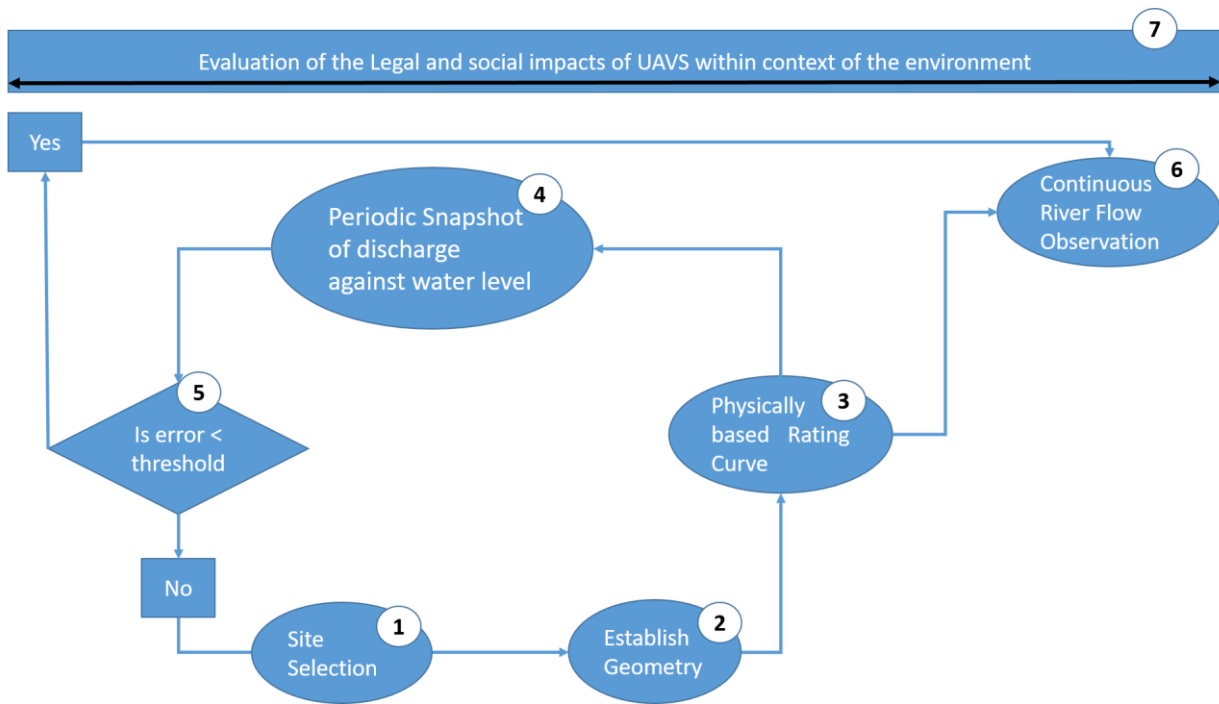


Figure 4.3 River monitoring framework.

It should be noted that site selection may also depend on the use case for the flow observations. Whether satellite proxies can be used strongly depends on this. For instance, for the forecasting use cases defined above, altimetry is not likely to provide sufficient coverage in time (once every 10–35 days approximately), as the likelihood of missing flood events is high. Other proxies such as surface area (from particularly passive microwave remote sensing) may be sufficient as these can be provided on a daily basis. For long-term water resources analysis, altimetry may prove a useful continuous observation as well. It should also be noted that the channel does not necessarily have to be entirely straight or uniform in shape as our rating relationship (further described in step 3) may also rely on a 2D or 3D physically based model.

Step 2, represented by node 2 on the framework diagram, involves, after site selection, establishment of geometry of the dry riverbed, floodplain and the wetted perimeter. In this step, a UAV, or other airborne platform such as kites, or balloons, is used to determine the geometry of a river reach using photogrammetry (see Section 4.4) in combination with sufficient sampling of Ground Control Points using a GNSS survey. For seasonal rivers, this is preferably done in the end of the dry season to maximise the visible area. An example of a point cloud captured in the dry season at Mfuwe is shown in Fig. 4.4. This survey took only one day with a team of 2 people to complete. UAVs should be employed with optimal flight conditions, using optimal settings and flight paths. These conditions and settings may be specific for the purpose of surveying a riverbed and therefore require investigation. The technique that is used to generate the geometry from UAV images is called photogrammetry.

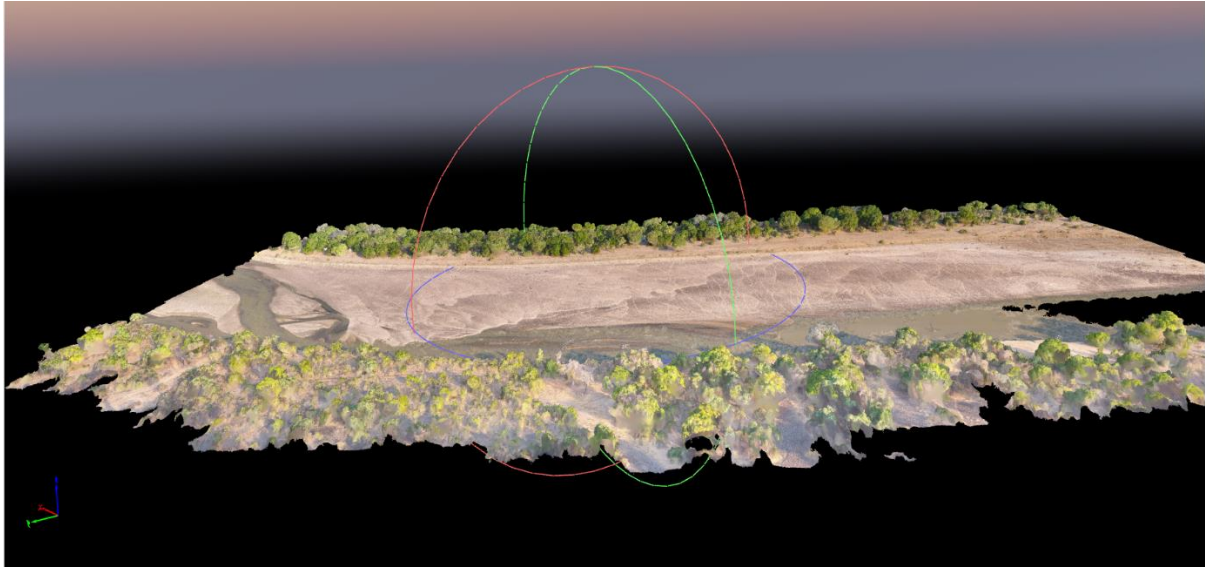


Figure 4.4 Point cloud of the Luangwa River at Mfuwe.

Photogrammetry makes use of these overlapping images to identify common points or objects on different images (Schenk and Quarter, 2005). There exists a line of sight between the location of the camera and the point of interest. The (x, y, z) coordinates are determined by the intersection of these lines of sight. Fig. 4.5 shows the Photogrammetric Process (Balogh and Kiss, 2014). Photogrammetry has been used by many different researchers to monitor rivers by establishing elevation models of river channels (Bird et al., 2010; Chandler et al., 2002; Lane, 2000; Westoby et al., 2012). Most of the monitoring has been for the purpose of assessing the hydromorphology of rivers. For instance, (2017a) used photogrammetry to assess river habitat and the hydromorphology, whilst Cucchiaro (2018) applied photogrammetry to assess the geomorphic effects of debris flow.

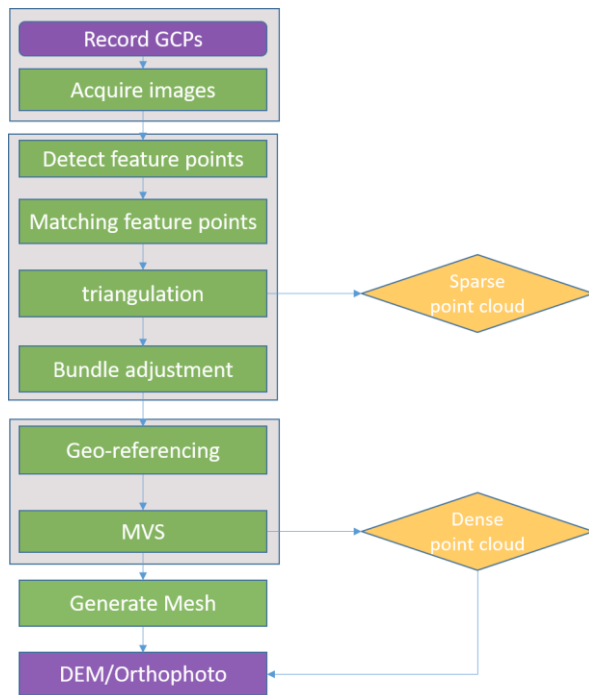


Figure 4.5 Photogrammetry process adapted from Balogh and Kiss (2014)

To our knowledge very little research has been conducted using photogrammetry to explicitly determine flows through hydraulic relationships. There are many different types of photogrammetry software available. The most well-known include Agisoft Photoscan (Metashape) (Jebur et al., 2018), Pix4D (Burns and Delparte, 2017) and the relatively recent package, OpenDroneMap (Burdziakowski, 2017). Of these three, ODM is the only photogrammetry package that is open source and free. For low-resource environments, it is of interest to determine if the output from this freely available software is similar to other relatively expensive commercial packages provided by Pix4D and Agisoft.

Areas which are constantly covered by the water may be compensated for, through use of simple methods such as point profile measurements using e.g. a rod with distance markers, or a Real-Time Kinematics GNSS equipment, attached to a long rod. The wet and dry geometry information needs to be combined into a complete and seamless terrain and bathymetry geometry. Validation of this method may be performed using real time kinematic GNSS surveys in the dry season and ADCP bathymetric surveys for under water spatial observations. In line with the aim to improve the quality of geometrical data, it can be argued that the high spatial resolution data collected from tools such as UAVs is an improvement on in situ surveys, but at specific locations, where GNSS survey point are taken, we can perform validation against these points as independent estimates of position and elevation. We will do this by leaving out several points from the DTM reconstruction process and keep these available as independent validation data.

Step 3 is a combination of node 3, 4 and 5 on the framework diagram and involves establishment of rating curves between flows, and proxies for flow such as classical water levels, surface velocities, width

or surface area, or a combination of these. To establish this relationship, we propose to utilize hydraulic simulations. There are 3 main methods of generating a physically based hydraulic simulation model, these are 1D (i.e. one-dimensional), 1D-2D (one-dimensional over the main flow direction, 2-dimensional in the floodplain) and 3D. Which of these 3 is to be used, depends on which proxy variable the user wishes to use to calibrate or validate the modelled relationship. For instance, if a user can collect total discharge (e.g. through an ADCP) along with water levels, and the river section is uniform enough (i.e. lateral transport is negligible) then a 1D model may be sufficient because a 1D hydraulic model can represent both water levels and integrated cross-sectional flow (Liu et al., 2014). If the channel section is more complex and/or the user cannot collect integrated flow but only surface velocities (for instance through LSPIV) or other surface proxies then a 3D model may be required, as a 3D model can represent more complex geometries, as well as surface variables such as velocity. Let us here assume a straight uniform section with moderately changing flow conditions so that steady-state conditions can be assumed. We also assume that the user can establish snapshot observations of cross-section integrated discharge and water levels at the same time. Under these conditions a simple 1D Manning's equation can be utilised to establish a physically based rating curve. It is simple and produces reliable results under the assumption that flow is steady and uniform (Herschy, 2009). The formula can be separated into two parts, roughness/slope constants and the conveyance. The conveyance part is attributed fully to the geometry of the river, i.e. it is in this case independent of roughness. This allows us to use a combination of UAV imagery and wetted profiles to establish a complete geometry in order to determine the conveyance. Manning's equation can be expressed as shown in equation 3.2

An estimation of slope can be established using the head drop in a saturated water hose or using GNSS equipment. The roughness may be estimated from a table which presents values of roughness against qualitative descriptions of those environments (Wu and Wang, 1999). In more complex environments the flow may not be steady or uniform, for instance when the direction of flow on the floodplain is highly unpredictable. Also, a user may want to rely on surface flow velocities to simulate cross-sectional discharge. These conditions require a 3D model application to simulate flow predictions in the x, y, and z directions, allowing for assimilation of surface velocities. The digital elevation and bathymetry model becomes critical in this application. Given that a low-cost drone can provide this information, a 3D model may be implemented in this case.

The combination of slope and roughness may be calibrated based upon field work snapshots, assimilated to the hydraulic model. This is done by collecting water level and discharge data or non-intrusive surface flow velocities within low, medium, high water regimes and comparing this snapshot data against the established hydraulic model to determine consistency and thus validity of the rating curve. When snapshots show that the observed flows or flow proxies cannot be matched against the observed water levels, widths or surface areas, apparently the geometry changed such, that a new geometry observation is required. The accuracy of this physically based method to establish a rating curve should be

investigated. Whether surface flow velocity estimates (e.g. through LSPIV) provide sufficient and certain enough information to calibrate the hydraulic relationships also requires investigation. For instance, the location of the illustration site (see Section 3) is in close proximity to already established Water Resources Authority of Zambia (WARMA) gauging stations. This allows us to compare the rating curves generated from the physically based rating curve developed here, with rating curves used by WARMA. Validation can be performed by generating a 95% confidence interval of the WARMA curve to establish if the physically based rating that has been modelled lies within limits in the range of the observations available. We will also investigate if the physically based rating curve is closer to existing rating points when only using relatively recently surveyed points as another form of validation. Our hypothesis is that in rapidly changing rivers, this will be true because the recent geometry is represented in the physically based rating curve.

Step 4 is represented by node 6 on the framework diagram. Continuous observation of one or more of the proxies for river flow is needed, either through a permanent instrument or satellite observations (dependent on the size and flow regime of the river). In order to be fully remote, a process of determining a permanent instrument such as a fixed camera or determining the most appropriate satellite-based monitoring method is required. If indeed a permanent instrument is to be used, we need to determine the location, orientation, data transmission method and applicability in the particular environment. In the case of satellite-based monitoring, a transfer model between the satellite view and what is visible on the ground is required. The decision to use altimetry or water surface proxies (e.g. from microwave remote sensing or optical methods) will be motivated by the expectation of a strong or weak relationship between changes in discharge against flow elevation (in the case of altimetry) or flow width (in the case of surface proxies). A combination of the two methods may be applied where a relationship is uncertain. This is to provide a proxy whereby the outputs of both methods should be within reasonable variation of each other. SWOT may provide key insights into the sensitivity of river flow to surface water level variations and surface extent variations. As SWOT observes both surface water level and extent at the same time, it may be used to translate other altimetry or surface extent methods into a continuous signal. The long-term observations of proxies of flow can be validated against in-situ observations. For instance, the surface area observed from satellite data can be cross checked against ground surveys or UAV surface area calculations.

Step 5 is represented by node 7 on the framework diagram. It is comprehensive analysis of the social and legal implication of using UAVs or other airborne methods is needed. As it stands, there are significantly different rules and regulations when it comes to utilisation of UAVs in different countries, and technologies also require different human resources. The reliance on UAVs of this workflow makes it important to determine how legal and social issues may impact on the framework's success. It becomes important to be able to confidently advice water managers and water authorities who intend on implementing this suggested framework. To address this questionnaires and interviews should be

conducted with users of the technology as well as related stakeholders (e.g. in Zambia, among others the Civil Aviation Authority, Wildlife Authority) to establish these social and legal implications, and conclude what is required for successful application of the framework.

Taking an all-inclusive look at the framework suggested, it is necessary to validate the hypothesis itself (“advanced techniques can contribute and even improve efficient river flow monitoring”). We will do this by conducting a pilot study and testing the hypothesis to establish the distribution of the responses which we obtain from the questionnaires and interviews and evaluating how this data deviates from the anticipated results.

4.4 Discussion

Through literature research, it is demonstrated that pieces of the puzzle have been laid that can be used to establish this framework. We identify that there are 4 general sets of specific research areas in need of analysis to be able to successfully implement remote river monitoring conclusively. These are related to the establishment of geometrical uncertainty, physically based rating curves, move from integrated direct, to non-contact proxies for determining flows, and finally, societal and institutional impacts of new technologies including UAVs. Here we identify the research questions in each area that require investigation in order to establish the framework for remote river observations presented in Section 4.3.

1. Which geometrical properties are important for flow estimation and how do uncertainties in these propagate into uncertainty of flows? This question requires experiments that identify what factors affect the quality of measurements of these properties. The factors are camera angles, flight height, light intensity, flight speed, and orientation with respect to the river channel, GCP formation and spread in the reach. Several flights with different combinations over a typical river and floodplain section must be performed to investigate the impact of these factors. There have been attempts to review UAV acquisition systems, orientation and regulation, (Colomina and Molina, 2014). There is need to go further and scrutinise hydrodynamic characteristics that need to be tested. These are, besides the overall terrain accuracy, the slope in the direction of flow and the shape of the cross-sectional area. Such experiments allow us to understand the best practices when it comes to photogrammetry with UAVs over river valleys, and will serve as a guideline for deployment.

2. How accurately can we establish rating curves by combining the generated geometry information with physically based hydraulic modelling? We anticipate that a hydraulic model, using the established geometry can translate continuously observed proxies for flow, including water levels, widths or surface water extents, into actual flows, by feeding such a model with boundary conditions of upstream flows across a wide range, and assess the resulting used proxy at surveyed cross-section locations. We will assess if this can be achieved with a 1-dimensional integrated model, which simulates integrated discharge estimates and uses water levels as continuously observed proxy. The model requires calibration against observed snap shots (during low, medium and high water) from e.g. ADCP

observations. We can then assess how uncertainties in the geometry propagate into uncertainties in flow estimation.

3. How accurately can we determine discharge using non-contact observation methods? Non-contact observations would alleviate the need to expose surveyors to dangerous, inaccessible river reaches and reduce the need for costly and sensitive equipment. Which seasonality factors may affect the output of measurement? To address this, we need to investigate if a hydraulic relationship can be calibrated based on non-contact surface observations only. This will allow us to replace the rather expensive and sometimes difficult to deploy ADCP or other intrusive observation methods, by a non-contact method such as LSPIV. It requires the use of a distributed 3-dimensional model (instead of 1-dimensional integrated) because surface flow velocities at specific locations in the vertical and horizontal must be evaluated and data on the surface assimilated. To this end, experiments can be conducted that only utilize the ADCP surface observations instead of the entire profile, and instead of an upstream boundary condition, assimilate these into a 3D model. Furthermore we can take advantage of the theoretical simulator proposed by (Hauet et al., 2008b). Finally, the impact of using less direct observations such as LSPIV-based surface flow on the rating curve, compared to traditional integrated flow estimates, must be investigated. The factors which may affect LSPIV results such as light reflection, tracer size and waves can be tested under varying conditions and using different tracer materials in time and space. Addressing question 2 and 3 requires taking snapshots using different observation methods at several moments during the season, traditional methods as benchmark, alternative observation such as LSPIV as test bed. The resulting rating curve can be evaluated against classical empirical rating curve points.

4. A final research questions relates to the socio-economical context: what skills and qualifications are needed by water authorities to adequately and effectively apply remote discharge observations. This concerns particularly the use of new technologies such as UAVs There seems to be resistance to use UAVs in most countries for many reasons which are mostly concerning security. What is the best strategy for water management institutions to induce a policy change to be granted permission to use UAVs in a manner which satisfies all parties involved? In what way can we make sure that water managers who are not familiar with new techniques can access training and what aspect of the institution must be amended to maximise adoption? What does the legal statute say about utilisation of UAV in these sensitive areas such as protected national parks? This also involves public opinion, co-design of use case development and appropriate licensing with aviation authorities, and social acceptance. The aim is to be able to fully advice all potential users of the implications. This part is fundamental in the sense that all the gains of the use of UAV remote river rating will not effectuate if certain aspects of the law, institutional requirements and social norms are not taken into consideration.

4.5 Conclusions (and recommendations)

There is indeed a need to design a framework specifically for monitoring flow in difficult environments such as our illustrative example, the Luangwa River in Zambia. The main principle is to utilize hydraulic

simulation of relationships between discharge and proxies for discharge based upon physics of momentum and mass balance, constrained by the observation location's geometry and roughness. This would allow for assimilation of any permanent observation of flow proxies into these hydraulic simulations, not just the classically observed water levels. This principle would also reduce the requirements for using a straight, uniform channel section as observation location. Although pieces of the puzzle are laid out in the scientific domain, there remain at least four main areas which we have identified as key to development of a holistic monitoring method and understanding its capabilities and accuracy. The first is in the area of mapping of the geometry of a river and its floodplains. We see low-cost UAVs as high potential, but there is no known (defined) flight method for surveying water bodies using UAVs. The unknown variables which can significantly affect the geometrical output, range from flight characteristics (application, altitude, speed, camera angle, light intensity, direction) to processing software settings. The second area of research emanates from the requirement to establish relationships (rating curves) between some continuously observed proxy for river flow and river flow itself. We propose that this is done through development of models which allow for non-contact or even space-based monitoring with occasional snapshots of both discharge and discharge proxies to validate if the geometry underlying the relationship is still accurate. The third aspect is in the snapshot observations. There is a knowledge gap how to assimilate non-contact surface flow observations (instead of integrated flow observation) such as LSPIV or satellite derived observations into the defined relationship, and how uncertainties in these observations propagate into uncertainties of flow estimates. In the case of large and extremely volatile rivers such as the Luangwa, non-contact observations may be easier to collect than contact observations. Advancements in affordable technologies allow for comparison of the available methods which best suits small budget water authorities. The fourth aspect concerns the context and environment of the user, for instance water authorities. To adopt this new framework, we require an evaluation of the social, legal and institutional implications of utilisation of new technology, in particular UAVs.

5 Evaluating low-cost topographic surveys for computations of conveyance

5.1 Introduction

Traditionally, flow measurements are performed through the use of current meters. A combination of measured depth and velocities across a profile can be integrated to calculate the total discharge. In order to attain continuous discharge data, river stage is recorded and plotted against corresponding discharge measurements to produce rating curves (Herschy, 2009; Mosley and McKerchar, 1993). Ideally, discharge measurements are carried out over a wide range of river stages. The low and medium river stages are usually relatively easy to record, whereas the high river stages are difficult as they are associated with dangerous conditions such as floods and inaccessible terrains. Peaks are also easy to miss, as deployment of personnel and materials takes time. Due to these difficulties, high stage discharge measurement is usually extrapolated from the rating curve. On the other hand, there is the risk of high variability in low flow measurements as a result of changing bed configurations, particularly in sand rivers which change every season. Measurements are usually taken at one particular point frequently despite physical changes in the profile. These problems lead to high levels of uncertainty in discharge estimates, which makes it difficult for water authorities to understand runoff generation processes, especially during high flows when management is mostly required (Petersen-Øverleir et al., 2009). Another limitation is the time validity of the measurements, which strongly depends on factors such as riverbed degradation, river course changes after floods, and overspill or ponding in areas adjoining the stream channel (Herschy, 2009; Rantz and Others, 1982). Changes in the geometry of the river due to these factors affect the rating curve output. Therefore, measurements may cease to be valid across time. Using a hydraulic modelling strategy has become an alternative for discharge estimation (Mansanarez et al., 2019). Physically based river rating is based on capturing geometry in a power-law expression. The physically based river rating makes use of the fact that river flow is a function of river slope, riverbed roughness, and channel geometry. In this instance discharge calculations of flow require information about the geometry of the channel in question (Costa et al., 2000). One of the most commonly used equations is Manning's formula, which is based on steady and uniform flow (Chow, 1959). The Manning equation can be rewritten as the power-law function as previously mentioned in equation 3.2.

The hydraulic geometry is a critical input in the production of rating curves (Zheng et al., 2018). Improvements in technology have allowed for a wide range of options for the establishment of geometry. These methods include survey equipment (levels, theodolites, differential GNSS), ground penetrating radar, and sensors mounted on satellites, aeroplanes, kites, unmanned aerial vehicles (UAVs), or hot air balloons (Feurer et al., 2008; Salamí et al., 2014). In general, manned aircraft which carry cameras are much more costly than other forms of image data collection (Yang et al., 2006). A low-cost means of

collecting geometry is through systematic capturing of images from one or multiple cameras mounted on an unmanned aerial vehicle (UAV). Advancements in technologies have resulted in the ability of surveyors to collect very high-resolution geometrical data in difficult-to-access places (Samboko et al., 2019).

The advantages of using UAVs are (i) the portability of UAVs, (ii) the option to self-design and modify integrated sensors, (iii) the availability of open-source and user-friendly data processing software, (iv) the collection of data in difficult-to-access terrains, and (v) the relatively low-cost of basic UAVs (Gindraux et al., 2017). UAVs, which operate at low altitudes, have a much higher spatial resolution than satellites and are not limited in temporal resolution. When used in combination with ground control points (GCPs), UAVs are capable of reconstructing dense and accurate terrains. Satellites with high spatial resolution usually have long revisit intervals. Only a very limited number of studies so far have used UAVs to collect data for hydraulic model purposes.

The application of UAV-based imagery for dry bathymetry reconstruction is relatively well practised and documented (Coveney and Roberts, 2017; Gustafsson and Zuna, 2017; Yao et al., 2019). Unfortunately, most low-cost UAVs with RGB sensors are incapable of mapping the geometry underwater. Given that many large rivers of interest are perennial, the common practice is to use subaqueous measuring tools such as acoustic Doppler current profilers (ADCPs) to determine the “wet” bathymetry of rivers (Vermeyen, 2007; Zedel et al., 2018). Depth profiling has become more affordable with recently developed low-cost echo-sounding devices, which are a viable alternative for typically high-cost ADCP devices. This was recently shown by Broere et al. (2021), who used a low-cost echo sounder to detect macro-plastics in streams. However, most ADCPs or echo sounders are equipped with consumer-grade GNSS instruments with 2m accuracy. This level of accuracy is unacceptable for accurate hydraulic modelling purposes.

The demand for both accurate and accessible measurements has driven the development of low-cost GNSS instruments (Glabsch et al., 2009; Poluzzi et al., 2019). Recent multi-frequency GNSS receivers are affordable (less than Euro 600), lightweight, and able to function in static and dynamic mode. They also act as accurate replacements for on-board consumer-grade GNSS instruments as they have been proven to be highly accurate and applicable as substitutes for traditional methods (Cina and Piras, 2014). A low-cost GNSS chip set (ZED-F9P) was released by U-blox in 2019. In this study the chip set is used on a breakout board of ArduSimple, type SimpleRTK2B. The set is uniquely capable of receiving corrections from both the L1 and L2 bands (U-blox, 2021). Research conducted using the SimpleRTK2B GNSS set has confirmed its ability to produce results comparable to accurate geodetic measurements (Hamza et al., 2020, 2021).

Apart from the impact of instrumental (GNSS, ADCP, and UAV) inaccuracies on hydraulic geometry, there are more factors to consider for conveyance calculations. These factors can be divided into three

groups: (i) pre-flight (UAV, flight application, flight path, and site selection), (ii) flight settings (camera angle, direction, velocity, altitude, light intensity, wind speed, overlap), and (iii) post-flight processing (photogrammetry software, camera lens distortion, GCP configuration, and slope). There have been a number successful attempts to review and evaluate best practices for pre-flight and flight settings of UAV acquisition systems, orientation, and regulation (Abou Chakra et al., 2020; Chaudhry et al., 2020; Seifert et al., 2019; Yao et al., 2019). We proceed by evaluating the four constituents (photogrammetry software, GCP configuration, camera lens distortion, and slope) of post-flight processing which are important for accurate reconstruction of hydraulic geometry.

Firstly, the post-flight processing of UAV-derived imagery is largely and increasingly facilitated by “structure-from-motion” (SfM) photogrammetry software. It offers image processing workflows which are easier to work with than traditional photogrammetry techniques. SfM-based approaches have been successfully used in various applications such as soil and coastal erosion and lava emplacement (Castillo et al., 2012; James and Robson, 2012; James and Varley, 2012; Smith et al., 2015). Unfortunately, SfM photogrammetry requires software which is usually available at a cost beyond the reach of most researchers and other interested parties. Some of the more common software packages are (commercial) Pix4D, Metashape meta-soft, and (non-commercial and open-source) OpenDroneMap (ODM). Several researchers have made some comparisons between the commercially available software (Alidoost and Arefi, 2017; Grussenmeyer and Khalil, 2008; Probst et al., 2018). ODM is an opensource software which can be used to generate digital elevation models and other photogrammetry results. Not only does the non-commercial nature of ODM make it more accessible to researchers and practitioners with limited resources, but it also presents an opportunity to tweak and investigate the impact of individual variables on the output (Burdziakowski, 2017).

The second aspect of post-processing which is important for hydraulic geometry is the GCP configuration. Similar to ADCPs, UAVs are equipped with a consumer-grade GNSS with an accuracy of 2 m. This means that all UAV-based images and outputs of photogrammetry have a maximum error of 2m (Udin and Ahmad, 2014). For the purposes of hydraulic modelling, this inaccuracy is unacceptable; therefore, the application of GCPs is paramount. A number of studies have investigated the number and distribution of GCPs necessary to generate accurate elevation models (Awasthi et al., 2020; Bandini et al., 2020; Ferrer-González et al., 2020; Rock et al., 2011). However, studies have not gone as far as to investigate how to adjust the number and distribution of GCPs specifically for the purposes of modelling flow in hydrodynamic conditions. For instance, the specific impact on hydraulic geometry of GCP proximity to a flowing river is largely unknown. This particular information would be handy for water managers who aim to survey the dry and wet bathymetry of a river using low-cost technologies.

The third aspect of post-processing which is important for hydraulic geometry is camera lens distortion. Investigation into camera lens distortion can be traced as far back as 1919 when A. Conrady developed the decentring distortion method (Conrady, 1919). Based on the decentring model, Brown developed the Brown–Conrady model (Brown, 1971; Clarke and Fryer, 1998). There have been a number of improvements and modifications to the Brown–Conrady model with respect to different applications (Beauchemin and Bajcsy, 2001; Ma et al., 2003; Shah and Aggarwal, 1996). Despite tremendous improvement in terms of reduced distortion, some DEMs show systematic broad-scale deformation, which is known as the “doming effect” (also known as the “bowling effect”) (Javernick et al., 2014; Rosnell and Honkavaara, 2012). The doming effect emanates from inaccuracies in modelling the radial distortion of camera lens (Fryer et al., 1987). This fundamental drawback makes it difficult to fully exploit the potential of SfM products in many situations such as gradient-sensitive applications, e.g. rainfall runoff and slope estimation. Some guidelines for avoiding the doming effect have been outlined (James and Robson, 2014a). A novel method which aimed at correcting the doming effect was presented by Magri (2017), who iteratively applied a planarity constraint through a bundle adjustment framework. The results were encouraging as they concluded that it was possible to mitigate the doming effect through manipulation of the bundle adjustment process. Bundle adjustment is a technique for calculating the errors that occur when we transform the x–y–z location of a point in the environment to a pixel point on a camera image.

Documentation from ODM suggests that making use of a configuration called the fixed camera parameter (FCP) can help reduce the doming effect (ODM, 2021). The FCP turns off camera optimisation while performing bundle adjustment. This is because in certain circumstances, particularly when mapping linear (low-amplitude, limited features) topographies, bundle adjustment performs poor estimation of distortion parameters (Griffiths and Burningham, 2019).

Finally, in order to estimate flow based on the Manning’s formula, it is important to accurately measure the slope of the terrain. Similar to hydraulic geometry, there is growing interest in non-contact methods of estimating slope. Common methods of slope measurement require accurate point data measured using GNSS and geodetically based methods. It is possible to extract elevations from photogrammetry outputs and derive slope; however, the accuracy of this method is largely unknown. Ultimately, the factors (photogrammetry software, GCP configuration, lens distortion, and slope) which affect hydraulic geometry can be evaluated in terms of their impact on discharge or flow proxies such as conveyance. A study was conducted by Mazzoleni (2020) on the potential for using UAV-derived topography for hydraulic modelling. The study concluded that these topographies extracted from UAVs presented results comparable to LIDAR and RTK-GNSS-based topographies. However, it did not accurately measure the permanently wetted bathymetry of the river. Rather, the study mechanically filtered out the river, which brought about some uncertainty. A similar study which investigated the impact of the number of GCPs on flood risk model performance concluded that UAVs could successfully be used for

data collection as long as a minimum number of control points were utilised (Coveney and Roberts, 2017). Nevertheless, the study was located in a large city and thus did not include the measurement of inundated areas, nor did it focus on the ability to reconstruct typical hydraulic properties.

The practical utility of accurate hydraulic geometry for flow estimation is unquestionable (Gleason, 2015). However, there is minimal research on how the factors which affect the accuracy of geometry can be adjusted to improve the quality of elevation models in hydrodynamic environments and when applied for the ultimate purposes of discharge estimation. Furthermore, earlier contributions did not put the focus on the ability to reproduce hydraulic geometry characteristics and did not focus on the entire bathymetry (including the permanently wet riverbed section). Hence, this paper investigates if low-cost methods for data collection and processing, i.e. a combination of precise wet bathymetry points with UAV photogrammetry, can be used to provide satisfactory quality elevation models for hydraulic models, quantified in hydraulic geometry characteristics. In this paper, a novel and practical method of correcting the doming effect using data collected using a low-cost GNSS mounted on a mobile cart is applied. The methods are tested on the Luangwa River in Zambia.

This paper is organised as follows: Sect. 5.2 describes the methodology and gives a brief outline of what materials were used in the study. In Sect. 5.2.1 we describe the study area (Luangwa Basin). Furthermore, the methodology section outlines how flow estimation was determined and software packages were compared. Furthermore, Sect. 5.3 presents results and a discussion of the results. The conclusion is Sect. 5.4, which presents a conclusion and recommendations for future studies. The following research questions are investigated and a determination of whether the said factors have a significant effect on the accuracy of results is made.

1. Can the freely available (open-source) ODM software package produce results that are comparable to commercial packages such as Agisoft Metashape?
2. What is the optimal GCP number and GCP distribution necessary to reconstruct accurate elevation models?
3. What impact do elevation models, reconstructed based on different GCP numbers, have on hydraulically simulated conveyance and hydraulic slope?

5.2 Materials and methods

This section first describes the data collection procedures, including flight plan, collection of ground control points, and dry and wet bathymetry. Then it describes which experiments are conducted to investigate our research questions.

5.2.1 Study site

The study was conducted along the Luangwa River, south of the Luangwa Bridge. A detailed description of this study site has been provided in section 2 and 4.2.

5.2.2 Data acquisition: Low-cost GNSS equipment

In 2019, U-blox launched the ZED-F9P chip capable of receiving satellite signals in the lower and upper bands (L1 and L2) from the BeiDou, Galileo, GLONASS, and GPS constellations.

The ZED-F9P chip was integrated with an Arduino simpleRTK2B board, which can function in RTK mode, produced by ArduSimple. The board can transmit or receive Radio Technical Commission for Maritime Services (RTCM) corrections and can be configured by the user using U-center, a freely available open-source software (U-blox, 2021). The simpleRTK2B set is low-cost (receiver EUR172 and patch antenna EUR50 at the time of writing) with the possibility to acquire <1 cm level precision with base rover and <1 cm level precision with RTCM corrections. The exact accuracy depends on multiple factors including the antenna used, the satellite reception quality and amount, the accuracy of the base station surveyed location, and the baseline distance. Long-range radio antennas were used to communicate RTCM messages. Figure 5.1a shows the SimpleRTK2B base and rover used to measure marker points. Figure 5.1b shows the simple RTK2B setup on-site. At the initial stages of configuration, the board was connected to a laptop which also provided a power supply and data storage through a USB port. Upon realisation that a laptop would not be able to supply power for a prolonged period of time in harsh fieldwork conditions, it was replaced with two 20 000mAh power banks and a Raspberry Pi. The time between starting the base station and actually beginning to take measurements using the rover has an impact on accuracy; i.e. an extended time period results in better results because the base is able to survey its location more precisely over time.

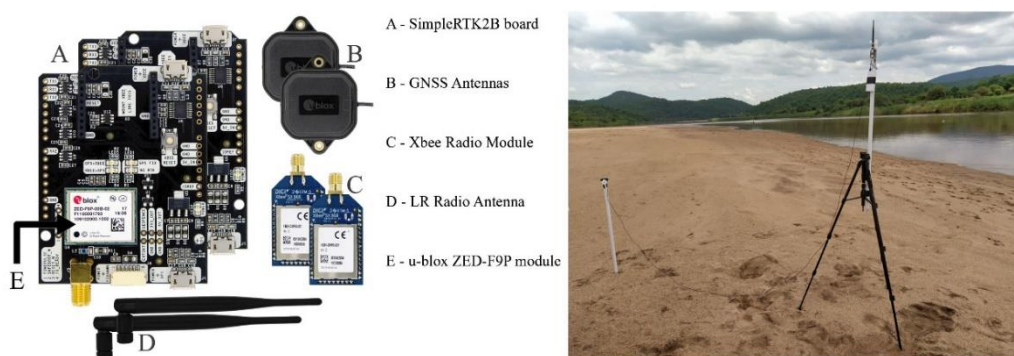


Figure 5.1 (a) RTK GNSS set and (b) RTK GNSS base station setup along the Luangwa River floodplain.

5.2.3 Flight plan

GCPs were recorded using RTK GNSS equipment on a 1 km long floodplain. Flights were conducted at two different heights (90 and 100 m) at a constant speed of 10 m/s, with a 10° camera angle used to optimise on 3D reconstruction results. The two flight patterns were separated by 20° from each other so

as to limit the effects of image lens distortion. The side and forward image overlap was set to 80 %. Figure 5.2 shows the flight paths of the two patterns which were flown. The UAV used is a DJI Phantom 4 Advance with a 12 Megapixel FC330 RGB camera with a focal length of 3.61 mm. A flight planning android application called Pix4D Capture was used to control the autonomous flights. This application was chosen due to its capability to tilt the camera forward during the image capturing process, which is important to capture more depth information than when using a nadir-looking configuration. The coordinate system was set to the WGS 84, UTM zone 36S (EPSG::32736).

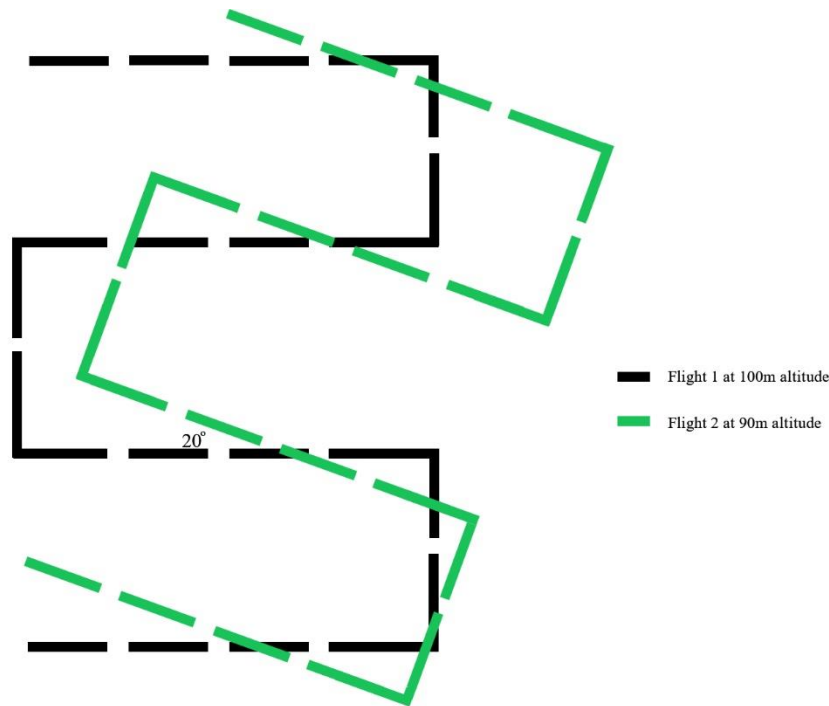


Figure 5.2 Flight paths flown at two different heights (90 and 100 m)

5.2.4 Dry river bathymetry

In order to refine the camera calibration parameters and to optimise the geometry of the output, GCPs have to be used. The dry bathymetry data collection can be divided into two procedures: placing the GCPs on the ground and collecting the images. A total of 17 GCP markers were placed on the floodplain, with some being closer to the road, others more in the middle of the dry floodplain, and the rest closer to the waterline. Figure 5.3 shows the location of the GCPs in relation to the floodplain. The GCPs were placed on one side of the floodplain because the other side was steep and covered with dense vegetation. An effort was made to make sure all elevation variations were covered by the placement of GCPs. This was achieved through a basic GNSS-based inspection of the terrain; the difference between the highest point on the terrain and the lowest was calculated and divided into 17 elevation levels. Taking the elevation levels into consideration, the 17 GCP markers were strategically distributed within an area of 25 hectares. A 2–1–2 formation was applied as practically as possible. The markers were 40 cm by 40 cm in dimension and had an alternating black–white colour. Different GCP numbers and combinations

were tested for two different experiments. The first experiment with the objective of determining if open-source software could perform as well as commercial software used 3 GCP numbers in a 2–1–2 formation. The 2–1–2 formation is sometimes known as the “checkerboard” method; it is a relatively common method of distributing marker points on a terrain. The GCP numbers used in this experiment were 5, 9, and 13. The second experiment with the objective to determine the impact of the number and distribution of GCPs used 5 GCP numbers and two different formations. The GCP numbers used in this experiment were 0, 5, 9, 13, and 17 GCPs. In the instance in which zero GCPs were used, we adjusted the calibration setting to FCP (see the Introduction, Sect. 1) to establish if this would improve results in situations when no GCPs are available. Both the 2–1–2 and the linear biased formations were used in the second experiment. The phrase “linear biased” distribution refers to a method of marker distribution whereby the markers are placed in a relatively straight line on one side of terrain. In this case, the markers were either closer to the river or further away from the river.

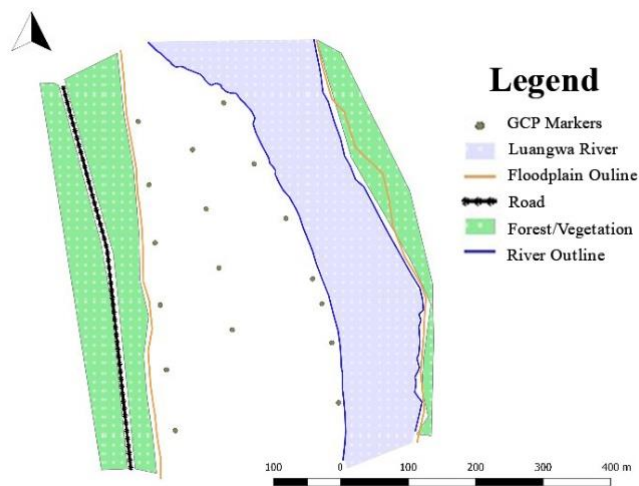


Figure 5.3 Spatial distribution of 17 GCPs on the floodplain.

5.2.5 Wet river bathymetry

The Luangwa River, similar to other large tributary rivers of the Zambezi, is perennial, meaning that the bathymetry of the river needs to be measured under flow conditions. The wet river bathymetry was recorded using a combination of an ADCP and RTK GNSS. The GNSS of the ADCP was not used in favour of the RTK GNSS for improved accuracy. The RTK GNSS was mounted directly onto the ADCP sonar beam, whilst the ADCP was attached to a canoe rowed by local fishermen, as shown in Fig. 5.5b. The ADCP and the RTK GNSS were configured to take measurements at 1 second intervals. The canoe moved from one side to the other in a zigzag manner and tried as much as possible to reach the edges on both sides. The GNSS crossed the river 21 times, and a total of 3102 measurements were recorded. The programme suitable for the particular ADCP, Winriver II, was used for real-time data collection. For the purposes of interpolation, the canoe was manoeuvred along both sides of the river. The river, however, was shallow, especially on the right bank; this means that it was not possible for the canoe to

adequately move close to the waterline. To capture the slope, the RTK GNSS was mounted on a wooden cart and towed manually along the waterline. An image of the cart is shown in Fig. 5.4a. The waterline tie line was subsequently used as the true value reference to enable establishment of the level of deviation of the ODM and Agisoft values.



Figure 5.4 (a) Low-cost RTK GNSS rover mounted on a mobile cart for recording RTK waterline 5 and (b) ADCP combined with an RTK

5.2.6 Processing the dry and wet bathymetry

Images taken by the UAV were collected and fed into the ODM and Agisoft software. The images were processed locally on a Dell Core i7 eighth-generation machine with 32GB of RAM. These computer specifications meet the requirements and fit the description of a “basic configuration” (Agisoft, 2021). The same settings were applied in the processing steps as far as was permissible. Figure 5.5 outlines the steps which were taken in the production of the point cloud and DEM. The first stage shown in Fig. 5.6 is fieldwork. As with all other images, aerial photographs are optically distorted. In order to correct these distortions, geometric corrections had to be made. These distortions are caused by the camera optics, the topographical relief, and the tilt of the camera (Verhoeven et al., 2013). One of the most effective ways to correct distortions is to make sure that accurate GCPs are recorded and applied. Over and above the traditional GCPs, an RTK waterline was measured so as to monitor and correct any potential systematic broad-scale distortion (doming effect) which may not have been dealt with by the GCP marker points. The second stage of the dry bathymetry processing is facilitated by Structure from Motion (SfM). The constituents that make up SfM commence with detection of feature points. This is the first step in many computer vision and photogrammetry applications. Despite the existence of approaches which detect edges, ridges, and regions of interest, the image features utilised in most SfM approaches are interest points (IPs). IPs can be defined as the most outstanding locations on an image which are also surrounded by a distinct texture. The following step matches the IPs from one image with the IPs from all other images; the algorithm has to determine which IPs are 2D representatives of the same 3D points. The process of determining the 3D location of interest points using views from different images is called triangulation. The triangulation step requires knowledge of the interior and exterior orientation of images, and the output is a sparse point cloud in a local coordinate frame. The final step in SfM, which optimises the sparse 3D structure and the projection matrices simultaneously through a robust iteration,

is called bundle adjustment. The third stage commences with the application of a coordinate reference system (geo-referencing) to the model. This step is necessitated by the inherent scale ambiguity of the SfM output. This is to say that if the sparse 3D structure is scaled by an arbitrary value and the distances between the camera's positions are simultaneously scaled by the same factor, then the structure will remain the same. The two main methods are either to import at least three well-distributed GCPs and transform the complete model or to import at least three accurately known camera positions or GCPs and use them as constraints during bundle adjustment (Barazzetti et al., 2012). The next step is multi-view stereo (MVS), which facilitates the creation of a dense point cloud. This MVS algorithm uses information on the orientation of images to compute a dense structure. This is possible because the outputs are pixel-based as opposed to feature-point-based. The final stage facilitates the creation of a digital elevation model (DEM) and the orthomosaic. The orthomosaic is important for visualisation of the terrain at a high resolution. This makes it possible to calculate the RMSE of GCPs, which would otherwise be difficult to identify. The processes summarised in Fig. 5.6 (third block until the last block) were repeated four times with different sets of GCPs each time (5, 9, 13, 17 GCPs) for both software packages. The Agisoft software version 1.5.1 reconstruction took approximately 9 h to process each set of images, whereas ODM took 2 h.

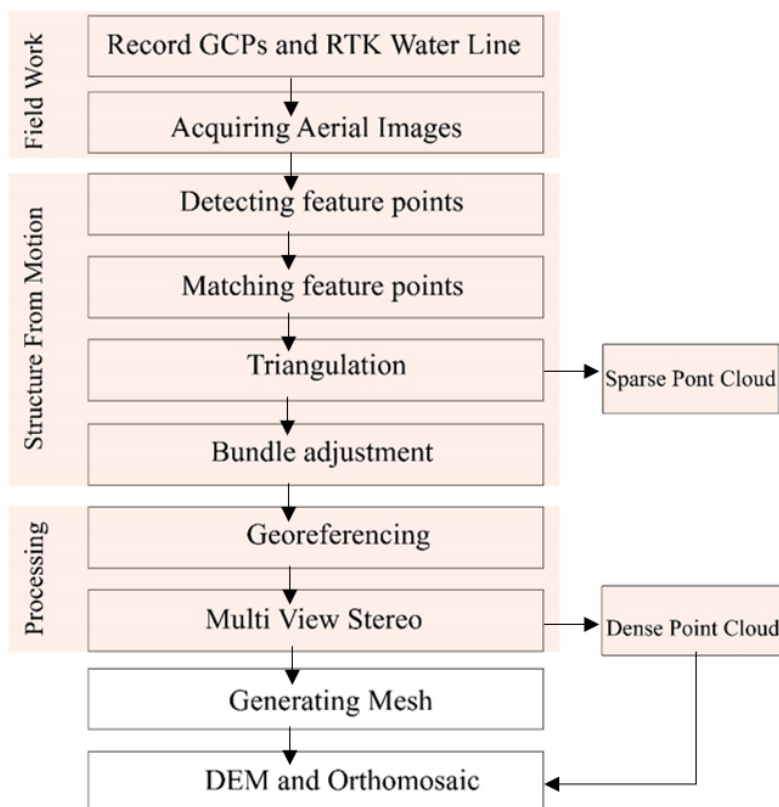


Figure 5.5 Photogrammetry process from image collection to reconstruction

The wet river bathymetry point cloud is then processed. Each measurement point taken on the river consists of the attributes depth (measured with the ADCP), latitude, longitude, and height (measured with the RTK GNSS). The depth measurement is subtracted from the water height to acquire the bed

level and combined with the longitudinal and latitudinal coordinates. Before the wet bathymetry is merged to the dry bathymetry, the wet river transects have to be volumized. This process entails conversion of the sparse point cloud made of transect points into pixels through linear interpolation with the nearest non-empty cell. In order to obtain the full bathymetry of the river, the dry bathymetry and the wet bathymetry are merged together in the software. In occurrences whereby there are overlaps or edges it is chosen to treat these through linear interpolation as well. After merging, three cross sections perpendicular to the river were extracted such that a relationship between area and perimeter could be established over the entire cross section, including both wet and dry bathymetry.

5.3 Reconstruction experiments

5.3.1 Impact of the processing software used

A relatively simple experiment to judge if ODM can be used as a viable alternative to proprietary software was employed. The experiment sought to validate the accuracy of open-source software versus commercially available software by comparing ODM (open-source) with Agisoft Metashape (commercial), respectively. The availability of GCPs made this possible. We considered the root mean square error (RMSE) of checkpoints. RMSE metric is widely employed as a measure of conformity between two DEMs (Alidoost and Arefi, 2017). If the RMSE values are of comparable nature when comparing one package against the other (magnitude, distribution, presence of outliers), then they perform similarly. To calculate these RMSE values, only reference points not used in the reconstruction were made use of; this allowed for an independent estimation made by both software packages. The RMSE was computed using Equations (5.1) and (5.2) in the horizontal and vertical direction, respectively:

$$RMSE_{xy} = \sqrt{\frac{1}{n} \sum_{i=1}^n (\Delta X_i^2 + \Delta Y_i^2)} \quad (5.1)$$

$$RMSE_z = \sqrt{\frac{1}{n} \sum_{i=1}^n (\Delta Z_i^2)} \quad (5.2)$$

Where ΔX_i = residual of the i^{th} value in the x axis

ΔY_i = residual of the i^{th} value in the y axis

ΔZ_i = residual of the i^{th} value in the z axis

n = number of check points (GCPs that were not used in the reconstruction)

DEMs based on 5, 9, 13, and 17 GCPs were exported from ODM and Agisoft. The DEMs were fed into the Geographic Information System (GIS) QGIS, and a point sampling tool was used to extract elevation values at the corresponding coordinates of the GCPs that were not used in the reconstruction.

This ensured that an independent estimate of the RMSE could be established. A bootstrapping experiment was conducted on the errors of the individual GCPs that were used to calculate the RMSE. This experiment was performed to test the stability of the RMSE. In the experiment random samples of error were drawn from the 5, 9, and 13 GCPs. The sampled errors, which were equal in number to the available GCPs, were sampled with replacement to obtain new RMSE values. The process was then repeated for 1000 drawn sample sets. Given that this first experiment led to the conclusion that ODM is a satisfactory choice and it is free and open-source the remaining experiments were only conducted with ODM.

5.3.2 Impact of GCP placement and density on accuracy

This experimental objective was divided into two parts. The first was to establish the impact of GCP density on DEM accuracy. The second part was to establish the impact of placing GCPs further from or closer to the flowing river. In both instances a comparison of absolute error was made with the RTK tie line, which was acquired using the RTK GNSS mounted on a mobile cart. The Python package Rasterio was used to extract elevation values at corresponding coordinates. For the first part, elevations from the DEMs with 5, 9, 13, and 17 GCPs were extracted and compared to the RTK line elevations. For each reconstruction, the maximum number of checkpoints available were used to verify the results. The total number of GCPs used in each reconstruction and checkpoints was always equivalent to the total number of GCPs available (17). The reconstruction with 5 GCPs had 12 checkpoints, the 9-GCP reconstruction had 8 checkpoints, the 13-GCP reconstruction had 4 checkpoints, and the 17-GCP reconstruction essentially had zero checkpoints available. The exact same GCP numbers and distributions were used for the reconstruction in both Agisoft and ODM. Figure 5.6 shows the locations and particular markers which were selected for each set of GCPs. The GCPs were placed in a 2–1–2 formation, which took into account the range of elevations as much as possible.

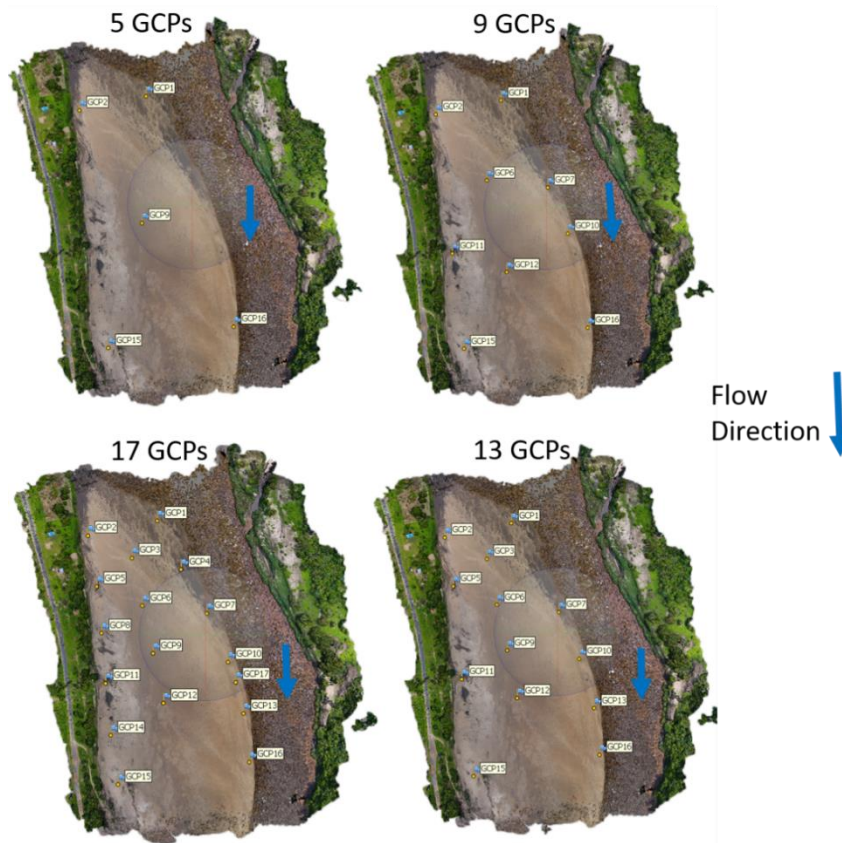


Figure 5.6 GCP marker distribution closer to and further from the river as well as the wetted river perimeter measured during the survey,

For the second part, many studies have indicated that photogrammetry is incapable of adequately mapping a flowing river because it reflects light (Bandini et al., 2018; Dai et al., 2018). The noise generated on the river surface has a negative impact on the overall accuracy of the DEM. In order to establish the significance of this noise, elevation extrapolations from the DEMs constructed using 9 GCPs closest to the river and 9 GCPs furthest from the river were compared. The GCP markers are placed in linear biased manner parallel to the RTK reference line. Figure 5.7 shows the positions of the GCPs placed further from and closer to the river. The figure also shows an orthophoto to be able to identify the river's water surface and other features such as the vegetation on the natural levee of the river's floodplain.

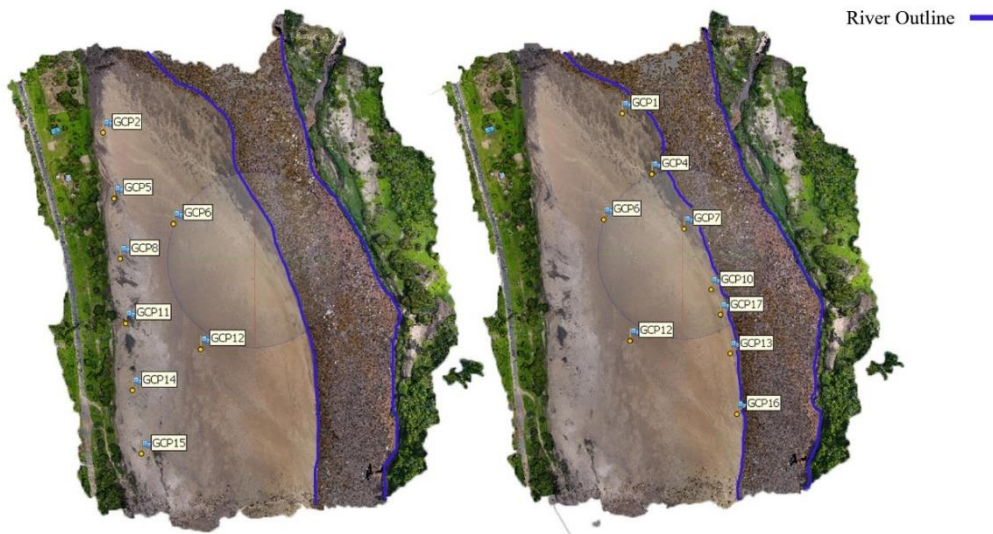


Figure 5.7 The location of the cross sections which were extracted from the respective reconstructions.

2.3.3 Impact of DEM variations on hydraulic conveyance

An investigation was conducted on how variations in DEM reconstruction choices impact conveyance characteristics. Conveyance versus depth relationships over several cross sections in each DEM created is determined. This was done for all the elevation models generated using a different number of GCPs so that the established relationships could be compared. Figure 5.8 shows the location of the cross sections which were extracted from the respective reconstructions.

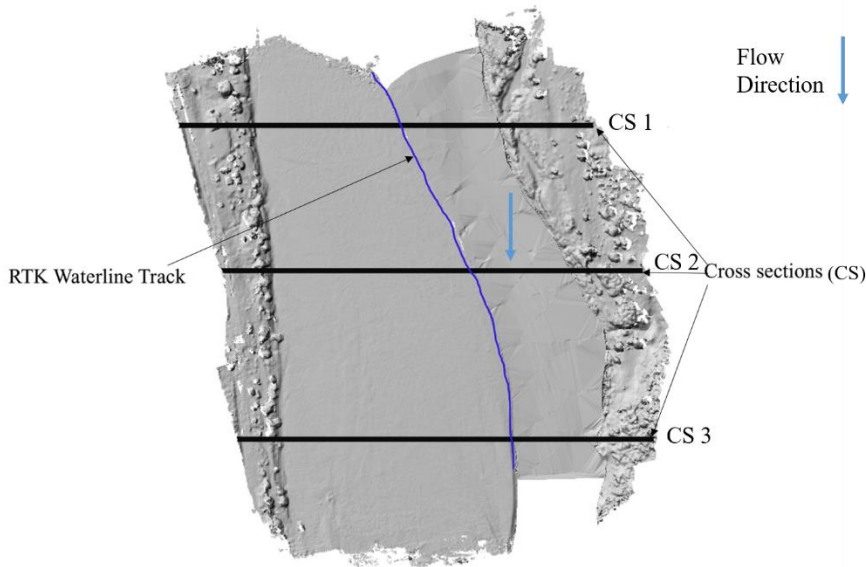


Figure 5.8 The location of 3 cross sections (CS1, CS2 and CS3)

In addition, DEM-derived hydraulic slope is compared with an independent estimate of slope using the in situ RTK GNSS tie line (see Sect. 2.2.3 for a description of the acquisition method). The first method calculated slope entirely based on an independent reference tie line. In order to attain the actual elevation values, the heights of the cart and the container were subtracted from the height measurements. The plot consists of 898 measurement points with a standard deviation of 0.018 m. A regression line was plotted

through the data and the waterline slope was determined to be 0.000230. A plot of the regression line is shown in Appendix B3. The second method involves the extraction of the slope from the terrain outputs produced by the photogrammetry process. The sample method of the Rasterio library in Python has been used. This method sampled the closest point to every coordinate in the RTK track. Thereafter, a regression line was fit through the various elevations so as to determine the slope of the various photogrammetry outputs. The outputs were then compared, taking the slope derived from the GNSS as the true value.

5.4 Results

In summary, the assessment of the impact of processing methods on the quality of terrain data, focussing on geometry of hydraulic properties, consisted of three steps: applicability of open-source versus proprietary photogrammetry software, the impact of GCP density and placement on DEM quality, and the impact of variations in DEMs on conveyance and slope. In this section, results of these three steps are presented.

5.4.1 Impact of the processing software used

In order to assess the applicability of open-source software the RMSEs of terrain models processed in ODM were compared with those from Agisoft Metashape. The results are presented in Table 5.1.

Table 5.1 RMSE of different GCP combinations

Configuration	Agisoft		ODM (m)	
	Horizontal RMSE [m]	Vertical RMSE [m]	Horizontal RMSE [m]	Vertical RMSE [m]
5 GCPs	0.415	0.594	0.686	0.592
9 GCPs	0.259	0.290	0.406	0.344
13 GCPs	0.300	0.395	0.431	0.380

The results indicate Agisoft RMSE values that are comparable to those calculated when ODM was used for reconstruction. The two software products generally follow a trend whereby increasing the number of GCPs from 5 to 9 results in a notable decrease in RMSE. A further increase from 9 to 13 GCPs results in an increase in RMSE. This result is counter-intuitive; however, given that the error was calculated based on GCPs which were not used in the reconstruction, it follows that increasing the number of GCPs

simultaneously decreased the sample size available for error calculation. A reduced sample size meant that outlier error values may well result in a poorer resultant RMSE. In general, the RMSE values of Agisoft and ODM were similar; however, the sample size of data used to calculate the RMSE was not large enough to provide statistical confidence. To that end, a bootstrapping experiment was conducted to establish if there was a significant similarity in the performance of ODM in comparison to Agisoft (see Sect. 2.3.1). The bootstrapping experiment is particularly appropriate for small sample sizes and data sets which do not necessarily follow a normal distribution (Freedman, 2007). The results of the bootstrap experiment are presented in Fig. 5.9.

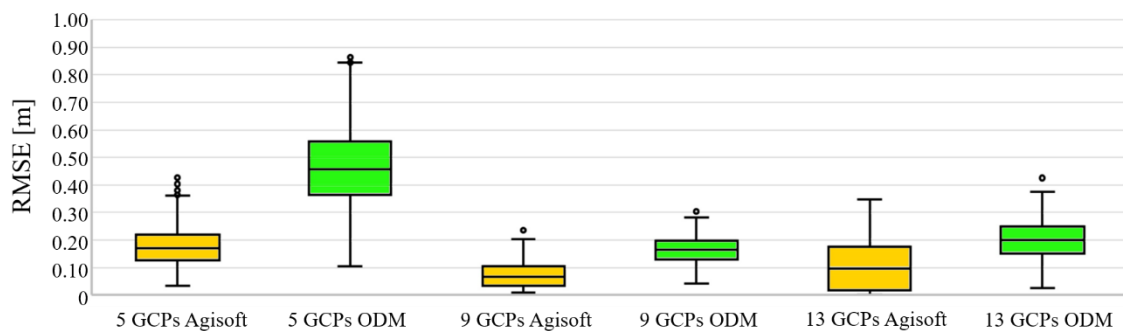


Figure 5.9 Bootstrap Box plot experiment comparing the performance of ODM against Agisoft for varying number of GCPs.

Using 5 GCPs, there is a relatively large difference between the RMSE of Agisoft and ODM. This difference is attributed to the inherent capacity of Agisoft to perform better than ODM in instances in which there are few control points. The graph suggests that, out of the selected number of comparisons, 13 GCPs is the optimal balance between GCPs that correct the reconstruction and checkpoints to calculate the RMSE. The representation indicates a strong resemblance between errors in ODM and Agisoft. The overlapping box plot in the 13-GCP configuration affirms the comparability of the products. However, a notable downside of ODM is indicated by the RMSE, which is twice that of Agisoft. Despite this downside, the absolute RMSE is limited to less than 0.20 m, which is acceptable for the purposes of merging with wet bathymetry. The results confirm the potential application of open-source software as an alternative for commercial options without significant compromise on accuracy. Accordingly, the remainder of the results are processed and analysed based on the ODM software package.

5.4.2 Impact of GCP placement and density on accuracy of hydraulic features

The aim of this investigation was to assess the impact of variations in the number of ground control points (GCPs) and the distribution of the GCP markers on the quality of DEMs, with particular emphasis on characteristics that impact hydraulics. Five different GCP numbers (0, 5, 9, 13, and 17) and two specialised settings (Brown–Conrady and fixed camera parameter) were compared. An observation of a dome-like deformations in all of the elevation extractions. This phenomenon, known as the doming

effect (also known as the bowing effect), is exemplified in Fig. 5.10. The effect is apparent despite attempts to avoid the aforementioned phenomena through deliberate flight practices such as a 10° camera angle and a 20° alternating flight path.

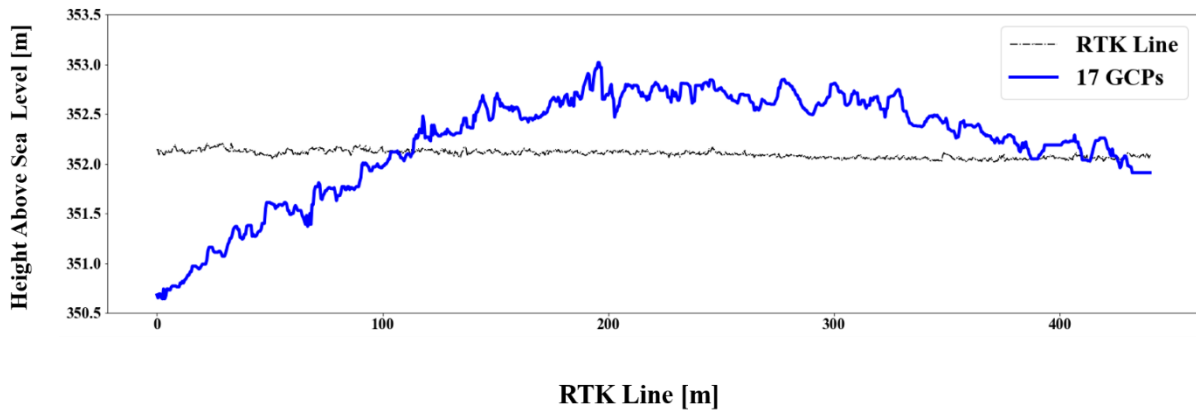


Figure 5.10 The doming effect visualised through comparison of elevation levels extracted from the RTK line vs. elevation values extracted

A rather practical approach was used to correct for the doming effect. A first-order polynomial was fitted through the RTK GNSS track. A second-order polynomial was then fitted through all the reconstructed point clouds. The error was then determined by calculating the absolute difference between the two polynomials for the given length. The respective clouds were divided into 1500 s from north to south whereby every point within each section was assumed to be deformed by the same elevation value. The absolute errors were then applied as corrections to the point clouds depending on which section each location fell in. Figure 5.11 shows corrections made to the reconstruction based on 5 GCPs. Appendix B shows the corrections which were performed on all other terrain models. The assessment was conducted based on the RTK waterline track, and the results are presented in Table 5.2.

Table 5.2 RMSE of different GCP combination and configurations

Configuration	RMSE _z [m] Based on RTK track
5 GCPs	0.558
9 GCPs	0.581
13 GCPs	0.486
17 GCPs	0.479
FCP	0.618

The results indicate a decrease in the RMSE as the number of GCPs is increased. However, the incremental benefit of increasing the number of GCPs beyond five becomes smaller as more control

points were added to the reconstruction. Noticeably, the RMSE derived based on the GCP checkpoints was similar to that which was obtained based on the RTK waterline as a reference. This implies that the RTK waterline track is a potential substitute when calculating the error in a photogrammetry reconstructed model. The RMSE values derived from the “no GCPs” and from using the Brown–Conrady configuration showed significant inaccuracy and were therefore rendered inapplicable. However, the fixed camera parameter (FCP) configuration performed reasonably well (RMSE 0.618 m), considering no control points were used. A bias is identified in terms of the errors calculated when GCPs are closer to or further from the river. Similar to the aforementioned experiment, the RTK track was used as a reference. The RMSE is less when GCPs closer to the river (approximately 20m away) are used in the reconstruction than when GCPs further away are used. The hypothesis is that the GCP distribution used in the experiment “closer to river” is such that GCPs are placed much closer

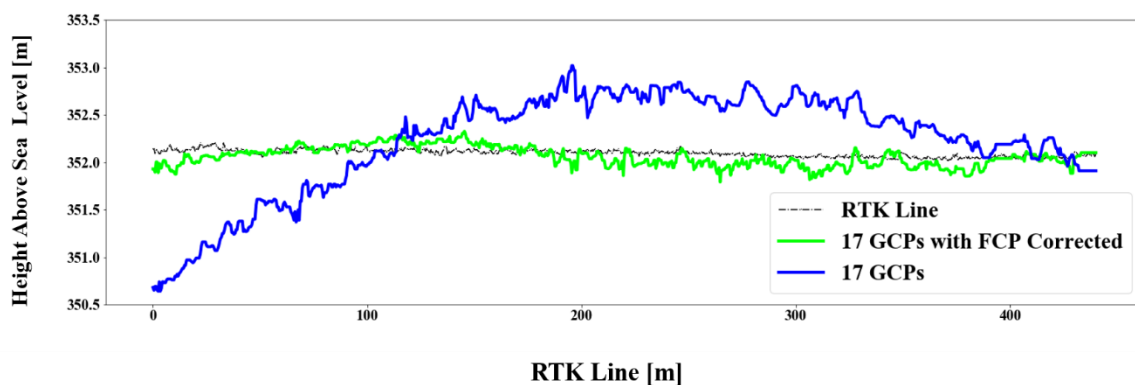


Figure 5.11 A visualisation of the effect of correcting the doming effect.

5.4.3 Impact of DEM variations on hydraulic conveyance and slope

Hydraulic conveyance was computed from the merged dry and wet bathymetry. A comparison of the hydraulic conveyance across various reconstructions is performed. Furthermore, the hydraulic slope of the various reconstructions is compared with an independent slope estimate measured from an in situ RTK GNSS tie line. In order to extract the cross section elevations, the full bathymetry of the river had to be utilised. Figure 5.12 is a visualisation of the process of generating a volumized wet bathymetry from separate components. The wet river point cloud, shown in Fig. 5.12, covers 555 m of the river length and consists of 5 164 points. The latitude and longitude originate from RTK GPS measurements, whereas the height component is determined using both RTK GNSS and an ADCP as described in Sect. 2.2. The maximum and minimum height of the point cloud are 352.20 and 348.45 m, respectively. The dry river bathymetry is constructed using photogrammetry and RTK. The various point clouds represent an area of approximately 679 551 m². Like the wet river, each point contains a latitude, longitude, and height component with a maximum and minimum height of 383.4 (hill in the south-east corner) and 350.2 m, respectively.

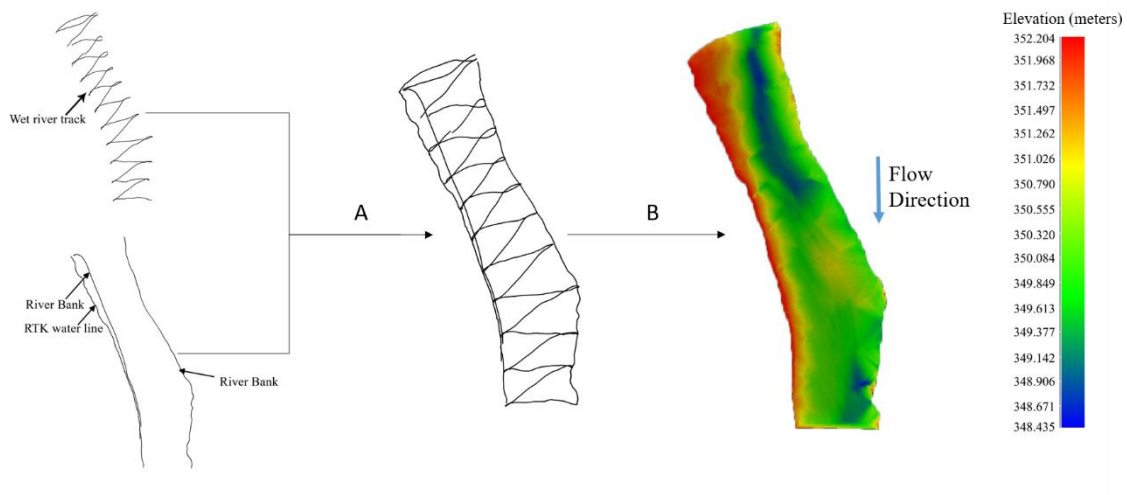


Figure 5.12 Wet bathymetry processing (a: merging the wet bathymetry transects which were measured using the ADCP with the RTK line)

In order to extract the cross sections, the dry and wet bathymetry had to be merged and subsequently volumized. These two processes that were conducted in Cloud Compare are exemplified in Fig. 5.13. Figure 5.14 shows an extraction of the cross section on the northern side of the terrain model (CS1). The GCP configuration with 5, 9, 13, and 17 GCPs present very similar cross-sectional properties. The results are similar for all cross sections (Appendix B4). The configuration with no GCPs and Brown–Conrady significantly underestimated the actual height by approximately 13 m. In an attempt to improve the results when no GCPs are available, applied fixed camera parameters were applied. The FCP results showed a significant improvement, and the shape of the cross section was similar to the experiments with GCPs though visibly below the rest.

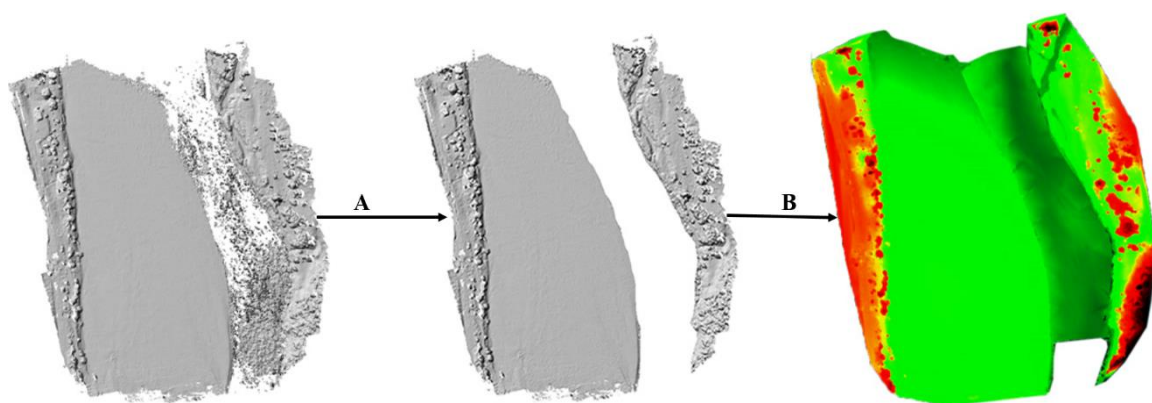


Figure 5.13 Floodplain processing (a: extraction of water surface river section, b: merging dry bathymetry with wet bathymetry and volumization).

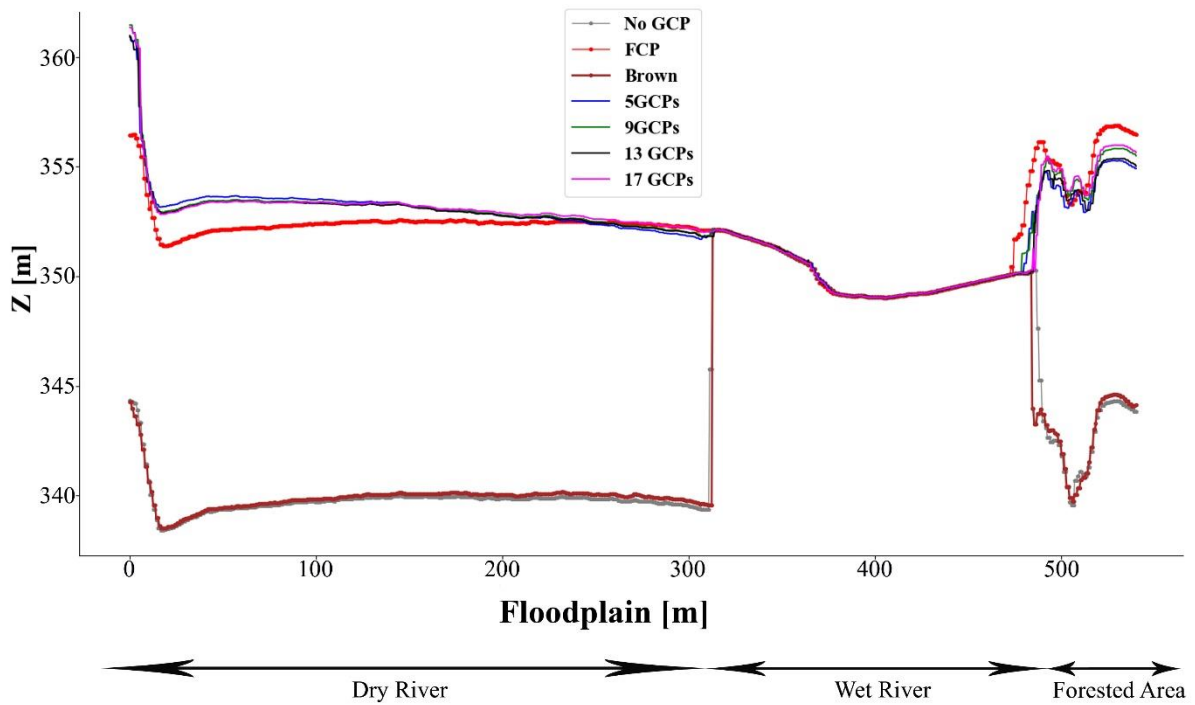


Figure 5.14 Extract of cross section 1 with the combined geometry of dry and wet bathymetry.

The hydraulic conveyance estimation graph is presented in Fig. 5.15. As anticipated, results indicate no significant difference among conveyances estimated based on 5, 9, 13, and 17 GCPs. The conveyances estimated based on the “no GCP” and Brown–Conrady configuration are not meaningful because of the clear offset between the photogrammetry results and the RTK results. The conveyance based on the FCP performed better than the Brown–Conrady and “no GCP” configuration. However, the estimated conveyance was significantly different from the conveyances estimated using GCPs. The results were similar for all three cross sections (Appendix A). The left bank of the river appears to be higher than the right bank. This is due to the riparian vegetation present on the left bank. This made access using the canoe (thus ADCP) difficult. Furthermore, the canopy cover from the riparian vegetation made it impossible for the photogrammetry to resolve the ground surface here.

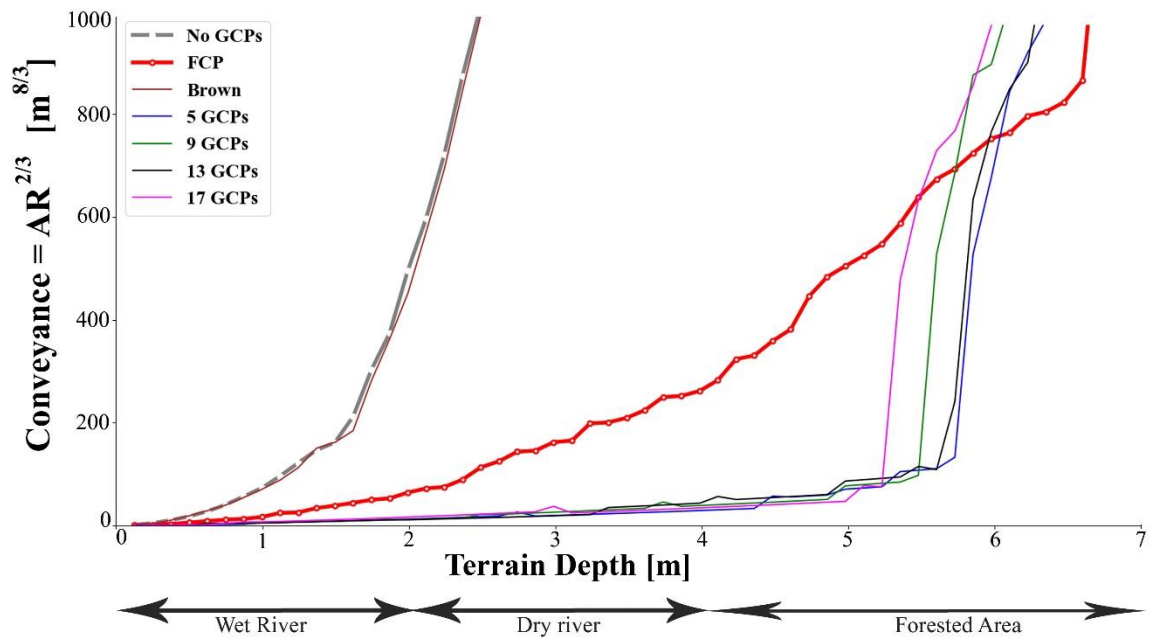


Figure 5.15 Cross section 3 (south of the terrain) for the conveyance vs. depth relationship.

The slope calculations, shown in Table 5.3, reveal a significant difference between the true slope (RTK GNSS) and the photogrammetry-derived slope values. This is despite a correction of the doming effect as described in Sect. 3.2. Among photogrammetry-based slope derivations, there were relatively large variations. Results indicate that for the purposes of hydraulic rating, slope derived from SfM is inapplicable due to high levels of inaccuracy.

Table 5.3 Slope estimations

Configuration	Hydraulic slope [* 10 ⁻⁴ m]
RTK GNSS Track	-2.300
5 GCPs	-3.935
9 GCPs	-3.286
13 GCPs	-3.749
17 GCPs	-3.891
No GCPs FCP	-3.995

5.5 Conclusions and recommendations

This study reinforced the capability of low-cost instruments, such as UAVs in combination with RTK GNSS, being applied to perform physically based remote discharge monitoring. The performance of the open-source photogrammetry software substantiated the hypothesis that free and open-source available packages are capable of producing results which are as good as proprietary alternatives as shown by the RMSE analyses. Across different GCP distributions, no significant difference was observed between the errors calculated based on open-source software and those calculated based on commercial software packages. This, combined with the fact that UAV data can be acquired relatively quickly and would be affordable to many water management institutions in low income economies, opens doors for use in low-resource settings. Apart from cost implications, the open-source software provided an option in the form of a “fixed camera parameter” configuration, which significantly reduced the RMSE of the reconstruction, even without the use of GCPs. The results had limitations in terms of the sample size used for calculating the RMSE of the GCPs. For instance, when reconstruction was performed based on 13 GCPs, only 4 GCPs were available to use as validation points. In future studies, it would also be useful not only to increase the number of independent checkpoints but also to measure the RTK track further away from the river to avoid the influence of poor river photogrammetry reconstruction. As anticipated, increasing the number of GCPs had an inverse effect on the RMSE. However, the gradual improvement in accuracy of the reconstruction diminished disproportionately. For the selected trials, a reconstruction based on 13 GCPs provides the most accurate RMSE results. It provides an optimal balance between the number of GCPs for reconstruction and the number of validation points. In addition, an observation that accuracy cannot be determined based on GCP density alone. The distribution of GCPs proves to be as critical as the GCP density in order to achieve optimal accuracy. In certain cases, priority must be placed on the GCP distribution so that the output is representative of a wider range of elevation values. Placing more GCPs in proximity to potentially problematic areas such as forests or water significantly improves the overall output of the reconstruction. The effective impact of variations in GCPs on geometry is realised in the form of conveyance. Despite the optimal number of GCPs being 13, the study concludes that 5 GCPs evenly spread out across a floodplain of approximately 40 ha and flying at an elevation of 100m is sufficient to generate an elevation model that meets the requirements of accurate conveyance estimation. Configurations such as the FCP advance the model reconstruction but do not achieve satisfactory accuracy without GCPs. Slope estimation based on photogrammetry reconstructions was not satisfactory under any GCP configuration tested. The novel method of measuring an RTK GNSS line is therefore a critical alternative to establish the slope by correcting for the doming effect. Furthermore, the conveyance is more impacted by the quality of the wet bathymetry collected by the GNSS than by the dry SfM bathymetry. Therefore, careful attention needs to be paid to making sure the wet bathymetry is measured as accurately as possible. A novel approach to generate a seamless bathymetry through merging and volumization was successfully tested. However, there was visible evidence of some mismatch in elevation, particularly on the upper part of the study area where

the wet bathymetry and dry bathymetry were merged. To counter this discrepancy, future studies may consider increasing wet bathymetry transects such that algorithms used to merge the two bathymetries (in this case Cloud Compare) have access to more transects. The additional transects would improve the quality of the wet bathymetry constructed through linear interpolation. Furthermore, results presented here encourage future studies to investigate the impact of variations in the number of GCPs on discharge estimations in a hydraulic model with different hydrodynamic boundary conditions. Within the envisioned hydraulic model it would be important to extend terrain downward to reduce backwater effects.

6 Towards Affordable 3D Physics-Based River Flow Rating: Application Over Luangwa River Basin

6.1 Introduction

Advancements in technology have led to new opportunities in river monitoring for dam operators, water resource authorities, environmental agencies and scientists with limited financial capacities (Rafik and Ibrenk, 2001). Hydraulic models play an important part in river discharge estimation procedures. However, several different data inputs are required in order to calibrate, apply and validate hydraulic models. One of the most sensitive of these data inputs is the geometry and bathymetry of a river (Dey et al., 2019). The geometry is usually described in the form of Digital Elevation Models (DEMs).

DEMs can be generated from a wide range of methods ranging from traditional ground surveying to remote sensing techniques applied to space- or air-borne imagery. Airborne-based Light Detection and Ranging (LiDAR) systems are capable of producing highly accurate DEMs (Liu et al., 2008). However, the data has limited spatial coverage and is expensive to acquire and process. In most cases, traditional ground surveying techniques are laborious, time inefficient, and potentially dangerous for personnel collecting the data (Samboko et al., 2019).

Space-borne methods provide a non-contact, thus safer, alternative for surveying river terrains. The most common satellite-based topography data sources are the Shuttle Radar Topography Mission (SRTM) DEM and the Advanced Space-borne Thermal Emission and Reflection Radiometer (ASTER) DEM. Unfortunately, there is a significant trade off which needs to be taken into account when applying satellite data for the purposes of river monitoring. Most freely available satellite-based terrain data sources such as ASTER (15m) and SRTM (30m) do not satisfy the required combination of spatial and temporal resolution necessary for accurate river monitoring. Consequently, while satellite data is promising for larger rivers, their spatial and temporal resolution is not appropriate for small to medium rivers (Kim, 2006).

Within this technological gap, Unmanned Aerial Vehicles (UAVs) equipped with cameras, continue to be developed and applied due to their relatively low-cost, high resolution and efficient application processes. The UAV collects overlapping images which are geotagged and subsequently merged together using photogrammetry (Skondras et al., 2022). The photogrammetric process in turn produces a number of outputs which include a digital elevation model (DEM). However, in order to reconstruct accurate geometries, the photogrammetry process requires Ground Control Points (GCPs) to identify the precise location of matter in the visible domain (Smith et al., 2015).

The process of distributing and surveying GCPs is laborious and time consuming, therefore it is important to minimise the number of GCPs collected without significant compromise on accuracy (Martínez-Carricondo et al., 2018; Smith et al., 2015; Woodget et al., 2017b). Several studies have been

conducted in order to determine the optimal number of GCPs necessary for accurate geometry reconstruction (Awasthi et al., 2019; Coveney and Roberts, 2017; Ferrer-González et al., 2020). Very few studies, however, have investigated the impact of uncertainties in geometry on the estimated flow when applied in a 3 D hydraulic model. One such study conducted by Samboko et al. (2022), investigated the impact of variations in the number of GCPs on the hydraulic conveyance. The study concluded that nine GCPs spread out across 25 hectares to optimally represent the full spectrum of elevation variations is sufficient for accurate conveyance estimation. However, the conveyance is a proxy of actual flow and may not be fully indicative of the actual discharge. Therein lies this research study gap, which seeks to develop a more physics-based rating curve using a combination of low-cost data collection equipment and 3D hydraulic modelling. The method is assessed by determining how inaccuracies in the geometry caused by varying GCP numbers, ultimately propagate into stage-discharge relationships. Furthermore, the study investigates how uncertainties in proxies of flow that may be derived from satellite platforms, such as river width (through surface water detection) or water level (from e.g. altimetry missions) propagate into uncertainties in discharge estimation.

The following research questions are investigated to determine whether the mentioned factors have a significant effect on the accuracy of results.

1. How does the rating curve produced by a 3 D hydraulic model compare with rating curves generated by conventional methods?
2. How do uncertainties in the surveyed geometry propagate into estimated discharge when applied in a 3D hydraulic model?
3. How do uncertainties in proxies of flows from satellite data propagate into uncertainties in discharge estimation?

6.2 Material and Methods

In brief, the investigation consists of the following steps; (i) select a suitable study site as far away as possible from impediments which may cause backwater effects and with a relatively straight river profile, (ii) use a combination of the UAV, RTK-GNSS, and ADCP to determine the wet /dry bathymetry and slope, (iii) merge the dry and wet bathymetries, (iv) subject the merged bathymetry to boundary conditions for a 3D hydraulic modelling environment to determine the roughness coefficient, (v) run the hydraulic model with different flow rates until a relationship between flow and stage (rating curve) can be determined, (vi) compare the rating curve with traditional rating curves then (vii) repeat this experiment using varying bathymetries and compare the outputs to determine if there is a significant difference in the results. *Figure 6.1* presents a schematic of the experiments conducted in this study.

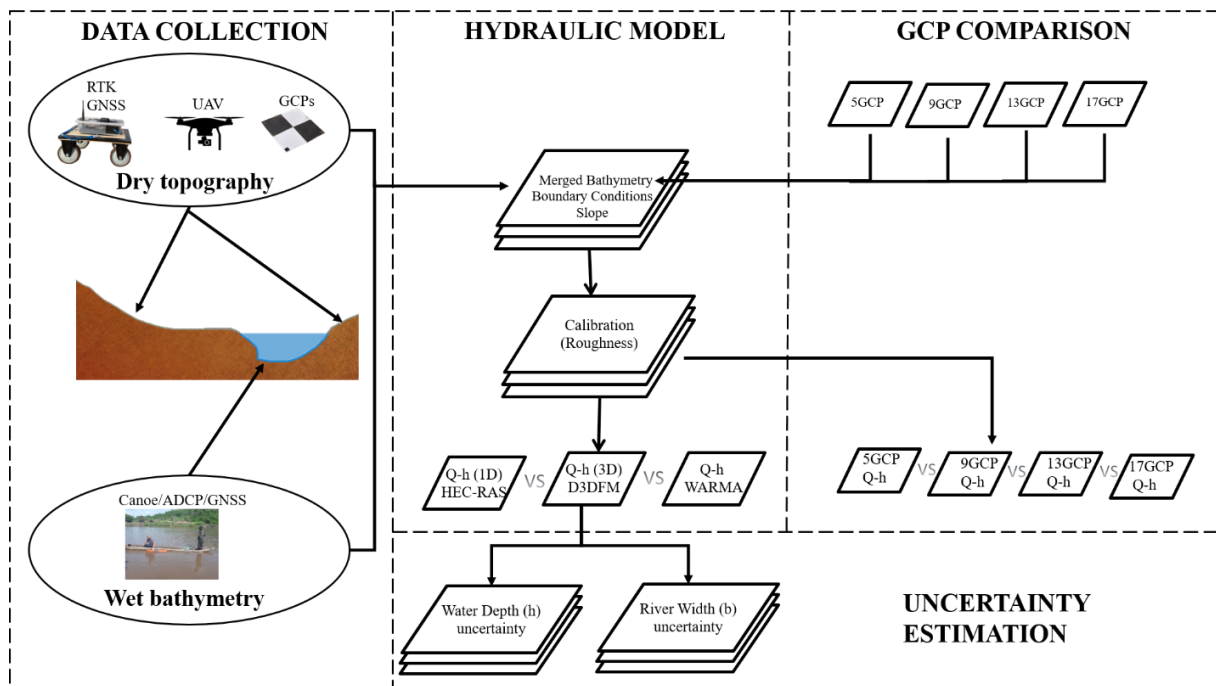


Figure 6.1 Schematic of experimental procedure

6.2.1 Data collection methods

A detailed description of how the dry and wet river bathymetry can be collected using low-cost UAV and GNSS device is introduced in section 2 of a study in Samboko et al. (2022). Similarly, a study by Alvarez (2018) applied an adaptive sampling technique to merge UAV derived images with echosoundings for bathymetric surveys. In short, the method consists of the following steps: an airborne instrument (e.g. UAV) is used to collect overlapping and geotagged images which are in turn converted into dry bathymetry through photogrammetry. Ground control points measured using low-cost RTK GNSS equipment are used to rectify inaccuracies in the bathymetry. The wet bathymetry is measured using a combination of an RTK GNSS and an echo sounding instrument (e.g. fish finder). The waterline is then measured using the RTK GNSS so as to correct any doming effect which may be caused by uncertainties in correcting radial lens distortions. Finally, the wet and dry bathymetries are merged through linear interpolation to form a seamless full bathymetry.

6.2.2 Study Site

The study which was similarly conducted on the Laungwa River is approximately 25 hectares. For purposes of comparison, the specific location of the study site is only a few kilometres from the Zambia Water Resources Management Authority (WARMA) permanent gauging station and a couple of hundred metres from the site where a similar study based on a 1D Hydrologic Engineering Center - River Analysis System (HEC-RAS) model (Abas et al., 2019). These sites may be considered similar in their hydraulic conveyance properties, given that they are geographically close to each other and their geomorphological characteristics are similar. A dataset of discharge and stage measurements, taken by

WARMA between 1948 and 2002 is available for rating curve comparison. The flow and water level is surveyed twice, at the end of the rainy season and at the end of the dry season so as to capture both low (only permanent channel) and intermediate (also partly floodplain) flow conditions. *Figure 6.2a* shows the location of the study site within the Luangwa Basin. *Figure 6.2b* shows the location of the study site in relation to the 2 other sites the WARMA gauging station and to the location where Abas et al., (2019) conducted a similar study based on a 1 D model.

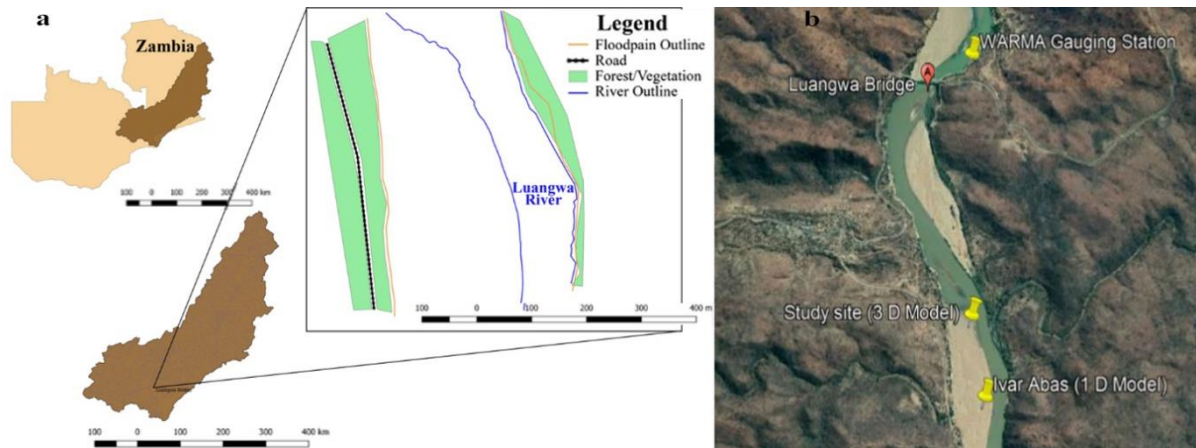


Figure 6.2 Study site along Luangwa River (b) location of study site in relation to other comparison sites.

6.2.3 Hydraulic Modelling

For hydraulic simulation, a software called D-Flow Flexible Mesh (D3DFM) (Deltares, 2020) is applied. D3DFM solves the nonlinear shallow water equations in 1D, 2D or 3D or combinations thereof using a flexible mesh domain. Within D3DFM two different layering methods are provided for 3D models, the sigma (σ) method and the Z-method. The Z-method is based on the Cartesian Z-coordinate system resulting in straight horizontal coordinate lines. Layers in the σ -model increase or decrease their thickness as the water depth in the model increases or decreases. The relative thickness distribution of the different layers however remains fixed (Deltares, 2020).

A hydraulic model consisting of a bed level, a grid structure, mathematical formulations describing the physical processes and corresponding necessary assumptions requires boundary conditions to simulate the desired hydraulic processes. In case of a river model these boundary conditions do often comprise an inflow and outflow of water implied by a discharge, velocity or water level. In D3DFM models these boundary conditions can be imposed as a time series or as a harmonic signal.

Besides the boundary conditions, there are initial conditions and physical parameter values to be assigned to the model, for example initial water levels, the water temperature and a uniform friction

coefficient. This friction coefficient influences the maximum velocity of the water at the river bed and therefore affects the discharge capacity and water level in the simulation (Saleh et al., 2013). The roughness can be described by different formulations like Chézy, Manning or White-Colebrook which all contain a certain roughness coefficient that needs to be specified. For the purpose of this study, the Manning coefficient is chosen as it is more applicable to open channels (Zidan, 2015).

6.2.4 Description of Data Requirements for D3DFM

Model setup and evaluation needed the bathymetry, boundary conditions (discharge and water level) and the roughness coefficient.

Bathymetry data requirements

The bathymetry of the terrain is established through merging and volumizing of photogrammetric data with sonar measurements. In brief, the Digital Terrain Model (dry bathymetry) is merged with river transects (wet bathymetry) and subsequently volumizing into a complete seamless bathymetric point cloud through linear interpolation. More details on this method can be found in Samboko et al., (2022).

The seamless bathymetry is then cut perpendicular to the flow direction on both sides in preparation for input into D3DFM. *Figures 6.3 (a) and 6.3 (b)* show an example of a DEM which has been volumized and subsequently cut on both sides perpendicular to river flow.

In order to use the point cloud in a model, the area should be extended both downstream and upstream. The extensions are required to ensure that upstream water can numerically spread over the entire width realistically, and downstream to ensure that backwater effects do not significantly alter water levels in the area of interest. In order to extend the point clouds using representative samples, a small selection of 1200 coordinates are extracted over the complete width on each side. This small stretch is reproduced every 36 meters in the direction of flow (or opposite for the extension to the north), this means the longitudinal and latitudinal values are shifted slightly and the height is subtracted or added with the corresponding slope. The point cloud is extended both upstream and downstream with 118 stretches, corresponding to 4248 meters, which is significantly more than the adaptation length (2.1 km). The adaptation length is the distance required to counter the effects of backwater. After volumizing the model for the last time, the final result is a point cloud containing 4.76×10^9 coordinates representing approximately 9.2 km of the Luangwa River. *Figure 6.3 (c)* shows the elongated bathymetry which is imported into D3DFM representing the bed level.

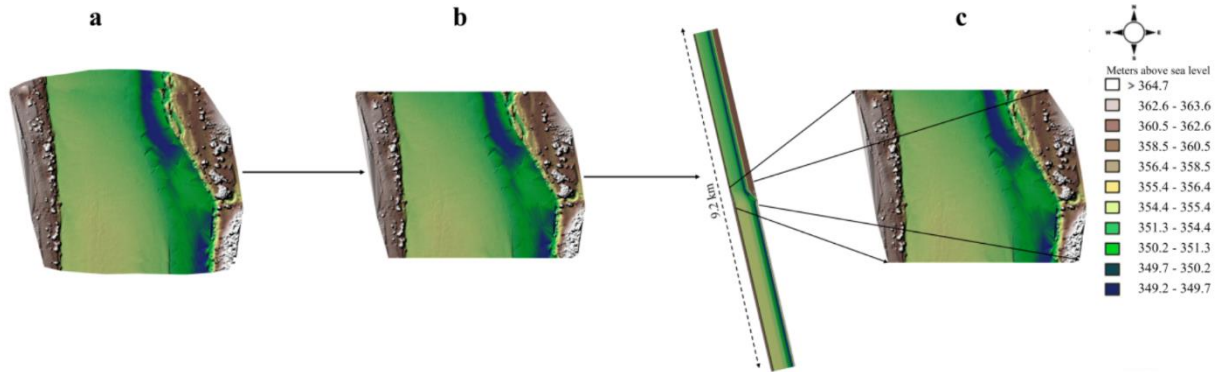


Figure 6.3 a) Study site volumised bathymetry b) bathymetry cut on both sides perpendicular to flow c) Elongated elevation model imported into D3DFM

6.2.5 D3DFM setup, calibration and evaluation

The model was setup with two Manning roughness configurations. One based on the main channel using the dry season observation set (water level, flow and velocimetry) and another where the degrees of freedom are extended to two roughness values (one main channel, one floodplain) using an observation taken during both the wet and dry season observations. This is to evaluate whether one visit is sufficient, or whether multiple visits are recommended.

In order to determine the optimal roughness coefficient of the main channel in the dry season, the model is constrained through optimisation of a combination of surface velocity and water level. The start value for Manning's friction coefficient was set at $0.018 \text{ s/m}^{-1/3}$, the median of the n value (Manning) for sandy straight uniform channels which ranges from 0.012 to $0.026 \text{ s/m}^{-1/3}$ (Arcement and Schneider, 1989). The upstream boundary condition which was measured in the field was kept constant at $191 \text{ m}^3/\text{s}$. The surface velocity distribution which were measured using Large Scale Particle Image Velocimetry (LSPIV) and a current meter was imported. Similarly, water level profile which were measured using an Acoustic Doppler Current Profiler (ADCP) were imported into the model and compared to the simulated water levels. Note that the use of ADCP could be replaced by the use of a more cost-efficient sonar, such as a fishfinder device, to keep the method entirely affordable. The comparison is based on the Mean Average Deviation (MAD).

$$MAD = \frac{\sum_{i=1}^n |x_i - \mu|}{n} \quad \text{Eq. 6.1}$$

Where n is the number of measurements, x_i is the term in question and μ is the mean of all measured values. The score was based on 5 measurements for the current meter and 10 for LSPIV. The simulated water level was similarly assessed with 5 observation points located in the centre of the wet bathymetry. A combination which yields the lowest values of MAD indicates an optimal roughness coefficient to proceed with.

The second model setup incorporated the wet and dry roughness coefficients. On the main channel, we applied the roughness which had been calibrated in the dry season. On the floodplain, a roughness coefficient of $0.040 \text{ s/m}^{-1/3}$ which was derived through a 1 D HEC RAS model in the wet season is applied. A summary of the derivation is described in *Annex 1*. After the model was constructed and calibrated, the next step was to accurately predict discharges other than $191 \text{ m}^3/\text{s}$. Establishing a stage-discharge relationship requires rating points (a discharge with corresponding stage) produced by the model. Hence, the model was run at least 20 times with changing boundary conditions. The upstream boundary condition was given by a discharge ranging from 5 to $3000 \text{ m}^3/\text{s}$ and the downstream boundary condition was determined through repetitive iterations which estimated the water level based on slope. Finally, both models were compared with a traditional rating curve constructed by WARMA. The 95% confidence interval of the WARMA rating curve will be used to generally judge the accuracy of the more physically constructed rating curve. Statistical model evaluation tools, Nash–Sutcliffe efficiency (E_{ns}) and Percentage bias (P_{bias}) are also used to determine significant differences among the simulated curves. The selected criteria are recommended for model evaluation because of their robust performance rating of simulating models. (Moriassi et al., 1983). P_{bias} measures the tendency of the simulated data to either under-estimate or over-estimate the observed WARMA readings. Low magnitudes indicate optimal model simulation. E_{ns} indicates how well the plot of observed versus simulated data fits the 1:1 line. NSE and PBIAS are computed as shown in *equation 6.2* and *equation 6.3*.

$$E_{ns} = 1 - \left[\frac{\sum_{i=1}^x (O_i - P_i)^2}{\sum_{i=1}^x (O_i - O_{mean})^2} \right] \quad \text{Eq 6.2}$$

$$P_{bias} = \frac{\sum_{i=1}^x (O_i - P_i)}{\sum_{i=1}^x O_i} \quad \text{Eq 6.3}$$

Where O is the observed value, O_{mean} is the mean of all observed values, P is the simulated value and x is the total number of values.

6.2.6 Comparison of discharge estimations based on varying geometries

In order to evaluate the impact of the number of GCPs on the estimated discharge, four elevation models reconstructed based on 5, 9, 13 and 17 GCPs are fed into the D3DFM hydraulic model under similar boundary conditions. The preparation of the bathymetries is similar to that which has been described in section 3.2. The different rating curves are compared individually to evaluate if there are any notable differences. *Figure 6.4* shows the varying GCP configurations used in the generation of bathymetries.

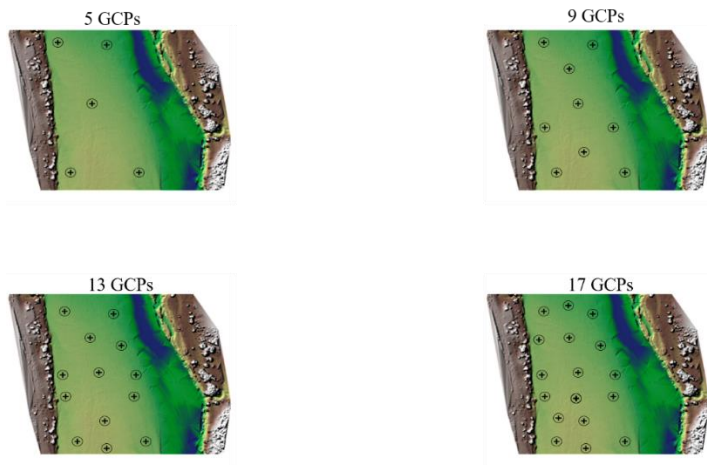


Figure 6.4 GCP distribution along floodplain of the Luangwa River

6.2.7 Evaluation of the propagation of continuous width and depth observations on uncertainty of discharge estimation

The two main proxies of flow that were assessed, and which potentially can be used for continuous monitoring through satellite observations, are water level and river width. In preparation to measure river width, a cross section is placed perpendicular to river flow where the cross-sectional must cut across the entire flood plain. *Figure 6.5* shows the location and orientation of the cross section.

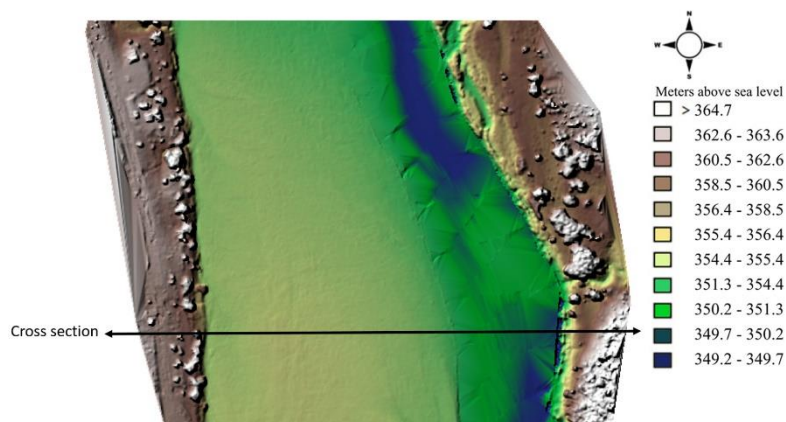


Figure 6.5 Location and orientation of cross-section

Thereafter, the model is run 20 times with varying upstream boundary conditions between 5 and 3000 m³/s. For each simulated upstream discharge value, the width in the simulation is measured and recorded. After calculating the average river width a relationship between discharge and river width relationship (Q-b) is established. Some of the satellite sensors that we may rely on are IceSAT-2 for river depth and Sentinel-1/2 for river width. Based on the resolutions of these sensors and with the assumption that our estimated widths could be +/- 5 meters uncertain, or in even more uncertain cases +/-10 meters, the river flow and its uncertainty is estimated through the established relationships between flow and depth, and flow and width respectively. This allowed us to assess at which point along the full stretch of the floodplain which proxy is more likely to produce accurate discharge estimations. This process was repeated with water depth as the proxy.

6.3 Results and discussion

The impact of photogrammetry-based geometry on the estimated discharge was assessed through three steps: comparing the rating curve of the D3DFM model with traditional methods, comparing rating curves based on geometries constructed using different GCP numbers in D3DFM, and evaluating how the uncertainty in models based on proxies of flow (width and water level) propagate into discharge inaccuracies.

6.3.1. Comparing the Rating Curve of the D3DFM Model with Traditional Methods

Before the comparison of D3DFM with other models, calibration and validation was performed. The surface flow velocity and the water depth were used to calibrate the model whilst model validation was performed based on a visual assessment of the RTK tie line and surface velocity. The measured variables are summarised in Table 6.1. There are sufficient surface velocity recordings to be able to partition them into a) calibration data and b) validation data.

Table 6.1 The experiments used for models' calibration and validation.

Phase	Data set	Description	Use
1	Surface velocity (a) (LSPIV, Current meter) and Water Depth (ADCP & RTK GNSS)	Determining the Roughness coefficient	(n) Calibration
2	RTK tie line and surface velocity (b)	Testing the models predictive capacity	Validation

The model setup required calibration of the roughness coefficient based on an optimal combination of the simulated water surface velocity and water level. The simulated velocities for the different roughness values were compared to the current meter and LSPIV measurements using the Mean Average Deviation (MAD) and percentage bias. *Table 6.2* provides the MAD of both the velocities and the water levels for each applied Manning coefficient (n). Lower values of MAD represent more optimal results.

Table 2.2 Mean Average Deviation for Roughness optimisation

Manning coefficient [s/m ^{1/3}]	MAD of Current metre [m/s]	[%]	MAD of LSPIV [m/s]	[%]	MAD of water level [m]
0.012	0.104	8.2	0.097	9.2	0.095
0.013	0.11	8.7	0.077	7.3	0.067
0.014	0.124	9.8	0.069	6.7	0.063
0.015	0.144	11.3	0.067	6.4	0.075
0.016	0.162	12.8	0.071	6.8	0.099
0.017	0.176	13.9	0.075	7.1	0.145
0.018	0.196	15.4	0.085	8.1	0.193

The first model simulation which was set at 0.018 s/m^{1/3} shows a relatively high average deviation (LSPIV: 15.4 % & CM: 8.1%) of the surface flow velocity and an overestimation of the water level by 19.3 cm. This results in a substantial widening of the river due to the uniform ‘flat’ floodplain. Both the velocity and the water level indicate a better performance when lower roughness value are applied since less resistance means faster flowing water and a lower water level with equal discharge. After further reductions in roughness values, results indicate that velocity and water levels are optimal when the Manning coefficient is set at either 0.013 s/m^{1/3} or 0.014 s/m^{1/3}. Since the CM measurements had to be performed from a boat, the expectation is that there are higher uncertainties in these measurements. Hence, 0.014 s/m^{1/3} (highlighted in grey in Table 6.1), is selected as the optimal roughness coefficient of the main channel.

The model validation was performed based on a visual analysis of the alignment between the measured RTK tie line and the simulated water level. *Figure 6.6* shows the RTK tie line which was measured along the water line and the simulated flow at $Q = 191 \text{ m}^3/\text{s}$, $n = 0.014 \text{ s/m}^{1/3}$ (main channel) and $n = 0.040 \text{ s/m}^{1/3}$ (floodplain). In the absence of varying seasonal gauge readings, the alignment between the

RTK tie line and the simulated water line on the right bank of the river provides visual evidence of good model performance.

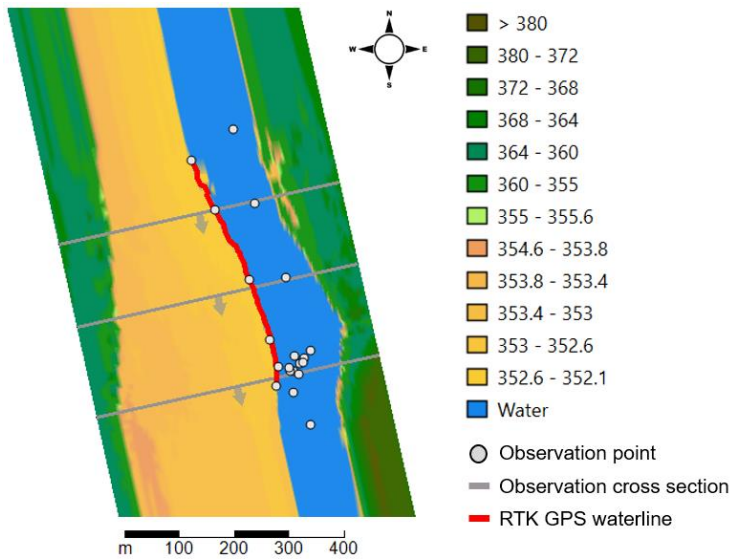


Figure 6.6 Visual representation of the discharge model at a discharge of $191 \text{ m}^3/\text{s}$ with $n = 0.014 \text{ s/m}^{1/3}$

After the model was setup and evaluated, simulations ranging from $5 \text{ m}^3/\text{s}$ to $3,000 \text{ m}^3/\text{s}$ with increments of $100 \text{ m}^3/\text{s}$ were performed. Figure 6.7 presents four rating curves,; one based on a single channel Manning coefficient (derived from dry-season flow survey in the main channel), the second is based on a combination of 2 coefficients (main channel and floodplain), the third curve shows the rating curve based on a 1D HEC-RAS model and the final curve is based on the conventional gauging method from WARMA. The discharge measurements are visualised in relation to a 95% confidence interval of the WARMA rating curve. In addition to the confidence interval, the significant differences among the curves based E_{ns} and $Pbias$ are evaluated in relation to the WARMA curve.

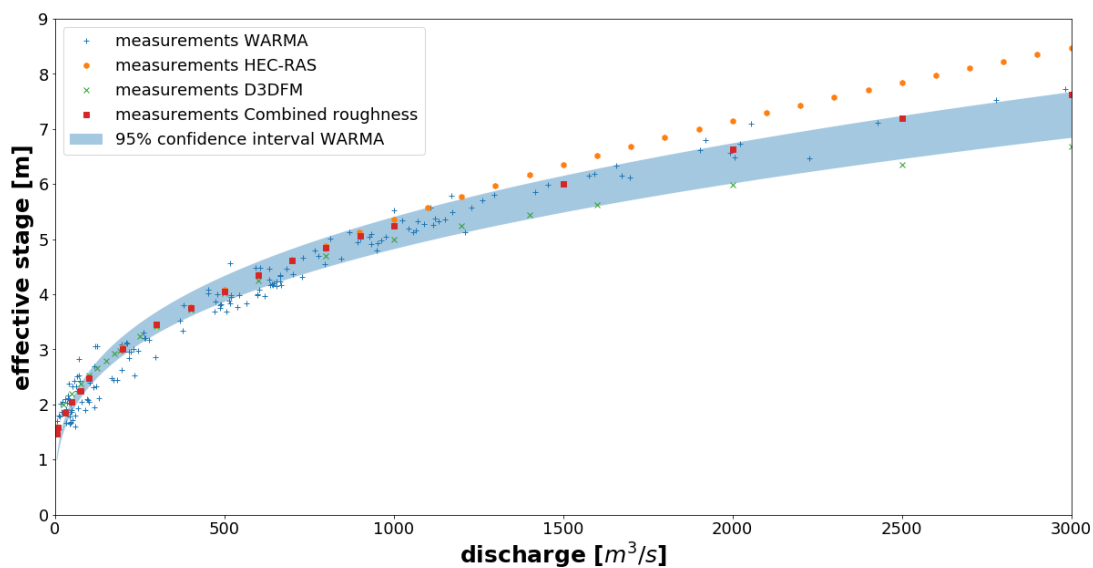


Figure 6.7 Rating curves comparing D3DFM with conventional methods

The D3DFM based model which combines two different roughness coefficients more closely resembles the WARMA curve than the 1D HEC-RAS curve and the D3DFM which applies only one roughness for the entire terrain. This is particularly the case for high flow conditions. This result may be attributed to better optimisation of the roughness coefficients (compared to 1D or 3D with only one Manning roughness) which acknowledges the fact that roughness in the main channel is different from roughness in the floodplain. It must however be noted that comparing with the relationships of WARMA and 1D HEC-RAS is only insightful to a certain extent as the experiment was not conducted at the exact same location as where the WARMA rating curve is maintained. Possible differences in the river geometry may cause that our results are not entirely equivalent with WARMA’s rating curve. The final stage-discharge relationship is expressed by *figure 6.8* and *equation 6.3*. This relationship should function as a basis on which adjustments can be made based on newly available stage-discharge data. Note that the river geometry will most likely change over time, due to the sandy bed-level, and therefore the constants are not stable over time.

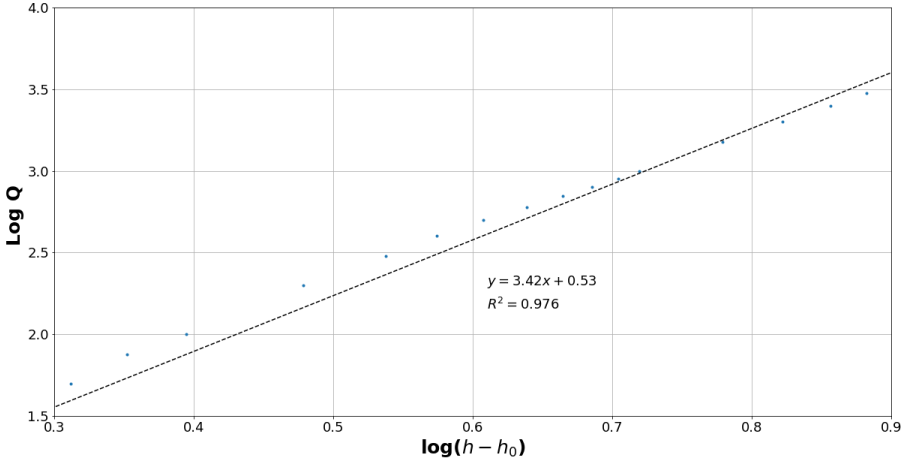


Figure 6.8 (Logarithm) Discharge vs stage relationship: combined roughness

$$Q = 3.42[h - h_0]^{3.39} \tag{Eq 6.3}$$

6.3.2. Comparison of discharge based on varying GCP numbers.

To assess the impact of the number of ground control points on the bathymetric chart and therewith on the modelled discharge, charts created with different GCP numbers were used to run the same hydraulic model with similar boundary conditions. *Figure 6.9* presents the rating curves of all four distributions.

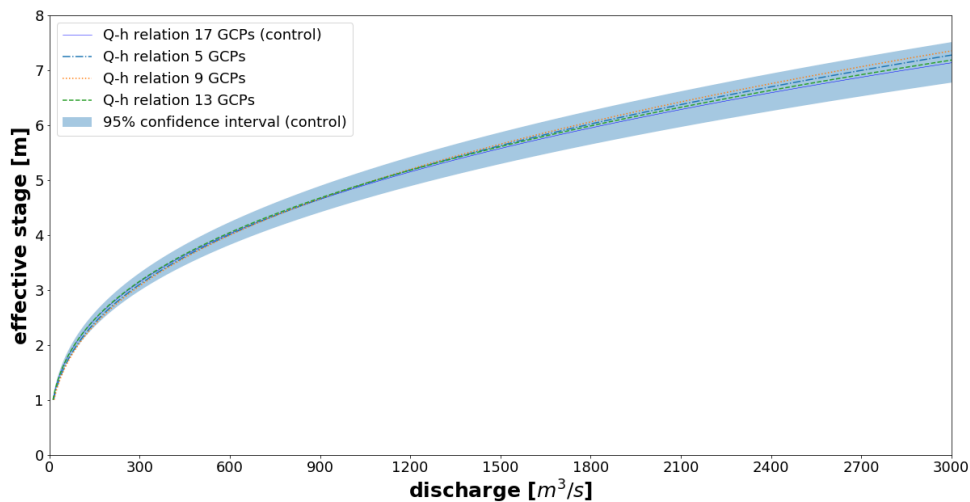


Figure 6.9 Comparison of Rating curves generated based on varying GCPs

Assuming the bathymetry based on 17 GCPs as the control, a 95% confidence interval on its rating curve is plotted. The confidence interval was plotted based on Ordinary Least Squares (OLS) regression results. These results are presented in *Annex 1*. The P_{bias} and E_{ns} results (comparing with 17 GCP control) indicate very similar curves derived among bathymetries based on 5, 9, 13 GCPs; PBIAS [3%, 0.7% & 0.6%] and NSE [0.982, 0.998, & 0.999] respectively. All 4 curves fell within the 95 % confidence interval of the control curve (17 GCPs). It must be noted that the bathymetry up until 191m³/s is determined by the ADCP/RTK measurements and therefore the number of GCPs does not influence the curve up until this point. In this study, a minimum of 5 GCPs spread over 25 hectares is sufficient for accurate discharge estimation. The conclusion is that for the purposes of physics-based river rating, a ratio of 5 ha/GCP is sufficient to accurately estimate discharge. However, in all instances including terrains less than 1 ha, the base-level/minimum number of GCPs required is 3 to allow for triangulation (Oniga et al., 2020). Finally, it is important to note that the distribution of the GCPs is likely to influence the final chart drastically as the most uncertain areas will be at the borders of the bathymetry (mostly due to the doming effect). Therefore, an optimal GCP distribution will be representative of the full spectrum of elevations, and will prioritise the placement of GCPs on the edges of the terrain being mapped.

6.3.3 The impact of uncertainty in proxies of flow on discharge estimation.

Finally, an investigation on the impact of proxy uncertainties (river width and water level) on discharge estimation is conducted. The term proxies refers to variables that can be more easily observed operationally. An uncertainty based on the resolution of satellite sensors is imposed seeing as we may rely on sensors such IceSAT-2 as investigated by Coppo Frias (2023) for river depth and Sentinel-1/2 for river width (Filippucci et al., 2022). *Figure 6.10* presents the relationship between discharge and

river width. The graph also highlights 2 different potential error intervals, +/- 5 meters (90 %) and +/- 10 meters (95 %) so as to visualise the amount of uncertainty which corresponds with specific sections of the terrain.

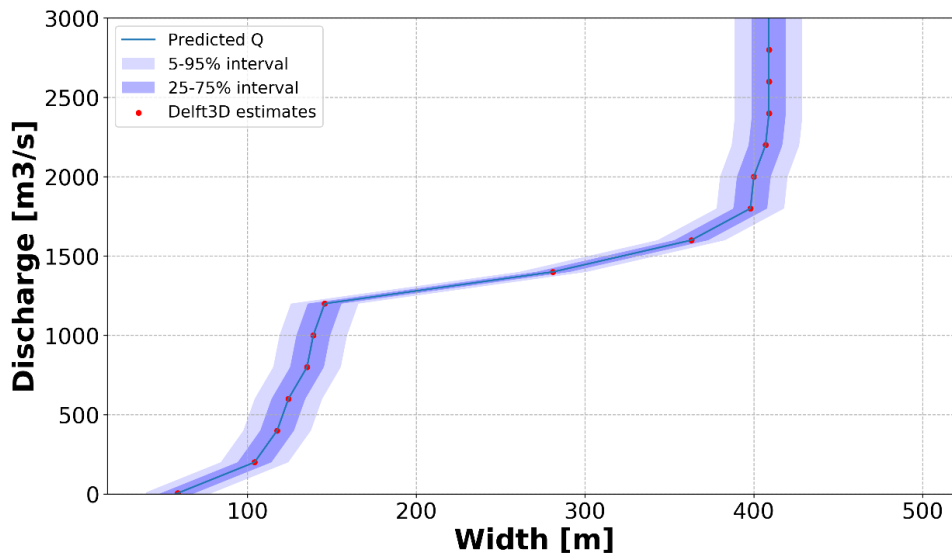


Figure 6.10 Discharge vs width relationship

If river widths would be used, this would result in high levels of flow uncertainty below 150 meters. These higher levels of uncertainty are as a result of low width sensitivity to changes in flow below 150 m. The low sensitivity in this low flow stage can be attributed to the steep bank, i.e. as flow increases the depth rises quickly but there are minimal changes in width. During medium level flows, between 150 m. and 370 m., results indicate lower levels of width uncertainty i.e. high river width sensitivity. The high sensitivity in this medium flow stage may be attributed to the gentle sloping floodplain (more stable roughness coefficient), i.e., as flow increases the width rises significantly faster than the water level. Finally, higher levels of width uncertainty are noted during high flows (above 370 meters). This region experiences low width sensitivity to changes in flow. The causal factor is the inundation of the entire floodplain, which has not been included in the hydraulic schematization.

Similar to width, water level uncertainties also result in varying discharge estimates. Figure 6.11 presents the relationship between discharge and water level as simulated by D3DFM. The graph also highlights 2 different potential error intervals, +/- 10 cm (90 %) and +/- 20 cm (95 %). These error intervals assist us in visualisation of the amount of uncertainty in flow that can be expected from using water levels as proxy. For lower flows (<1 000 m³/s), results indicate lower levels of water level uncertainty i.e. high water level sensitivity. The justification for the high sensitivity in this low flow stage can be attributed to the steep bank, i.e. as flow increases the depth rises quickly but there are minimal changes in width. During medium level flows, between 1 000 m³/s and 1 500 m³/s, results indicate higher levels of water level uncertainty i.e. low water level width sensitivity. The low

sensitivity in this medium flow stage may be attributed to the gentle sloping floodplain, i.e. as flow changes, the water level does not change significantly. Finally, during high flows the floodplain is inundated with water, thus, the expectation is that in this regime high water level sensitivity i.e. low water level uncertainty. Contrary to our expectation, this segment experiences high water level uncertainty.

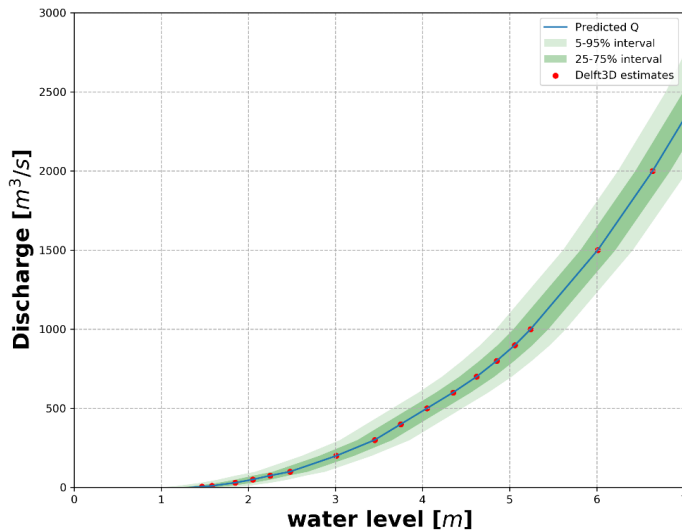


Figure 6.11 Discharge vs water level relationship

As shown in figures 6.10 and 6.11, the proxies of flow (water level and river width), are antagonistic in nature. This implies that when one of the proxies exhibits high uncertainty, the other is more likely to presents low levels of uncertainty.

An observation that different proxies of flow, namely water level and river width, perform optimally at different segments. At low flows the shape of the wet river channel (steep slope) is more likely to induce high water level sensitivity and low river width sensitivity to changes in discharge. At higher flow levels the shape of the wet river channel (gentle slope) is more likely to induce low water level sensitivity and high river width sensitivity to changes in flow. At even higher flows, ideally, the floodplain is inundated and becomes insensitive to river width. In the absence of more accurate discharge estimation methods, the water level is once again the more reliable proxy. Above the natural levee, the assumptions of the schematization of the D3DFM model no longer hold, and therefore any flows above that level should not be considered reliable.

6.3.4 Discussion

This study offers us the unique opportunity to compare a 1D model and a 3 D model for the purposes of river discharge estimation. This comparison is made with the understanding that the 1 D HEC-RAS model data (collected: April 2019) was collected approximately one hydrological cycle (1year) before the D3DFM model data (collected: November 2020). Therefore, the roughness was established at two different flow regimes (high flow and medium). The comparison of two or more rating curves based on

potentially varying bathymetries/floodplain geometries will not yield precisely identical results. However, the close proximity of the study sites and the hydrogeological similarities of the two locations means that our ability to extract meaningful comparison is not compromised.

Results indicate that the 1D model is similar to the 3D model in its capacity to generate accurate rating curves for the purpose of river monitoring. In addition to being freely available (open-source), the 1D model requires significantly less computing power than the 3D model, which may be a limitation for water authorities with limited financial capabilities. However, there are two significant benefits of the 3D model over the 1D model. Firstly, the 3D model takes into account the heterogeneity of the river geometry and roughness at much higher spatial resolution. In contrast, the 1D relies more on point-based measurements which would suggest that the 3D model is capable of estimating more accurate flow discharge when applied correctly. Secondly, the 3D model introduces a unique validation method which is not available in the 1D model. This is referring to the ability to extract the surface velocity within the 3D model and compare it to surface velocities derived from direct methods such as the current meter or LSPIV. It is not possible to extract surface velocities from a 1D model.

Apart from comparing the 3D model with the 1D model, this study derived some validation by comparing the 3D model with traditionally derived rating curves. The fact that the more physics-based method was within a 95% confidence interval of the WARMA (traditional curve) provides evidence that flow can be accurately estimated through non-contact means and the constant improvement in technologies.

6.4 Conclusion and Recommendations

The study reaffirms and provides insight into the potential of applying low-cost and readily available technologies for river monitoring. The methods described in the study are well within reach of water authorities with limited resources and are particularly useful for small to medium sized rivers in sub-Saharan Africa. The D3DFM discharge model resembles actual river in depth, width and location when using a combination of two Manning's coefficients ($0.014 \text{ s/m}^{1/3}$ & $0.040 \text{ s/m}^{1/3}$) and a discharge value of $191 \text{ m}^3/\text{s}$.

Based on the *confidence interval*, all four (5, 9, 13, 17) bathymetries fell within the 95% confidence interval. 5GCPs are sufficient to simulate a curve which falls within the 95% confidence interval of a WARMA curve (control). Therefore, 5 GCPs are adequate for physically based river rating on condition that the GCPs are accurately measured using an RTK GNSS and are optimally distributed to represent the full spectrum of terrain elevations.

The slope, which is an important input to the model, must be measured as accurately as possible for the longest possible distance along the water line. Ideally, measuring the waterline height at 200 m intervals

for a 5 km stretch is sufficient to avoid the impact of wave distortions. The impact of backwater distortions is of particular concern for high water levels as opposed to low water levels and therefore a longer measuring distance is required in high water level instances. However, the magnitude of slope has a bearing on the length that is required to reduce the impact of backwater distortions, i.e. in Luangwa's case, a long distance would be needed but for streams with a large bottom slope, a much shorter distance is sufficient. Furthermore, the stretch chosen for observation must be long enough to cancel out the effects of sand banks (uneven silt deposition) which may have an impact on the slope accuracy. However, identifying and measuring such long stretches is problematic due to difficult terrains and inaccuracies caused by the need to move the base station. The most feasible compromise is to use one base station location and then measure continuously for as far as possible to both sides, use correction via satellites, or use a spirit level. In that way the relative accuracy stays the same and will be adequate.

It is established that the proxies of flow (water level and river width) perform well at different stages of discharge. For instance, at low discharge values and steep banks, the water level is more sensitive to changes in flow, thus more accurate. For higher discharge values and gentle floodplain slopes where the floodplain fills up, the river width is more sensitive to flow changes and thus more appropriate to use. As a result of the two proxies acting antagonistically in performance, a combination of both methods in different flow regimes gives a more accurate flow monitoring assessment. Alternatively, determining the river geometry and then deciding on which proxy would be most helpful to measure i.e., for gently sloping riverbed using the width since a slight change in discharge will have a larger impact on the width and therefore be easier to measure. And vice versa for steeply sloping riverbeds (rectangular channel will be only interesting for water level measurements).

We reiterate that the accurate measurement of a tie line is critical not only to correct the doming effect, but to provide an extra validation check for the hydraulic model. The study demonstrated that this is feasible and affordable using a simple combination of an RTK GNSS and a mobile cart. The tie line must be measured simultaneously with the river discharge so that it can be compared against the simulated water line as derived by the hydraulic model. Finally, a recommendation is put forward that the approach is applied in the dry season so as to minimize the amount of water flowing in the river for more efficient photogrammetry processing. However, it is important to occasionally measure flows and corresponding water levels at different times of the year so as to validate the efficiency of the model simulation and differentiate roughness in the main channel and floodplain.

7 Conclusions and Outlook

The overall aim of this research was to investigate the possibility of applying low-cost technologies to further improve water resource management in data scarce catchments such as the Luangwa Basin. This was done by focusing on modern technologies which are within reach for water authorities with limited budgets. More specifically, an attempt was made to combine low-cost UAV derived data with low-cost RTK GNSS equipment to predict flow within a 3D hydraulic modelling environment. Additionally, the study assessed how uncertainty in proxies of flow and geometry may affect the estimated flows. A framework for remote river monitoring with limited contact between survey equipment and measured variables was proposed. This framework was tested and exemplified in a case study of the Luangwa River in Zambia. Inputs derived from low-cost devices were successfully integrated within a 3D hydraulic model and results comparable to known gauge station readings were found.

This physics-based approach was successful in providing an alternative for traditional river rating. The proposed approach proved to be of acceptable accuracy through statistical comparison with traditional rating curves. The ‘real’ value of this approach lies in the increased capacity of water resource authorities with financial limitations to accurately monitor river flows for the benefit of all stakeholders including the sustainability of the river system itself. Table 7.1 shows a range of indicative costs associated with the traditional and more physics based methods. A lower cost of river monitoring means that a more consistent network of data collection points can be established and maintained within large basins to improve upon systems such as early flood/drought warnings, water allocations, environmental flows, hydro-power management and water infrastructure construction.

Table 7.1 Indicative prices for materials used in each method

Method			Item	Cost range (Euro)
Traditional	river discharge estimation equipment		ADCP	15 000 ~ 30 000
			Differential GNSS	3 000 ~ 5 000
			Motorised engine boat	4 000 ~ 5 000
Proposed	river discharge estimation equipment		UAV	1500 ~ 2 500
			Fish Finder	200 ~ 300
			RTK GNSS	400 ~ 600

As the impact of anthropogenic activities and climate change increase, the dependence of all species including human inhabitants on the river system will grow significantly. Therefore, to safeguard the ecosystem, it is critical to continue to explore technologies which make it possible for more efficient, safe and affordable flow predictions while as little as possible negatively influencing the river system.

7.1 A proposed framework for remote river rating

During the inception of this thesis there was no known method of river rating which combined different low-cost technologies in order to estimate river flow in complex locations. Therefore, the first step was to propose a framework for monitoring rivers using low-cost technologies. This step is described in detail in chapter 4. An inventory of flow observation techniques which include in-situ flow observations for natural control sections and satellite observations has been investigated. The output of this literature review informed the process of framework development. A list of individual components providing the framework and the order in which the elements were to be placed was determined. The manner in which each critical step is related to the other and how modern technologies are assimilated into an interconnected framework was explained. The proposed framework includes checks and balances in the form of error thresholds to make sure that the estimation remains accurate. Up until this point, the proposed framework was only theoretical. In order to determine the proposed frameworks practicality, it had to be exemplified within a real-life setup. A resolution was made that the Luangwa Basin is an ideal location which satisfies all the environmental properties of a remote, and difficult to work in location with limited data availability. The main principle was to utilize hydraulic simulations of relationships between discharge and proxies for discharge based upon physics of momentum and mass balance, constrained by the observation location's geometry, slope and roughness. This would allow for assimilation of any permanent observation of flow proxies into these hydraulic simulations, not just the classically observed water levels. The framework directs that after identification of a suitable site, the next stage is to determine the geometry of the river channel.

7.2 Evaluation of the geometry for remote river rating in hydrodynamic environments.

In order to partially fulfil the previously proposed framework, Chapter 5 focused on the development of geometry for the purpose of physically based remote-river monitoring. The hypothesis is that the UAV based reconstruction using Real Time Kinematic Global Navigation Satellite System (RTK GNSS) equipment leads to accurate geometries particularly fit for hydraulic simulation. It was determined that open-source photogrammetry software is perfectly capable of reconstructing geometries with similar precision and accuracy as commercial packages. Additionally, it was established that the optimal number of GCPs necessary for satisfactory geometrical reconstruction is 13. Furthermore, it is recognised that there are viable alternatives to the application of UAVs for mapping the dry bathymetry. To that point, it is put forward a rather elementary, yet highly effective and affordable method of dry bathymetry mapping using a low-cost RTK GNSS mounted on a 'DIY' mobile cart. The importance of the mobile cart was demonstrated through its application in the measurement of an RTK GNSS line (slope) which was in turn used to correct the doming effect (distortions in the photogrammetry solution due to imperfectness of the intrinsic lens matrix). Furthermore, a novel approach of merging the dry

bathymetry with the wet bathymetry using linear interpolation was successfully implemented to produce a seamless bathymetry.

Finally, given that the terrain data must be used to estimate channel conveyance, the correctness of the derived terrain was measured in the form of conveyance parameters and the effect of variations in the used amount and configuration of Ground Control Points (GCPs) on these parameters and the resulting actual discharge estimation was investigated. This was investigated in the subsequent chapter of this thesis.

7.3 The impact of geometry variations on discharge estimations

To conclude the realization of the proposed framework in Chapter 4 of this thesis, Chapter 6 attempted to establish the impact of variations in geometry on discharge estimation in a hydraulic modelling environment. Unlike the preceding chapter which based its evaluation on a proxy of flow (conveyance), this section evaluates performance based on actual flow (discharge). The study reaffirms and provides insight into the potential of applying low-cost and readily available technologies for river monitoring. It is recognised that for the purposes of UAV based river rating, a limited number of GCPs are required. This is on the condition that the control points are evenly distributed to represent the full spectrum of elevation within the terrain in question. Holding all other factors constant (slope, roughness), there is no significant benefit of increasing the number of control points beyond a minimum threshold. This threshold varies depending on the area of interest of the terrain and thus the size of the river system. This is important due to the rigorous, time consuming and at times dangerous process of GCP placement and recording.

Outlook

This research highlighted the added value of innovations in low-cost technology for remote-river monitoring. However, there remain many opportunities yet to be explored as illustrated in the next sections.

7.4 Integration of satellite data to achieve truly remote river rating

In this research, the available remote sensing products are not accurate enough for relatively narrow rivers (less than 100 meters). The unavailability of free and high-resolution satellite data meant that tools such as UAVs had to be applied to map the dry bathymetry. However, to truly be labelled as 'remote' river monitoring, surveyors must be able to obtain similarly accurate discharge estimations without having to repeatedly make trips to the study site for recalibration. This would have significant implications on the capacity and cost of monitoring entire basins remotely. To that end, the recently launched Surface Water Ocean Topography Mission (SWOT) is promising, as it will present altimetry at an even higher resolution and a much more robust temporal scale than current sensors such as ICESat-2 (Cooley et al., 2021). The SWOT mission is designed to observe all rivers wider than 100m. The

mission will observe all rivers regardless of nadir (camera/sensor looking vertically downwards) overpass. It will provide the very first discharge variations and river storage data in a globally consistent manner. The altimetry method is however more applicable in instances where the expectation that sensitivity is high in response to water level changes.

7.5 Bathymetric Chart

In this research an ADCP with a single-beam sonar was attached to a wooden canoe to extract the wet river bathymetry. In future research, perhaps other methods to manoeuvre a floating sonar can be applied considering that the canoe is somewhat unstable and was carrying valuable equipment like a laptop, smartphone and RTK GPS in a crocodile and hippo infested river. Given that motorized engine boats are generally expensive for water authorities with smaller budgets, one can think of a floating sonar dragged over the river surface by a drone. Larger battery power would be required for this procedure to be successful. An ADCP is not strictly the only tool which can be applied for under water measurements. An echo sounder or fish finder could do the job. These instruments are significantly more affordable, however, some thought must be put into how exactly the position for the angle can be corrected. It may be useful to apply drones with more and larger rotors.

7.6 Discharge Model

In this research the roughness coefficient is used to calibrate the discharge model, which is common practice (Ardıçlıoğlu and Kuriqi, 2019). However, while calibrating the model to the test data most of the uncertainty will be encapsulated in the roughness coefficient. Therefore, it is recommended to estimate a range of bed roughness values, based on grain or pebble size, ground surface irregularities and vegetation elements.

The surface flow velocities computed with the discharge model are extracted as the average velocity in the upper layer. In this research an equal layer distribution is used of ten layers, resulting in an upper layer that represents ten percent of the river depth. It could be worthwhile to change this layer distribution towards a smaller upper layer and assess the differences in produced surface flow velocity and therewith possibly obtain a different value for the roughness coefficient.

In our view, the implementation of remote river rating methods presented in this thesis would yield significant improvements in accurate and consistent river monitoring at a substantially lower cost. However, for institutions such as WARMA to operationalise these techniques, some foundational work needs to be done. This includes human resource capacitation with respect to the ability to use relevant hydraulic models, safely operating remotely piloted aircrafts (drones) and learning how to use advanced low-cost RTK GNSS devices. At policy level, institutions such as WARMA may need to lobby for relaxation of the laws which govern the use of drones as these stringent regulations may present a

significant hurdle for genuinely productive programs. Overall, it may be necessary to perform a bottom-up system analysis which takes up the opinions of all stakeholders into account to determine what steps are required to shift from traditional river monitoring methods to remote river monitoring.

Appendix A

A1. Data Collection

This appendix contains figures, tables and photo which complement the data collection method.

Figure A.1 shows the components and setup of the constructed Real Time Kinematic GNSS. The container on the right-hand side in Figure A.1 contains the base, the other container contains the rover. Both containers include two SimpleRTK2B boards with a u-blox-ZED9P module, a Raspberry Pi, two GNSS antennas, an XBEE shield and a long range radio antenna. With this hardware, two complete RTK GNSS sets can be constructed, one based on long range radio communication and one based on a 4G internet connection. The SimpleRTK2B board with the XBEE shield works with the radio module and is used during the fieldwork.

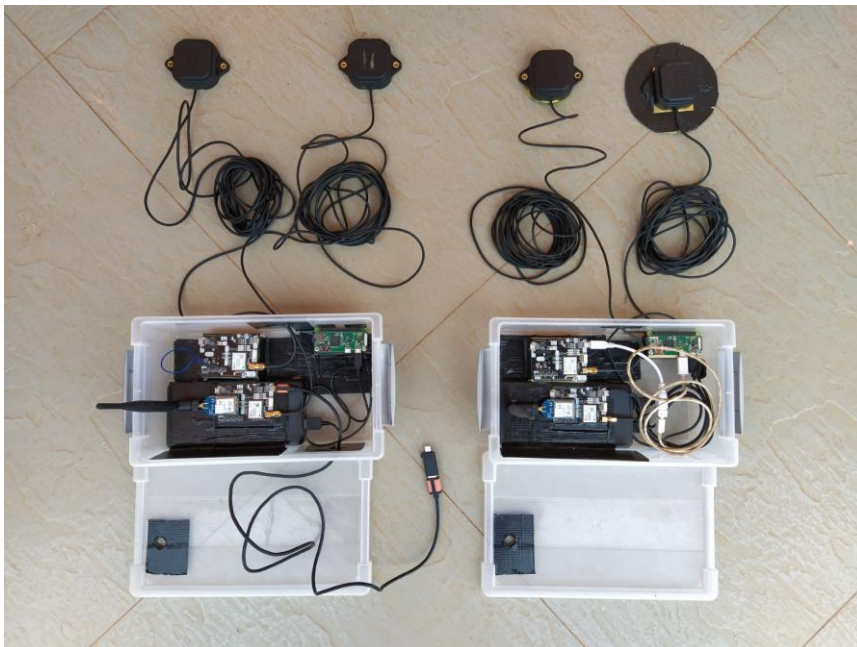


Fig. A1. 2 sets of RTK GNSS Equipment, one base of a long range radio connection and one based on 4G connection.

Figure B.1 shows the bathymetric data collection setup with the ADCP tied to the wooden canoe of a local boatman. On top of the sonar an RTK GNSS receiver is mounted which is, via a SimpleRTK2B board, connected to a smartphone logging the location measurements with a one second time interval. The ADCP is connected to a laptop running Winriver II which stores the depth measurements.



Fig. A1. ADCP with a Low-cost RTK GNSS attached to canoe

A2. Wet and Dry Bathymetry

Figure A2.1 shows the ‘bowling’ or ‘doming’ effect on terrain models. The top left graph represents the relationship between height and track for the 5 GCP terrain. The centre left graph represents the relationship between and track for the 5 GCP terrain after FCP correction. The bottom left graph represents the relationship between and track for the 5 GCP terrain after both FCP and doming correction. The top right graph represents the relationship between height and track for the 9 GCP terrain. The centre right graph represents the relationship between and track for the 9 GCP terrain after FCP correction. The bottom right graph represents the relationship between and track for the 9 GCP terrain after both FCP and doming correction.

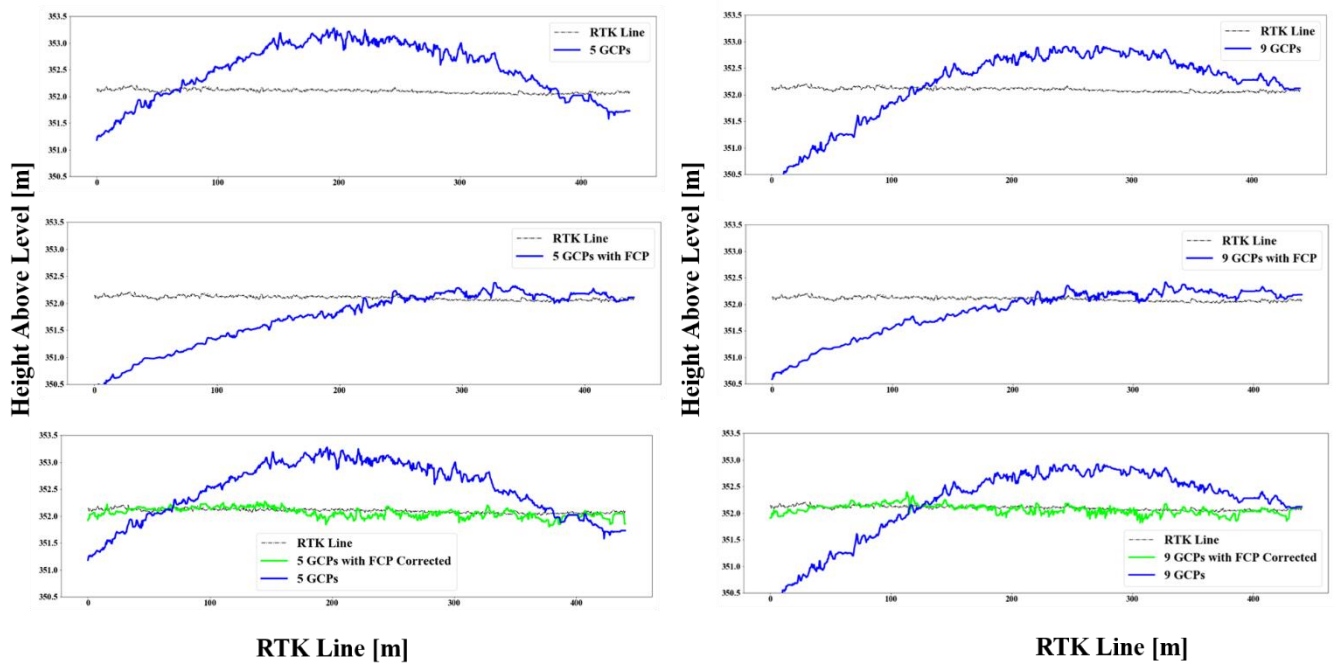


Fig.A2.1 Correction for the doming effect

Figure A2.2 shows the ‘bowling’ or ‘doming’ doming effect on terrain models. The top left graph represents the relationship between height and track for the 13 GCP terrain. The centre left graph represents the relationship between and track for the 13 GCP terrain after FCP correction. The bottom left graph represents the relationship between and track for the 13 GCP terrain after both FCP and doming correction. The top right graph represents the relationship between height and track for the 17 GCP terrain. The centre right graph represents the relationship between and track for the 17 GCP terrain after FCP correction. The bottom right graph represents the relationship between and track for the 17 GCP terrain after both FCP and doming correction.

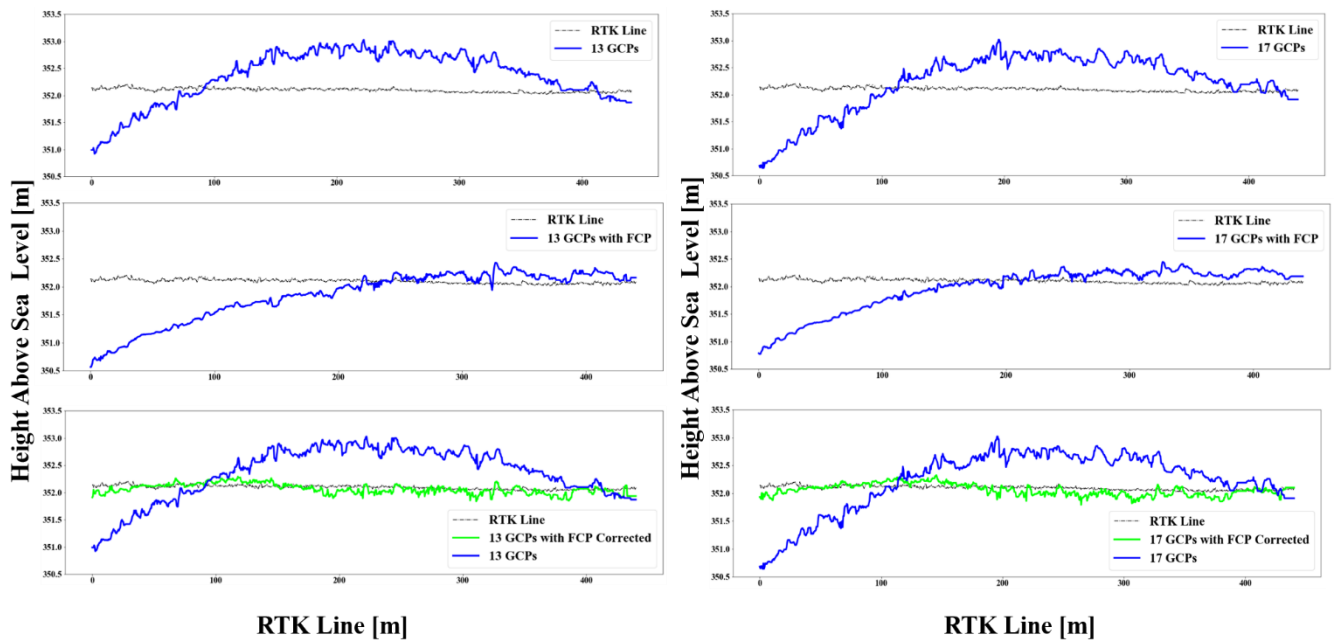


Fig. A2.2 Correcting the doming effect

Figure A2.3 shows the regression line fit through extracted tracks lines. The top left graph represents the relationship between height and track for the RTK track. The centre left graph represents the relationship between height and track for the 9 GCP. The bottom left graph represents the relationship between height and track for the 17 GCP terrain. The top right graph represents the relationship between height and track for the 5 GCP terrain. The centre right graph represents the relationship between height and track for the 13 GCP. The bottom right graph represents the relationship between height and track for the no GCP terrain

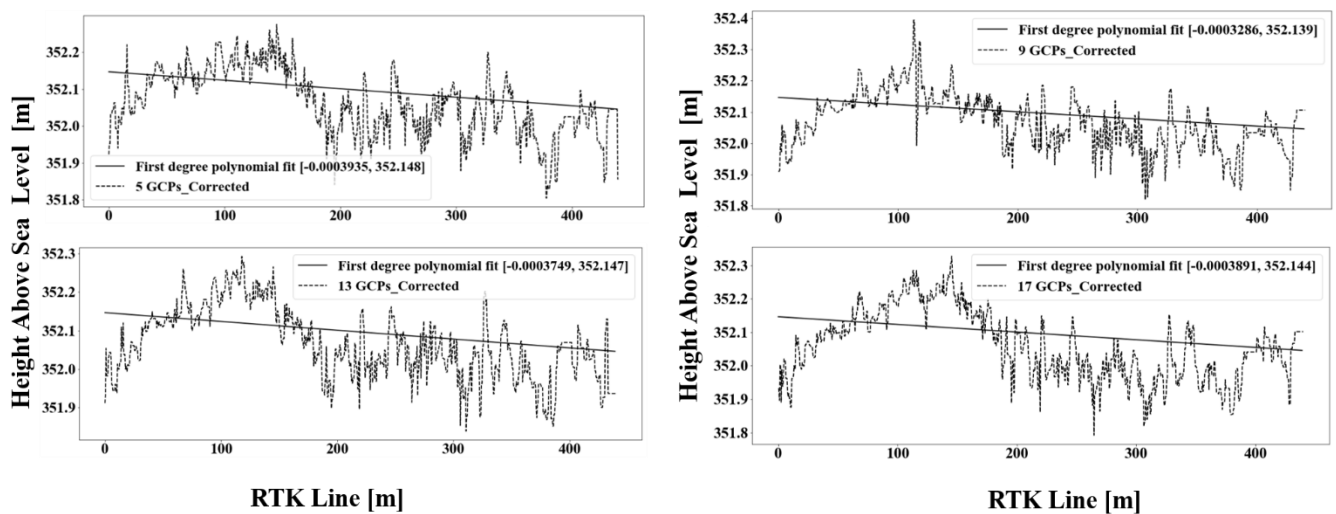


Fig.A2.3. First order polynomials through extracted tracks

Figure A2.4 shows the relationship between depth and area, as well as the relationship between depth and conveyance. The top left graph represents the relationship between depth and area at the cross section on the northern part of the terrain. The top right graph represents the relationship between depth and conveyance at the cross section on the northern part of the terrain. The two bottom left graphs represents the relationship between depth and area at the cross section on the northern part of the terrain. The bottom right graph represents the relationship between depth and conveyance at the cross section on the northern part of the terrain.

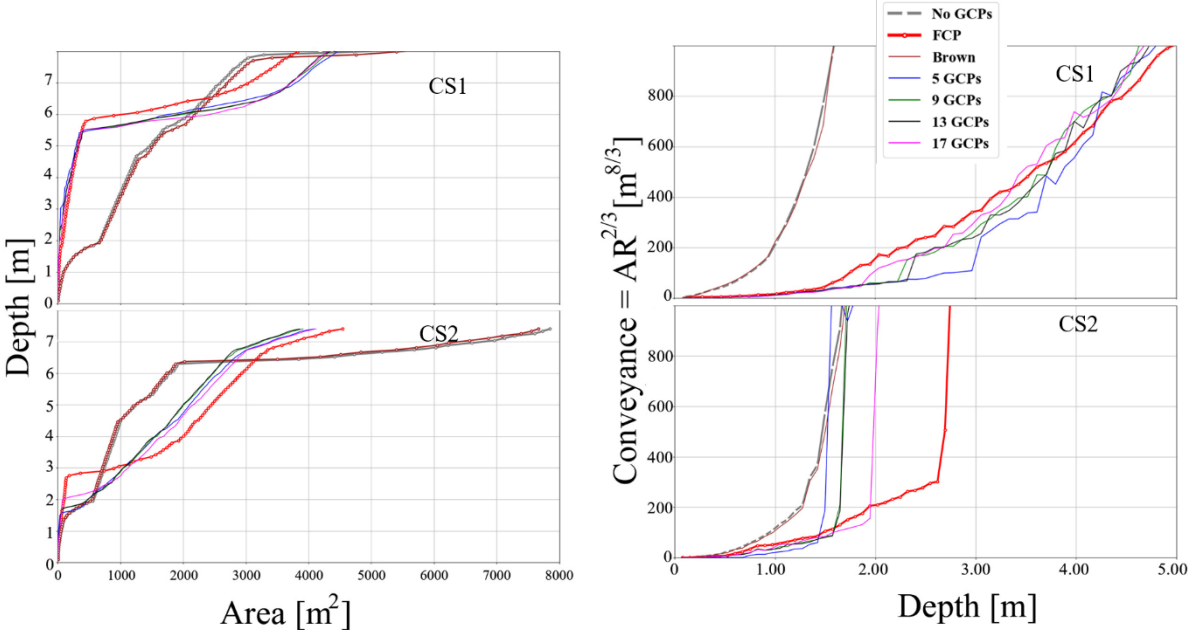


Fig. A2.4 Depth vs Area Map and Conveyance vs Depth

Figure A2.5 shows the relationships between floodplain width and height above mean sea level, as well as the relationships between wetted perimeter and area. The top left graph represents the relationship between floodplain width and height above mean sea level at the cross section on the northern part of the terrain (CS1). The top right graph represents the relationship between wetted perimeter and area at the cross section on the northern part of the terrain. The bottom left graph represents the relationship between floodplain width and height above mean sea level at the cross section on the northern part of the terrain. The bottom right graph represents the relationship between wetted perimeter and area at the cross section on the northern part of the terrain.

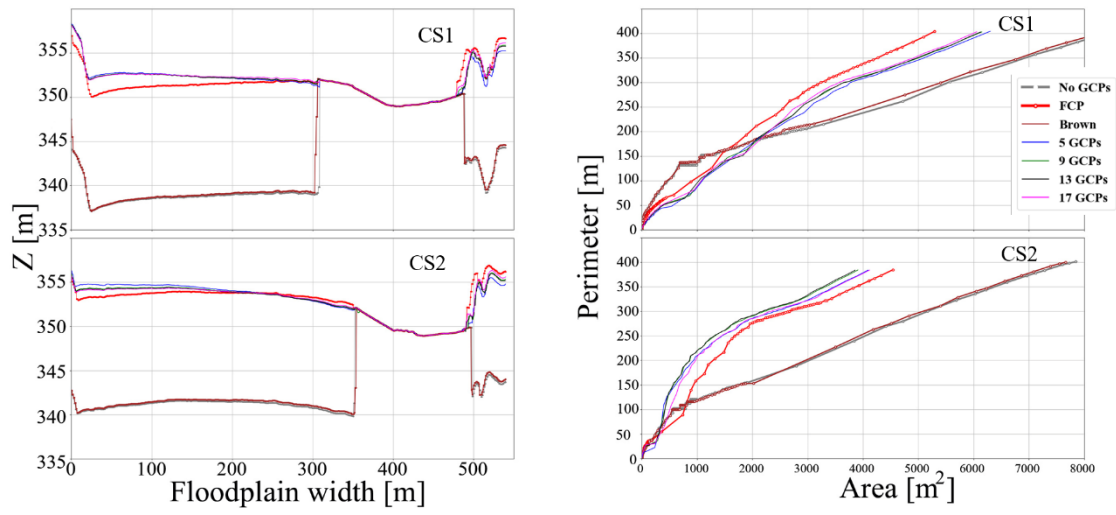


Fig. A2.5 Height vs width graph and Perimeter vs Area

Appendix B

B.1 1 D HEC-RAS model

In this annex, we describe a preliminary study which was conducted in order to determine the optimal roughness coefficient during high flows. The preliminary research was conducted in close proximity to the study currently in question. Both study locations have similar geophysical and hydraulic properties, thus, are comparable. The research methodology was divided in four stages. The first stage was data collection of discharge, bathymetry and aerial data. A DJI phantom 4 Unmanned Aerial Vehicle (UAV) with a 12 MP camera was used to collect. The second stage was processing of images and transects collected using the Unmanned Aerial Vehicle (UAV) and Acoustic Doppler Current Profiler (ADCP) respectively. The images were merged together and used to reconstruct the dry topography through photogrammetry. The third stage involved hydraulic modelling using the HEC-RAS model. The 1D steady-state hydraulic model was built and calibrated based on the ADCP measurements. In the final stage, the more physically based rating curve from the hydraulic model was compared with a traditional rating curve from the Zambian Water Resources Management Authority (WARMA).

The model output was evaluated by the Root Mean Squared Error (RMSE). The lowest value for the RMSE is obtained for a Manning's roughness coefficient of $n = 0.040 \text{ s/m}^{-1/3}$. According to literature this seems to be a reasonable value. We proceed to utilise this roughness value in the current study as a representation of the optimal roughness during high flows.

B.2 OLS Regression Results

```

=====
                        OLS Regression Results
=====
Dep. Variable:          log_Q      R-squared:                0.995
Model:                  OLS        Adj. R-squared:           0.994
Method:                 Least Squares  F-statistic:              2976.
Date:                   Thu, 03 Nov 2022  Prob (F-statistic):       1.32e-19
Time:                   07:58:12     Log-Likelihood:           28.325
No. Observations:      18          AIC:                      -52.65
Df Residuals:          16          BIC:                      -50.87
Df Model:               1
Covariance Type:       nonrobust
=====

```

	coef	std err	t	P> t	[0.025	0.975]
Intercept	1.0797	0.030	36.337	0.000	1.017	1.143
log_control	2.8092	0.051	54.552	0.000	2.700	2.918

```

=====
Omnibus:                16.412    Durbin-Watson:            0.683
Prob(Omnibus):          0.000    Jarque-Bera (JB):        16.859
Skew:                   -1.571    Prob(JB):                 0.000218
Kurtosis:               6.551    Cond. No.                 5.28
=====

```

Annex 1 OLS regression for Control

References

- Abas, I., Luxemburg, W., Banda, K. and Hubert, S.: A robust approach to physically-based rating curve development in remote rivers through UAV imagery, *Geophys. Res. Abstr.*, 21(1), 2019–5765, 2019.
- Alsdorf, D. E., Melack, J. M., Dunne, T., Mertes, L., Hess, L. and Smith, L. C.: Interferometric radar measurements of water level changes on the Amazon floodplain., *Nature*, 404, 174–177., 2000.
- Alvarez, L. V., Moreno, H. A., Segales, A. R., Pham, T. G., Pillar-Little, E. A. and Chilson, P. B.: Merging Unmanned Aerial Systems (UAS) Imagery and Echo Soundings with an Adaptive Sampling Technique for Bathymetric Surveys, *Remote Sens.* 2018, Vol. 10, Page 1362, 10(9), 1362, doi:10.3390/RS10091362, 2018.
- Arcement, G. J. and Schneider, V. R.: Guide for selecting Manning's roughness coefficients for natural channels and flood plains, *Water Supply Pap.*, doi:10.3133/WSP2339, 1989.
- Ardıçlıoğlu, M. and Kuriqi, A.: Calibration of channel roughness in intermittent rivers using HEC-RAS model: case of Sarımsaklı creek, Turkey, *SN Appl. Sci.*, 1(9), 1–9, doi:10.1007/S42452-019-1141-9/FIGURES/6, 2019.
- Armstrong, D. W., Holnbeck, S. R. and Chase, K. J.: Evaluating the use of video cameras to estimate bridge scour potential at four bridges in southwestern Montana, *Fact Sheet*, doi:10.3133/FS20223040, 2022.
- Awasthi, B., Karki, S., Regmi, P., Dhimi, D. S., Thapa, S. and Panday, U. S.: Analyzing the Effect of Distribution Pattern and Number of GCPs on Overall Accuracy of UAV Photogrammetric Results, *Lect. Notes Civ. Eng.*, 51, 339–354, doi:10.1007/978-3-030-37393-1_29, 2019.
- Balogh, A. and Kiss, K. A.: Photogrammetric processing of aerial photographs acquired by UAVs, *Hungarian Archaeol.*, 40, 1–8. [online] Available from: https://www.academia.edu/7070293/Photogrammetric_processing_of_aerial_photographs_acquired_by_UAVs (Accessed 2 April 2019), 2014.
- Bandini, F., Olesen, D., Jakobsen, J., Kittel, C. M. M., Wang, S., Garcia, M. and Bauer-Gottwein, P.: Bathymetry observations of inland water bodies using a tethered single-beam sonar controlled by an Unmanned Aerial Vehicle, *Hydrol. Earth Syst. Sci. Discuss.*, 1–23, doi:10.5194/hess-2017-625, 2017.
- Beat, L., Philippe, T. and Peña-Haro, S.: Mobile device app for small open-channel flow measurement. [online] Available from: <https://scholarsarchive.byu.edu/iemssconference/2014/Stream-A/36> (Accessed 5 January 2019), 2014.
- Biancam, S., Lettenmaier, D. P. and Pavelsky, T. M.: The SWOT mission and capabilities for land hydrology, *T.M. Surv Geophys*, 2016.
- Bird, S., Hogan, D. and Schwab, J.: Photogrammetric monitoring of small streams under a riparian forest canopy, *Earth Surf. Process. Landforms*, 35(8), 952–970, doi:10.1002/esp.2001, 2010.

- Bjerklie, D. M., Moller, D., Smith, L. C. and Dingman, S. L.: Estimating discharge in rivers using remotely sensed hydraulic information, *J. Hydrol.*, 309(1–4), 191–209, doi:10.1016/j.jhydrol.2004.11.022, 2005.
- Bogning, S., Frappart, F., Blarel, F., Niño, F., Mahé, G., Bricquet, J.-P., Seyler, F., Onguéné, R., Etamé, J., Paiz, M.-C. and Braun, J.-J.: Monitoring Water Levels and Discharges Using Radar Altimetry in an Ungauged River Basin: The Case of the Ogooué, *Remote Sens.*, 10(3), 350, doi:10.3390/rs10020350, 2018.
- Le Boursicaud, R., Pénard, L., Hauet, A., Thollet, F. and Le Coz, J.: Gauging extreme floods on YouTube: Application of LSPIV to home movies for the post-event determination of stream discharges, *Hydrol. Process.*, 30(1), 90–105, doi:10.1002/HYP.10532, 2016.
- Brakenridge, G. R., Nghiem, S. V., Anderson, E. and Mic, R.: Orbital microwave measurement of river discharge and ice status, *Water Resour. Res.*, 43(4), doi:10.1029/2006WR005238, 2007.
- Burdziakowski, P.: Evaluation of open drone map toolkit for geodetic grade aerial drone mapping – case study, *Int. Multidiscip. Sci. GeoConference Surv. Geol. Min. Ecol. Manag. SGEM*, 17(23), 101–110, doi:10.5593/SGEM2017/23/S10.013, 2017.
- Burns, J. H. R. and Delparte, D.: Comparison of commercial structure-from-motion photogrammetry software used for underwater three-dimensional modeling of coral reef environments, *Int. Arch. Photogramm. Remote Sens. Spat. Inf. Sci. - ISPRS Arch.*, 42(2W3), 127–131, doi:10.5194/isprs-archives-XLII-2-W3-127-2017, 2017.
- CDS: Flood Management in Mozambique, [online] Available from: www.wmo.int (Accessed 31 January 2023), 2007.
- Chandler, J., Ashmore, P., Paola, C., Gooch, M. and Varkaris, F.: Monitoring River-Channel Change Using Terrestrial Oblique Digital Imagery and Automated Digital Photogrammetry, *Ann. Assoc. Am. Geogr.*, 92(4), 631–644, doi:10.1111/1467-8306.00308, 2002.
- Chauhan, M., Kumar, V., Dikshit, P. and Dwivedi, S.: Comparison of discharge data using ADCP and current meter., *Int J Adv Earth Sci* 3(2), 81–86, 2014.
- Chawla, I., Karthikeyan, L. and Mishra, A. K.: A review of remote sensing applications for water security: Quantity, quality, and extremes, *J. Hydrol.*, 585, 124826, doi:10.1016/J.JHYDROL.2020.124826, 2020.
- Chow, V.: *Open-channel hydraulics.*, McGraw-Hill Book Company, New York., 1959.
- Colomina, I. and Molina, P.: Unmanned aerial systems for photogrammetry and remote sensing: A review, *ISPRS J. Photogramm. Remote Sens.*, 92, 79–97, doi:10.1016/J.ISPRSJPRS.2014.02.013, 2014.
- Comina, C., Lasagna, M., De Luca, D. and Sambuelli, L.: Geophysical methods to support correct water sampling locations for salt dilution gauging., *Hydrol Earth Syst Sci* 18(8)3195–3203, 2014.
- Cooley, S. W., Ryan, J. C. and Smith, L. C.: Human alteration of global surface water storage variability, *Nat.* 2021 5917848, 591(7848), 78–81, doi:10.1038/s41586-021-03262-3, 2021.

- Coppo Frias, M., Liu, S., Mo, X., Nielsen, K., Rannal, H., Jiang, L., Ma, J. and Bauer-Gottwein, P.: River hydraulic modeling with ICESat-2 land and water surface elevation, *Hydrol. Earth Syst. Sci.*, 27(5), 1011–1032, doi:10.5194/HESS-27-1011-2023, 2023.
- Costa, J., Cheng, R., Haeni, F., Melcher, N., Spicer, K., Hayes, E., Plant, W., Hayes, K., Teague, C. and Barrick, D.: Use of radars to monitor stream discharge, by noncontact methods. *Water Resour. Res.* 42(7), 1–14, 2006.
- Costa, J. E., Spicer, K. R., Cheng, R. T., Haeni, F. P., Melcher, N. B., Thurman, E. M., Plant, W. J. and Keller, W. C.: Measuring stream discharge by non-contact methods: A proof-of-concept experiment. [online] Available from: <http://citeseerx.ist.psu.edu/viewdoc/download;jsessionid=402EFED54B1E25BD2513F8455430828D?doi=10.1.1.469.2760&rep=rep1&type=pdf> (Accessed 26 December 2018), 2000.
- Coveney, S. and Roberts, K.: Lightweight UAV digital elevation models and orthoimagery for environmental applications: data accuracy evaluation and potential for river flood risk modelling, *Int. J. Remote Sens.*, 38(8–10), 3159–3180, doi:10.1080/01431161.2017.1292074, 2017.
- Le Coz, J., Hauet, A., Pierrefeu, G., Dramais, G. and Camenen, B.: Performance of image-based velocimetry (LSPIV) applied to flash-flood discharge measurements in Mediterranean rivers, *J. Hydrol.*, 394(1–2), 42–52, doi:10.1016/J.JHYDROL.2010.05.049, 2010.
- Le Coz, J., Jodeau, M., Hauet, A., Marchand, B. and Le Boursicaud, R.: Image-based velocity and discharge measurements in field and laboratory river engineering studies using the free FUDAA-LSPIV software, *Proc. Int. Conf. Fluv. Hydraul. RIVER FLOW 2014*, 1961–1967, doi:10.1201/B17133-262, 2014.
- Cucchiaro, S., Cavalli, M., Vericat, D., Crema, S., Llena, M., Beinat, A., Marchi, L. and Cazorzi, F.: Monitoring topographic changes through 4D-structure-from-motion photogrammetry: application to a debris-flow channel, *Environ. Earth Sci.*, 77(18), 632, doi:10.1007/s12665-018-7817-4, 2018.
- Dal Sasso, S. F., Pizarro, A., Pearce, S., Maddock, I. and Manfreda, S.: Increasing LSPIV performances by exploiting the seeding distribution index at different spatial scales, *J. Hydrol.*, 598, 126438, doi:10.1016/J.JHYDROL.2021.126438, 2021.
- Deltares: D-Flow Flexible Mesh User Manual., 2020.
- Dey, S., Saksena, S. and Merwade, V.: Assessing the effect of different bathymetric models on hydraulic simulation of rivers in data sparse regions, *J. Hydrol.*, 575, 838–851, doi:10.1016/J.JHYDROL.2019.05.085, 2019.
- Van Dijk, A. I. J. M., Brakenridge, G. R., Kettner, A. J., Beck, H. E., De Groeve, T. and Schellekens, J.: River gauging at global scale using optical and passive microwave remote sensing, *Water Resour. Res.*, 52(8), 6404–6418, doi:10.1002/2015WR018545, 2016.
- Dobriyal, P., Badola, R., Tuboi, C. and Hussain, S. A.: A review of methods for monitoring streamflow for sustainable water resource management, *Appl. Water Sci.*, 7(6), 2617–2628,

doi:10.1007/s13201-016-0488-y, 2017.

- Donchyts, G., Baart, F., Winsemius, H., Gorelick, N., Kwadijk, J. and van de Giesen, N.: Earth's surface water change over the past 30 years, *Nat. Clim. Chang.*, 6(9), 810–813, doi:10.1038/nclimate3111, 2016.
- Du, T. L., Lee, H., Bui, D. D., Arheimer, B., Li, H.-Y. and Kim, D.: Streamflow prediction in “geopolitically ungauged” basins using satellite, 2020.
- Fakhri, A., Ettema, R., Aliyari, F. and Nowroozpour, A.: Large-Scale Particle Image Velocimetry for Estimating Vena-Contracta Width for Flow in Contracted Open Channels, *Water* 2021, Vol. 13, Page 31, 13(1), 31, doi:10.3390/W13010031, 2020.
- Ferrer-González, E., Agüera-Vega, F., Carvajal-Ramírez, F. and Martínez-Carricondo, P.: UAV photogrammetry accuracy assessment for corridor mapping based on the number and distribution of ground control points, *Remote Sens.*, 12(15), 2447, doi:10.3390/RS12152447, 2020.
- Feurer, D., Bailly, J.-S., Puech, C., Le Coarer, Y. and Viau, A.: Very-high-resolution mapping of river-immersed topography by remote sensing. [online] Available from: <https://hal.archives-ouvertes.fr/hal-00585200> (Accessed 20 April 2021), 2008.
- Fiedler, K., Strobl, T., Zunic, F. and Matthes, H.: Velocity gauging with ADCP in rivers with bedload and sediment transport, 2009.
- Filippucci, P., Brocca, L., Bonafoni, S., Saltalippi, C., Wagner, W. and Tarpanelli, A.: Sentinel-2 high-resolution data for river discharge monitoring, *Remote Sens. Environ.*, 281, 113255, doi:10.1016/J.RSE.2022.113255, 2022.
- Flener, C., Wang, Y., Laamanen, L., Kasvi, E., Vesakoski, J.-M., Alho, P., Flener, C., Wang, Y., Laamanen, L., Kasvi, E., Vesakoski, J.-M. and Alho, P.: Empirical Modeling of Spatial 3D Flow Characteristics Using a Remote-Controlled ADCP System: Monitoring a Spring Flood, *Water*, 7(12), 217–247, doi:10.3390/w7010217, 2015.
- Fujita, I. and Hino, T.: Unseeded and Seeded PIV Measurements of River Flows Videotaped from a Helicopter, *J. Vis.*, 6(3), 245–252, doi:10.1007/BF03181465, 2003.
- Gindraux, S., Boesch, R. and Farinotti, D.: Accuracy Assessment of Digital Surface Models from Unmanned Aerial Vehicles' Imagery on Glaciers, *Remote Sens.*, 9(2), 186, doi:10.3390/rs9020186, 2017.
- Gordon, N., TA, M., BL, F., CJ, G. and RJ, N.: (2013), in *Stream hydrology: an introduction for ecologists*. Wiley, England., 2013.
- De Groeve, T.: Flood monitoring and mapping using passive microwave remote sensing in Namibia., *Geomatics, Nat. Hazards Risk*, 1(1), 19–35., 2010.
- Gumindoga, W., Rientjes, T. H. M., Tamiru Haile, A., Makurira, H. and Reggiani, P.: Performance of bias-correction schemes for CMORPH rainfall estimates in the Zambezi River Basin, *Hydrol. Earth Syst. Sci.*, 23(7), 2915–2938, doi:10.5194/HESS-23-2915-2019, 2019.
- Gustafsson, H. and Zuna, L.: Unmanned Aerial Vehicles for Geographic Data Capture: A Review,

- [online] Available from: <http://www.diva-portal.org/smash/record.jsf?pid=diva2%3A1116742&dsid=9725> (Accessed 26 December 2018), 2017.
- Hamududu, B. H. and Ngoma, H.: Impacts of climate change on water resources availability in Zambia: implications for irrigation development, *Environ. Dev. Sustain. A Multidiscip. Approach to Theory Pract. Sustain. Dev.*, 22(4), 2817–2838, doi:10.1007/S10668-019-00320-9, 2020.
- Hauet, A., Creutin, J.-D. and Belleudy, P.: Sensitivity study of large-scale particle image velocimetry measurement of river discharge using numerical simulation, *J. Hydrol.*, 349(1–2), 178–190, doi:10.1016/J.JHYDROL.2007.10.062, 2008a.
- Hauet, A., Creutin, J.-D. and Belleudy, P.: Sensitivity study of large-scale particle image velocimetry measurement of river discharge using numerical simulation, *J. Hydrol.*, 349(1–2), 178–190, doi:10.1016/j.jhydrol.2007.10.062, 2008b.
- Herschty, R. W.: *Streamflow measurement*, Routledge. [online] Available from: <https://epdf.tips/streamflow-measurement-third-edition.html> (Accessed 28 March 2019), 2009.
- Heusinkveld, H.: *Mobile Water Management*, [online] Available from: <https://www.tudelft.nl/myanmar/innovations/mobile-water-management/> (Accessed 17 April 2019), 2014.
- Hrachowitz, M., Savenije, H. H. G., Blöschl, G., McDonnell, J. J., Sivapalan, M., Pomeroy, J. W., Arheimer, B., Blume, T., Clark, M. P., Ehret, U., Fenicia, F., Freer, J. E., Gelfan, A., Gupta, H. V., Hughes, D. A., Hut, R. W., Montanari, A., Pande, S., Tetzlaff, D., Troch, P. A., Uhlenbrook, S., Wagener, T., Winsemius, H. C., Woods, R. A., Zehe, E. and Cudennec, C.: A decade of Predictions in Ungauged Basins (PUB)—a review, *Hydrology and Earth System Sciences*, 17(6), 1198–1255, doi:10.1080/02626667.2013.803183, 2013.
- Hudson, N.: *Field measurement of soil erosion and runoff*, Rome : Food and Agriculture Organization of the United Nations. [online] Available from: <https://www.worldcat.org/title/field-measurement-of-soil-erosion-and-runoff/oclc/49888870> (Accessed 20 January 2019), 1993.
- International Monetary Fund: *Building resilience in developing countries vulnerable to large natural disasters.*, , 55 [online] Available from: <https://www.bookstore.imf.org/books/building-resilience-in-developing-countries-vulnerable-to-large-natural-disasters> (Accessed 31 January 2023), 2019.
- Jebur, A., Abed, F. and Mohammed, M.: Assessing the performance of commercial Agisoft PhotoScan software to deliver reliable data for accurate 3D modelling, edited by T. S. Al-Attar, M. A. Al-Neami, and W. S. AbdulSahib, *MATEC Web Conf.*, 162, 03022, doi:10.1051/mateconf/201816203022, 2018.
- Jiang, Y., Cui, Y. and Li, B.: Study on Differential GPS (DGPS): Method for Reducing the Measurement Error of GNSS, *Adv. Mater. Res.*, 482–484, 75–80,

doi:10.4028/WWW.SCIENTIFIC.NET/AMR.482-484.75, 2012.

- Jodeau, M., Hauet, A., Le Coz, J., Bercovitz, Y. and Lebert, F.: Laboratory and field LSPIV measurements of flow velocities using Fudaa-LSPIV a free user-friendly software Fudaa-Lspiv : a user friendly software View project Fluorimetry for hydrogeology View project HydroSenSoft, International Symposium and Exhibition on Hydro-Environment Sensors and LABORATORY AND FIELD LSPIV MEASUREMENTS OF FLOW VELOCITIES USING FUDAA-LSPIV, A FREE USER-FRIENDLY SOFTWARE, in HydroSenSoft, International Symposium and Exhibition on Hydro-Environment Sensors and Software. [online] Available from: <https://forge.irstea.fr/projects/fudaa-lspiv/files>. (Accessed 17 April 2019), 2017.
- Kim, E. and Kim, S. K.: Global Navigation Satellite System Real-Time Kinematic Positioning Framework for Precise Operation of a Swarm of Moving Vehicles, *Sensors* 2022, Vol. 22, Page 7939, 22(20), 7939, doi:10.3390/S22207939, 2022.
- Kim, Y.: Uncertainty analysis for non-intrusive measurement of river discharge using image velocimetry, [online] Available from: <https://www.gettextbooks.com/isbn/9780542833311/> (Accessed 6 January 2019), 2006.
- Kim, Y., Muste, M., Hauet, A., Krajewski, W. F., Kruger, A. and Bradley, A.: Stream discharge using mobile large-scale particle image velocimetry: A proof of concept, *Water Resour. Res.*, 44(9), 9502, doi:10.1029/2006WR005441, 2008.
- Kuzmin, V., Pivovarova, I., Shemanaev, K., Sokolova, D., Batyrov, A., Tran, N. A. and Dang, D. K.: Method of Prediction the Stream Flows in Poorly Gauged and Ungauged Basins, *J. Ecol. Eng.*, 20(1), 180–187, doi:10.12911/22998993/94915, 2019.
- Lamichhane, S. and Shakya, N. M.: Integrated Assessment of Climate Change and Land Use Change Impacts on Hydrology in the Kathmandu Valley Watershed, Central Nepal, *Water* 2019, Vol. 11, Page 2059, 11(10), 2059, doi:10.3390/W11102059, 2019.
- Lane, S. N.: The Measurement of River Channel Morphology Using Digital Photogrammetry, *Photogramm. Rec.*, 16(96), 937–961, doi:10.1111/0031-868X.00159, 2000.
- Lewis, Q. W. and Rhoads, B. L.: LSPIV Measurements of Two-Dimensional Flow Structure in Streams Using Small Unmanned Aerial Systems: 2. Hydrodynamic Mapping at River Confluences, *Water Resour. Res.*, 54(10), 7981–7999, doi:10.1029/2018WR022551, 2018.
- Lewis, Q. W., Lindroth, E. M. and Rhoads, B. L.: Integrating unmanned aerial systems and LSPIV for rapid, cost-effective stream gauging, *J. Hydrol.*, 560, 230–246, doi:10.1016/J.JHYDROL.2018.03.008, 2018a.
- Lewis, Q. W., Lindroth, E. M. and Rhoads, B. L.: Integrating Unmanned Aerial Systems and LSPIV for Rapid, Cost-effective Stream Gauging, [online] Available from: <http://www.elsevier.com/open-access/userlicense/1.0/> (Accessed 4 February 2023b), 2018.
- Lin, Y.-T., Han, J.-Y. and Lin, Y.-C.: Automatic Water-Level Detection Using Single-Camera Images with Varied Poses, , doi:10.1016/j.measurement.2018.05.100, 2018.

- Liu, H., Shao, Q., Kang, C. and Li, J.: Flow Characteristics and Cavitation Effect of the Submerged Water Jet Discharged from a Central-Body Nozzle, *World J. Eng. Technol.*, 2, 281–288, doi:10.4236/wjet.2014.24029, 2014.
- Liu, X., Zhang, Z., Peterson, J. and Chandra, S.: Large Area DEM Generation Using Airborne LiDAR Data and Quality Control, 2008.
- Mansanarez, V., Westerberg, I. K., Lam, N. and Lyon, S. W.: Rapid Stage-Discharge Rating Curve Assessment Using Hydraulic Modeling in an Uncertainty Framework, *Water Resour. Res.*, 55(11), 9765–9787, doi:10.1029/2018WR024176, 2019.
- Martínez-Carricondo, P., Agüera-Vega, F., Carvajal-Ramírez, F., Mesas-Carrascosa, F. J., García-Ferrer, A. and Pérez-Porras, F. J.: Assessment of UAV-photogrammetric mapping accuracy based on variation of ground control points, *Int. J. Appl. Earth Obs. Geoinf.*, 72, 1–10, doi:10.1016/J.JAG.2018.05.015, 2018.
- Moore, D.: Introduction to Salt Dilution Gauging for Streamflow Measurement Part 2: Constant-rate Injection. [online] Available from: <https://pdfs.semanticscholar.org/4210/42e4d7a842b6be48ec746b1453a82fb3ed5e.pdf> (Accessed 20 January 2019), 2004.
- Moramarco, T. and Ranzi, R.: Advances in Hydro-Meteorological Monitoring, *Adv. Hydro-Meteorological Monit.*, doi:10.3390/BOOKS978-3-03842-978-4, 2018.
- Moriasi, D. N., Arnold, J. G., Liew, M. W. Van, Bingner, R. L., Harmel, R. D. and Veith, T. L.: MODEL EVALUATION GUIDELINES FOR SYSTEMATIC QUANTIFICATION OF ACCURACY IN WATERSHED SIMULATIONS, *Trans. ASABE*, 50(3), 1983.
- Mosley, M. . and McKerchar, A. .: Handbook of hydrology. [online] Available from: http://dl.watereng.ir/HANDBOOK_OF_HYDROLOGY.PDF (Accessed 27 April 2021), 1993.
- Mueller, D. S., Wagner, C. R., Rehmel, M. S., Oberg, K. A. and Rainville, F.: Measuring discharge with acoustic Doppler current profilers from a moving boat, *Tech. Methods*, doi:10.3133/TM3A22, 2013.
- Muste, M., Fujita, I. and Hauet, A.: Large-scale particle image velocimetry for measurements in riverine environments, *Water Resour. Res.*, 44(4), 0–19, doi:10.1029/2008WR006950, 2008.
- Muste, M., Fujita, I. and Hauet, A.: Large-scale particle image velocimetry for measurements in riverine environments, *Water Resour. Res.*, 46(4), doi:10.1029/2008WR006950, 2010.
- Oniga, V. E., Breaban, A. I., Pfeifer, N. and Chirila, C.: Determining the suitable number of ground control points for UAS images georeferencing by varying number and spatial distribution, *Remote Sens.*, 12(5), doi:10.3390/RS12050876, 2020.
- Pearce, S., Ljubicic, R., Peña-Haro, S., Perks, M., Tauro, F., Pizarro, A., Dal Sasso, S. F., Strelnikova, D., Grimaldi, S., Maddock, I., Paulus, G., Plavšic, J., Prodanovic, D. and Manfreda, S.: An Evaluation of Image Velocimetry Techniques under Low Flow Conditions and High Seeding Densities Using Unmanned Aerial Systems, *Remote Sens.* 2020, Vol. 12, Page 232, 12(2), 232,

doi:10.3390/RS12020232, 2020.

- Petersen-Øverleir, A., Soot, A. and Reitan, T.: Bayesian rating curve inference as a streamflow data quality assessment tool, *Water Resour. Manag.*, 23(9), 1835–1842, doi:10.1007/s11269-008-9354-5, 2009.
- Peyret, F., Bétaille, D. and Hintzy, G.: High-precision application of GPS in the field of real-time equipment positioning, *Autom. Constr.*, 9(3), 299–314, doi:10.1016/S0926-5805(99)00058-8, 2000.
- Plant, W. J. and Keller, W. C.: Evidence of Bragg scattering in microwave doppler spectra of sea return, *J. Geophys. Res.*, 95, 299–16,310, 1990.
- Rafik, H. and Ibrenk, H. O.: Environmental and Water Resources Management ENVIRONMENT STRATEGY PAPERS NO. 2 Rafik Hirji Hans Olav Ibrenk, 2001.
- Rantz, S. E. and Others, A.: Measurement and Computation of Streamflow: Volume 1. Measurement of Stage and Discharge, Vol. 1 - Meas. Stage Discharge, USGS Water Supply Pap. 2175, 1, 313, doi:10.1029/WR017i001p00131, 1982.
- Revilla-Romero, B., Thielen, J., Salamon, P., De Groeve, T. and Brakenridge, G. R.: Evaluation of the satellite-based Global Flood Detection System for measuring river discharge: influence of local factors, *Hydrol. Earth Syst. Sci.*, 18(11), 4467–4484, doi:10.5194/hess-18-4467-2014, 2014.
- Sainz Sanchez, G.: The Zambezi River Basin: water resources management Energy-Food-Water nexus approach, 2018.
- Salamí, E., Barrado, C. and Pastor, E.: UAV Flight Experiments Applied to the Remote Sensing of Vegetated Areas, *Remote Sens.*, 6(11), 11051–11081, doi:10.3390/rs61111051, 2014.
- Saleh, F., Ducharme, A., Flipo, N., Oudin, L. and Ledoux, E.: Impact of river bed morphology on discharge and water levels simulated by a 1D Saint-Venant hydraulic model at regional scale, *J. Hydrol.*, 476, 169–177, doi:10.1016/J.JHYDROL.2012.10.027, 2013.
- Salguero, L., Quinones, A. and Ackerman, L.: Wastewater flow management., US Environ. Prot. Agency Sci. Ecosyst. Support Div. Georg., 2008.
- Samboko, H. T., Abasa, I., Luxemburg, W. M. J., Savenije, H. H. G., Makurira, H., Banda, K. and Winsemius, H. C.: Evaluation and improvement of Remote sensing-based methods for River flow Management, *Phys. Chem. Earth*, 2019.
- Samboko, H. T., Schurer, S., Savenije, H. H. G., Makurira, H., Banda, K. and Winsemius, H.: Evaluating low-cost topographic surveys for computations of conveyance, *Geosci. Instrumentation, Methods Data Syst.*, 11(1), 1–23, doi:10.5194/gi-11-1-2022, 2022.
- Schaefer, M. and Woodyer, T.: Assessing absolute and relative accuracy of recreation-grade and mobile phone GNSS devices: A method for informing device choice, *Area*, 47(2), 185–196, doi:10.1111/AREA.12172, 2015.
- Schenk, T. and Quarter, A.: Introduction to Photogrammetry. [online] Available from: <http://www.mat.uc.pt/~gil/downloads/IntroPhoto.pdf> (Accessed 2 April 2019), 2005.

- Schweitzer, S. A. and Cowen, E. A.: Large Scale Infrared-Based Remote Sensing of Turbulence Metrics in Surface Waters: Going Beyond Mean Flow, 14th Int. Symp. Part. Image Velocim., 1(1), doi:10.18409/ISPIV.V1I1.53, 2021.
- Sentlinger, G.: Salt Dilution Flow Measurement: Automation and Uncertainty. [online] Available from: <https://meetingorganizer.copernicus.org/EGU2019/EGU2019-58.pdf> (Accessed 20 April 2019), 2019.
- Sheffield, J., Wood, E. F., Chaney, N., Guan, K., Sadri, S., Yuan, X., Olang, L., Amani, A., Ali, A., Demuth, S. and Ogallo, L.: A drought monitoring and forecasting system for sub-sahara african water resources and food security, *Bull. Am. Meteorol. Soc.*, 95(6), 861–882, doi:10.1175/BAMS-D-12-00124.1, 2014.
- Shiklomanov, A., Lammers, R. and Vörösmarty, C.: Widespread decline in hydrological monitoring threatens pan- Arctic research., *AGU EOS- Trans.*, (83,), 16–17, 2002.
- Skondras, A., Karachaliou, E., Tavantzis, I., Tokas, N., Valari, E., Skalidi, I., Bouvet, G. A. and Stylianidis, E.: UAV Mapping and 3D Modeling as a Tool for Promotion and Management of the Urban Space, *Drones 2022*, Vol. 6, Page 115, 6(5), 115, doi:10.3390/DRONES6050115, 2022.
- Smith, M. W., Carrivick, J. L. and Quincey, D. J.: Structure from motion photogrammetry in physical geography:, <http://dx.doi.org/10.1177/0309133315615805>, 40(2), 247–275, doi:10.1177/0309133315615805, 2015.
- Strijker, B.: Improving Rating Curve Computation, 2017.
- Tauro, F., Petroselli, A. and Arcangeletti, E.: Assessment of drone-based surface flow observations, *Hydrol. Process.*, 30(7), 1114–1130, doi:10.1002/hyp.10698, 2016a.
- Tauro, F., Porfiri, M. and Grimaldi, S.: Surface flow measurements from drones, *J. Hydrol.*, 540, 240–245, doi:10.1016/J.JHYDROL.2016.06.012, 2016b.
- Temimi, M., Leconte, R., Brissette, F. and Chaouch, N.: Flood monitoring over the Mackenzie River Basin using passivemicrowave data., *Remote Sens. Environ.*, 98, 344–355., 2005.
- The World Bank: The Zambezi River Basin. Technical report, Washington DC., 2010.
- u-blox: u-center | u-blox, [online] Available from: <https://www.u-blox.com/en/product/u-center> (Accessed 21 September 2021), 2021.
- Vermeyen, T. B.: Using an ADCP, Depth Sounder, and GPS for Bathymetric Surveys, *Examining Conflu. Environ. Water Concerns - Proc. World Environ. Water Resour. Congr. 2006*, 1–10, doi:10.1061/40856(200)172, 2007.
- Ward, D. P., Hamilton, S. K., Jardine, T. D., Pettit, N. E., Tews, E. K., Olley, J. M. and Bunn, S. E.: Assessing the seasonal dynamics of inundation, turbidity, and aquatic vegetation in the Australian wet-dry tropics using optical remote sensing, *Ecohydrology*, 6(2), 312–323, doi:10.1002/eco.1270, 2013.
- WARMA: Luangwa Catchment., [online] Available from: <http://www.warma.org.zm/index.php/%0Acatchments/luangwa-catchment> (Accessed 4

September 2019), 2016.

- Westoby, M. J., Brasington, J., Glasser, N. F., Hambrey, M. J. and Reynolds, J. M.: 'Structure-from-Motion' photogrammetry: A low-cost, effective tool for geoscience applications, *Geomorphology*, 179, 300–314, doi:10.1016/j.geomorph.2012.08.021, 2012.
- WinRiver: WinRiver User's Guide RD Instruments Acoustic Doppler Solutions, 2001.
- Winsemius, H.: Satellite data as complementary information for hydrological modelling., 2008.
- Woodget, A. S., Austrums, R., Maddock, I. P. and Habit, E.: Drones and digital photogrammetry: from classifications to continuums for monitoring river habitat and hydromorphology, *Wiley Interdiscip. Rev. Water*, 4(4), e1222, doi:10.1002/wat2.1222, 2017a.
- Woodget, A. S., Austrums, R., Maddock, I. P. and Habit, E.: Drones and digital photogrammetry: from classifications to continuums for monitoring river habitat and hydromorphology, *Wiley Interdiscip. Rev. Water*, 4(4), e1222, doi:10.1002/WAT2.1222, 2017b.
- Wu, W. and Wang, S. S. Y.: Movable Bed Roughness in Alluvial Rivers, *J. Hydraul. Eng.*, 125(12), 1309–1312, doi:10.1061/(ASCE)0733-9429(1999)125:12(1309), 1999.
- Yamazaki, D., Ikeshima, D., Sosa, J., Bates, P. D., Allen, G. H. and Pavelsky, T. M.: MERIT Hydro: A High-Resolution Global Hydrography Map Based on Latest Topography Dataset, *Water Resour. Res.*, 55(6), 5053–5073, doi:10.1029/2019WR024873, 2019.
- Yang, C., Everitt, J. H. and Bradford, J. M.: Comparison of QuickBird Satellite Imagery and Airborne Imagery for Mapping Grain Sorghum Yield Patterns, *Precis. Agric.*, 7, 2006.
- Yao, H., Qin, R. and Chen, X.: Unmanned Aerial Vehicle for Remote Sensing Applications—A Review, *Remote Sens.* 2019, Vol. 11, Page 1443, 11(12), 1443, doi:10.3390/RS11121443, 2019.
- Zambia: Water Resources Management Act, 2011 (No. 21 of 2011). | UNEP Law and Environment Assistance Platform, [online] Available from: <https://leap.unep.org/countries/zm/national-legislation/water-resources-management-act-2011-no-21-2011> (Accessed 31 January 2023), 2011.
- Zedel, L., Wang, Y., Davidson, F. and Xu, J.: Comparing ADCP data collected during a seismic survey off the coast of Newfoundland with analysis data from the CONCEPTS operational ocean model, <https://doi.org/10.1080/1755876X.2018.1465337>, 11(2), 100–111, doi:10.1080/1755876X.2018.1465337, 2018.
- Zheng, X., Tarboton, D. G., Maidment, D. R., Liu, Y. Y. and Passalacqua, P.: River Channel Geometry and Rating Curve Estimation Using Height above the Nearest Drainage, *J. Am. Water Resour. Assoc.*, 54(4), 785–806, doi:10.1111/1752-1688.12661, 2018.
- Zhu, X. and Lipeme Kouyi, G.: An Analysis of LSPIV-Based Surface Velocity Measurement Techniques for Stormwater Detention Basin Management, *Water Resour. Res.*, doi:10.1029/2018WR023813, 2019.
- Zidan, A.: REVIEW OF FRICTION FORMULAE IN OPEN CHANNEL FLOW, *Int. water Technol.*, 5(1), 2015.

Zimba, H., Kawawaa, B., Chabalaa, A., Phiria, W., Selsamb, P. and Markus Meinhardt Nyambe, I.:
Assessment of trends in inundation extent in the Barotse Floodplain, upper Zambezi River Basin:
A remote sensing-based approach, J. Hydrol. Reg. Stud., 2018.

Acknowledgements

This PhD research was part of the research project “Enhancing Water, Food and Energy Security in the Lower Zambezi” (ZAMSECUR). The overall objective of this project was to improve the water management in the Lower Zambezi basin by enhancing knowledge on the water resources of its mostly ungauged tributaries in Zimbabwe, Zambia and Mozambique. This study was a phenomenal journey which started well before the official commencement in 2018. I would say it began with a fascinating trip to the Lower Zambezi in the company of Bart Strijker, Wim Luxemburg and Hubert Savenije in 2017. Apart from the deep level impartation of hydrological concepts from Dr Wim and Prof Hubert, we (Bart and I) learnt a lot about perseverance, ethics and how to use astronomy when lost in a cloud free African forest with no compass, courtesy of the ‘southern cross’. The PhD itself did not disappoint in terms of extraordinary interactions. First on the list are Ivar and Esther. These two have outgrown the sphere of PhD interactions and have become part of my family. The long drives across Zambia with Ivar and the joy rides on Kings’ day in Amsterdam with Esther will forever be treasured. These two were not the only ones who gravitated from title of colleague to friend. My karaoke partner and highly intelligent friend, Sten, is a firm member of that family. Within the ZAMSECUR project itself I acknowledge the immense assistance I received from my research partners, Henry Zimba and Petra Hulsman. From the Technical University of Delft, nothing beats Psor on a Thursday afternoon next to the lake with Juancho (the smartest guy to come out of Colombia-terrific artist and musician), Monica (the best Spanish rocket scientist and dancer I have ever met), Ties (the smartest Dutchman on campus) and Boran (The funniest all round amazing Turkish guy to come out of the TU). My TU family would not be complete without a mention of my good friend and marathon fanatic from Tanzania, Martha. My partner Keziah, your constant encouragement will live with me forever. Within the great city of Delft, I learnt how to ride a bicycle. I credit this to two amazing people, Shelly and Marylyn. Marylyn, I wish you all the best in your new life in Zoetermeer. And Shelly, thank you for all your insights, it was a pleasure. The research itself would not have been possible without assistance from UNZA and WARMA; I would especially like to mention Beauty Shamboko, Chewe Chishala, Dr Kawawa Banda, Prof Nyambe. Finally, to the best supervisor I have ever had and will probably ever have, thank you Hessel.

Funding and Support

This research was supported by the TU Delft | Global Initiative, a program of the Delft University of Technology to boost Science and Technology for Global Development, and NWO-WOTRO, a Dutch

Organization for Scientific Research which aims to carry out research in support of the Sustainable Development Goals. The ZAMSECUR project was a collaboration of Delft University of Technology (TU-Delft), University of Zimbabwe (UZ), University of Zambia (UNZA) and WaterNet. A summary of the research activities within this project can be found on [https:// zamsecur.wixsite.com/home](https://zamsecur.wixsite.com/home). This study would not have been possible without the help of those who provided us with equipment and data from our local partners, WARMA (Water Resources Management Authority in Zambia), Department of National Parks, Zambia Civil Aviation Authority (CAAZ) and Zambia Air force (ZAF).

Curriculum Vitae

Hubert T Samboko

15-09-1991 Born in Bulawayo, Zimbabwe.

Education

2010–2014 *BSc Agricultural Engineering*

University of Zimbabwe

2015–2016 *MSc Water Resources Engineering and Management*

University of Zimbabwe

2023 *PhD. Water management*

Delft University of Technology, Netherlands

Thesis: Remote river rating in Zambia: Exploring opportunities for ungauged basins through low-cost technological advancements

Promotor: Prof. dr. ir. H.H.G. Savenije & Dr H. Winsemius

Experience

2016-2018 Agriculture and mining Drone pilot/engineer

Drone Solutions

List of Publications

H.T. Samboko, S. Schurer, H.H. G. Savenije, H. Makurira, K. Banda, and H. Winsemius:
Evaluating low-cost topographic surveys for computations of conveyance, *Geosci. Instrum. Method. Data Syst.*, 11, 1–23, <https://doi.org/10.5194/2022> : Chapter 4

H.T. Samboko, I. Abas, H.H. G. Savenije, H. Makurira, K. Banda, and H. Winsemius:
Evaluation and improvement of remote sensing-based methods for river flow management,
Physics and Chemistry of the Earth, <https://doi.org/10.1016/j.pce.2020.102839>, 2020: Chapter 5

H.T. Samboko, S. Schurer, H.H. G. Savenije, H. Makurira, K. Banda, and H. Winsemius:
Evaluating low-cost topographic surveys for computations of conveyance, *Geosci. Instrum. Method. Data Syst.*, submitted : Chapter 6

